



UNIVERSITY OF  
**KWAZULU-NATAL**  
INYUVESI  
**YAKWAZULU-NATALI**

DISCIPLINE OF MECHANICAL ENGINEERING  
MECHATRONICS AND ROBOTICS RESEARCH GROUP (MR<sup>2</sup>G)  
BIO-ENGINEERING UNIT

**A MODULAR PROSTHETIC ARM WITH HAPTIC  
INTERFACING FOR TRANSRADIAL/TRANSHUMERAL  
AMPUTEES**

---

**Mr Drew van der Riet (BEng, NMMU) – 213569879**

**In fulfilment of the MScEng, College of Agriculture, Engineering and Science, University  
of KwaZulu-Natal**

**August 2014**

**Supervisors:**

**Dr Riaan Stopforth**

**Prof Glen Bright**

**Prof Olaf Diegel**

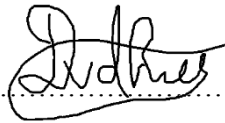
## COLLEGE OF AGRICULTURE, ENGINEERING AND SCIENCE

### DECLARATION 1 - PLAGIARISM

I, Drew van der Riet, declare that

1. The research reported in this dissertation, except where otherwise indicated, is my original research.
2. This dissertation has not been submitted for any degree or examination at any other university.
3. This dissertation does not contain other persons' data, pictures, graphs or other information, unless specifically acknowledged as being sourced from other persons.
4. This dissertation does not contain other persons' writing, unless specifically acknowledged as being sourced from other researchers. Where other written sources have been quoted, then:
  - a. Their words have been re-written but the general information attributed to them has been referenced
  - b. Where their exact words have been used, then their writing has been placed in italics and inside quotation marks, and referenced.
5. This dissertation does not contain text, graphics or tables copied and pasted from the Internet, unless specifically acknowledged, and the source being detailed in the dissertation and in the References sections.

Signed:



.....

### Supervisor's Agreement

As the candidate's Supervisor I agree/do not agree to the submission of this dissertation.

Signed:



.....

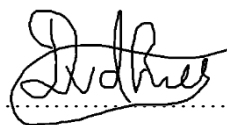
## COLLEGE OF AGRICULTURE, ENGINEERING AND SCIENCE

### DECLARATION 2 - PUBLICATIONS

DETAILS OF CONTRIBUTION TO PUBLICATIONS that form part and/or include research presented in this dissertation:

- van der Riet, D., Stopforth, R., Bright, G. and Diegel, O., “An overview and comparison of upper limb prosthetics,” IEEE AFRICON Conference, Mauritius, September 2013.
  - van der Riet, D. - 1<sup>st</sup> author
  - Stopforth, R. - supervisor
  - Bright, G. - supervisor
  - Diegel, O. - supervisor
- van der Riet, D., Stopforth, R., Bright, G. and Diegel, O., “Simultaneous vibrotactile feedback for multi-sensory upper limb prosthetics,” 6<sup>th</sup> IEEE Robotics and Mechatronics Conference of South Africa, Durban, October 2013.
  - van der Riet, D. - 1<sup>st</sup> author
  - Stopforth, R. - supervisor
  - Bright, G. - supervisor
  - Diegel, O. - supervisor
- van der Riet, D., Stopforth, R., Bright, G. and Diegel, O., “The low cost design of a 3D printed multi-fingered myoelectric prosthetic hand,” Mechatronics: Principles, Technologies and Applications, Nova Science Publishers Inc., submitted.
  - van der Riet, D. - 1<sup>st</sup> author
  - Stopforth, R. - supervisor
  - Bright, G. - supervisor
  - Diegel, O. - supervisor
- van der Riet, D. and Stopforth, R., “A low cost, extendable prosthetic leg for trans-fermoral amputees,” Mechatronics: Principles, Technologies and Applications, Nova Science Publishers Inc., submitted.
  - van der Riet, D. - 1<sup>st</sup> author
  - Stopforth, R. - supervisor

Signed:



## ACKNOWLEDGEMENTS

---

I would like to acknowledge and thank the following people for their assistance during this research:

- My loving wife, Alexi, for all the encouragement and support given to me during my research.
- Riaan Stopforth, for the constant assistance and feedback provided to me during the course of this research.
- Olaf Diegel, for the generous donation of the 3D printed hand parts.
- John Harris, for volunteering as a double transradial amputee to assist in the research and experimentation.
- Clive Leppens, for the fabrication and donation of the prosthetic socket used for experimentation.
- The various test subjects, for assisting in the research process.
- All other people from UKZN that have been involved in the project in some capacity, for there assistance and support.
- The National Research Foundation, for granting me a scholarship and travel grant to allow me to complete this research.

## ABSTRACT

---

Contemporary upper extremity prosthetics bring a lot of benefit to the amputee community. However, there are still a number of challenges facing the field of upper extremity prosthetics. These challenges include high cost and low functionality. This dissertation looks into a low-cost solution to provide a modular upper extremity prosthetic that will be suitable for both transradial and transhumeral amputees.

A novel method of myoelectric control is investigated with the introduction of a haptic user interface which will enhance the functionality of the prosthesis. This approach uses haptic feedback to display information (through the use of haptic displays) about the status of the control of the prosthetic arm.

The hand of the prosthetic arm is equipped with tactile sensors. These sensors read grip force, object slip, object temperature and object texture. In a novel approach to haptic feedback, this sensory information is displayed to the user simultaneously through a multi-sensory haptic feedback system. The haptic display uses vibrotactile displays to communicate the information to the user through vibrations. This approach gives the user a more holistic sensory representation.

The UKZN Touch Hand was developed at a cost of US\$ 1'000 for materials and parts. It is capable of gripping with 19.5 N using a power/cylindrical grip and 3.7 N using a lateral/key grip. It can hold up to 8 kg passively using a hook grip. The hand weighs 540 g including all electronics. It is equipped with pressure, temperature and vibration sensors to sense grip force, object temperature, slippage and texture. A novel simultaneous multi-sensory haptic feedback system was designed, tested on nine test subjects and shown to be a suitable form of feedback using a single vibrotactile display per sensory channel. A novel electromyography control method was developed to allow the amputee to select from a limitless list of pre-set grip types and hand gestures using only two muscles.

The Touch Hand was successfully tested on a transradial amputee who used it to perform tasks such as picking up various objects, pouring a bottle of water and drinking from a cup. Future work in this research should investigate alternative haptic feedback communication protocols to optimise the communication of information. Future work should also be done in developing fitting and training software to improve the amputees fitting and learning experience of the control of the prosthetic hand.

## CONTENTS

---

|   |    |
|---|----|
| 1. Introduction.....                                    | 1  |
| 1. Introduction .....                                   | 1  |
| 1.1 An overview of contemporary prostheses.....         | 1  |
| 1.1.1 Contemporary commercial hand prostheses .....     | 1  |
| 1.1.2 Shortcomings of commercial hand prostheses .....  | 2  |
| 1.1.3 Research and development of hand prostheses ..... | 2  |
| 1.2 Haptic feedback.....                                | 4  |
| 1.2.1 The role of senses in the hand .....              | 4  |
| 1.2.2 Contemporary haptic feedback systems .....        | 5  |
| 1.2.3 Novel haptic feedback research.....               | 5  |
| 1.3 Myoelectric control .....                           | 7  |
| 1.3.1 Problems in electromyography .....                | 8  |
| 1.3.2 Approaches to myoelectric control .....           | 8  |
| 1.4 Comparative results.....                            | 10 |
| 1.5 Discussion .....                                    | 13 |
| 1.5.1 Grip and load force.....                          | 13 |
| 1.5.2 Weight.....                                       | 13 |
| 1.5.3 Hand positions and myoelectric control.....       | 13 |
| 1.5.4 Haptic feedback.....                              | 14 |
| 1.5.5 Cost .....  | 14 |
| 1.6 Biological anatomy of hand and arm .....            | 15 |
| 1.6.1 Hand skeletal structure.....                      | 15 |
| 1.6.1.1 Finger joint anatomy .....                      | 15 |
| 1.6.1.2 Finger ligaments and tendons .....              | 16 |
| 1.6.2 Upper extremity skeletal anatomy.....             | 16 |
| 1.6.3 Upper extremity amputation .....                  | 18 |
| 1.6.3.1 Wrist disarticulation.....                      | 19 |
| 1.6.3.2 Transradial .....                               | 19 |
| 1.6.3.3 Elbow disarticulation .....                     | 19 |
| 1.6.3.4 Transhumeral .....                              | 20 |
| 1.6.4 Muscles in the human arm .....                    | 20 |

|         |  |    |
|---------|--|----|
| 1.6.4.1 | Biceps Brachii.....                          | 20 |
| 1.6.4.2 | Brachialis .....                             | 21 |
| 1.6.4.3 | Brachioradialis .....                        | 21 |
| 1.6.4.4 | Triceps brachii .....                        | 21 |
| 1.6.4.5 | Anconeus .....                               | 22 |
| 1.6.4.6 | Muscles in the forearm.....                  | 22 |
| 1.7     | Research objectives and specifications ..... | 23 |
| 1.8     | Contributions.....                           | 24 |
| 1.9     | Publications .....                           | 24 |
| 1.10    | Chapter summary .....                        | 25 |
| 2.      | Mechanical Design.....                       | 26 |
| 2.1     | Considered designs.....                      | 26 |
| 2.1.1   | Finger designs .....                         | 26 |
| 2.1.2   | Wrist and forearm design.....                | 29 |
| 2.1.3   | Upper limb actuation design .....            | 30 |
| 2.2     | Final design .....                           | 32 |
| 2.2.1   | Stress analysis .....                        | 34 |
| 2.3     | Kinematic models.....                        | 35 |
| 2.3.1   | Hand .....                                   | 36 |
| 2.3.2   | Arm .....                                    | 39 |
| 2.4     | Hand manufacturing process .....             | 41 |
| 2.4.1   | The working zone.....                        | 41 |
| 2.4.2   | Manufacture of fingers and thumb .....       | 42 |
| 2.4.3   | Finger and palm assemble .....               | 45 |
| 2.4.4   | Assembly of actuator and drive system.....   | 47 |
| 2.5     | Arm and socket manufacturing process .....   | 49 |
| 2.5.1   | Wrist.....                                   | 50 |
| 2.5.2   | Prosthetic socket.....                       | 53 |
| 2.5.2.1 | Socket fabrication .....                     | 53 |
| 2.5.2.2 | Suspension system .....                      | 55 |
| 2.5.3   | Device modulation .....                      | 56 |
| 2.5.3.1 | Transradial .....                            | 56 |
| 2.5.3.2 | Transhumeral .....                           | 57 |

|         |   |    |
|---------|---|----|
| 2.5.4   | Upper limb .....                                | 59 |
| 2.5.4.1 | The chassis plate .....                         | 59 |
| 2.5.4.2 | Fluidic muscle.....                             | 60 |
| 2.5.4.3 | Muscle support structure.....                   | 61 |
| 2.5.4.4 | Transhumeral socket connector .....             | 61 |
| 2.5.4.5 | Pulley redirection system.....                  | 62 |
| 2.5.4.6 | The rigid pulley.....                           | 63 |
| 2.5.4.7 | The valves .....                                | 63 |
| 2.5.5   | Chemical investigation.....                     | 65 |
| 2.6     | Chapter summary .....                           | 66 |
| 3.      | Electronic Design .....                         | 68 |
| 3.1     | Tactile sensory system .....                    | 69 |
| 3.1.1   | Grip force .....                                | 70 |
| 3.1.2   | Object temperature .....                        | 72 |
| 3.1.3   | Object slippage.....                            | 77 |
| 3.1.4   | Object texture .....                            | 80 |
| 3.2     | Electromyography .....                          | 85 |
| 3.3     | Haptic feedback and user interfacing .....      | 86 |
| 3.3.1   | Methodology .....                               | 87 |
| 3.3.1.1 | Sensory extraction.....                         | 87 |
| 3.3.1.2 | Feedback design.....                            | 88 |
| 3.3.1.3 | Placement.....                                  | 88 |
| 3.3.2   | Haptic user interfacing .....                   | 89 |
| 3.4     | Actuating and position feedback circuitry ..... | 90 |
| 3.4.1   | Electronic hardware integration .....           | 90 |
| 3.4.2   | Complete assembly of the hand .....             | 93 |
| 3.5     | Chapter summary .....                           | 94 |
| 4.      | Control .....                                   | 95 |
| 4.1     | Haptic user interface .....                     | 95 |
| 4.1.1   | Navigation .....                                | 95 |
| 4.1.2   | Feedback .....                                  | 98 |
| 4.1.3   | Training .....                                  | 99 |
| 4.2     | Electromyography .....                          | 99 |



|         |   |     |
|---------|---|-----|
| 4.2.1   | Calibration and filtering .....                   | 100 |
| 4.3     | Position control .....                            | 102 |
| 4.3.1   | Grip control process .....                        | 103 |
| 4.4     | Haptic sensory feedback .....                     | 103 |
| 4.5     | Chapter summary .....                             | 105 |
| 5.      | Tests and Results.....                            | 106 |
| 5.1     | Sensory system.....                               | 106 |
| 5.1.1   | Temperature test.....                             | 106 |
| 5.1.2   | Grip force test.....                              | 107 |
| 5.1.3   | Discussion .....                                  | 108 |
| 5.2     | Haptic feedback.....                              | 109 |
| 5.2.1   | Setup.....  | 109 |
| 5.2.2   | Experimental procedure .....                      | 109 |
| 5.2.2.1 | Test 1 - Spatial discrimination .....             | 110 |
| 5.2.2.2 | Test 2 - Intensity discrimination .....           | 110 |
| 5.2.2.3 | Test 3 - Intensity variation discrimination ..... | 110 |
| 5.2.2.4 | Test 4 - Full spectrum .....                      | 110 |
| 5.2.2.5 | Qualitative report .....                          | 111 |
| 5.2.3   | Results .....                                     | 111 |
| 5.2.4   | Discussion .....                                  | 112 |
| 5.2.4.1 | Spatial discrimination .....                      | 112 |
| 5.2.4.2 | Intensity discrimination .....                    | 113 |
| 5.2.4.3 | Intensity variation discrimination .....          | 113 |
| 5.2.4.4 | Simultaneous multi-sensory feedback .....         | 114 |
| 5.3     | HUI control .....                                 | 114 |
| 5.4     | Physical capabilities .....                       | 116 |
| 5.4.1   | Grip force test.....                              | 116 |
| 5.4.2   | Grip stability test.....                          | 118 |
| 5.4.3   | Kinematic video analysis .....                    | 119 |
| 5.4.4   | Passive loading test .....                        | 123 |
| 5.5     | Practical testing .....                           | 124 |
| 5.5.1   | Gripping objects .....                            | 124 |
| 5.5.2   | Live testing with a transradial amputee.....      | 126 |

|       |                                   |     |
|-------|-----------------------------------|-----|
| 5.6   | Chapter summary .....             | 127 |
| 6.    | Conclusion .....                  | 129 |
| 6.1   | Research achievements .....       | 130 |
| 6.2   | Future work .....                 | 132 |
| 6.2.1 | Control .....                     | 133 |
| 6.2.2 | Haptic feedback.....              | 134 |
| 6.3   | Chapter summary .....             | 134 |
| 7.    | References .....                  | 136 |
| 8.    | Appendix A .....                  | 138 |
| 8.1   | Mechanical drawings of hand ..... | 138 |

## LIST OF FIGURES

---

### 1. Introduction

- Figure 1-1: i-limb ultra from Touch Bionics© has multi-fingered grip resulting in more realistic movement and a variety of grips.
- Figure 1-2: Eight different grips/hand postures made by a prosthetic hand.
- Figure 1-3: Lateral stretch idea shown from side (a) and top-down (b) views. The crowns swing laterally when the actuators move up and down.
- Figure 1-4: Rotational skin stretch device.
- Figure 1-5: (a) Grip strength and object slip display using a vibrator and (b) stroking belt.
- Figure 1-6: Grip strength (in Newtons) of prosthesis in power and lateral grip types.
- Figure 1-7: Passive load (in kilograms) of prosthesis in the hook grip position.
- Figure 1-8: The number of available grip and hand positions the prosthesis is able to form.
- Figure 1-9: Complete system weight (in grams) of prosthesis including the wrist.
- Figure 1-10: Three groups of bones in the hand
- Figure 1-11: Finger joints
- Figure 1-12: Bones of the human arm
- Figure 1-13: Elbow flexion/extension
- Figure 1-14: Forearm supination/pronation
- Figure 1-15: Wrist flexion/extension
- Figure 1-16: Wrist abduction/adduction
- Figure 1-17: Types of amputation (a) wrist disarticulation, (b) transradial, (c) elbow disarticulation (d) transhumeral
- Figure 1-18: The bicep brachii (a), the brachialis (b) and the brachioradialis (c)
- Figure 1-19: Anterior of the forearm
- Figure 1-20: Posterior of the forearm

### 2. Mechanical design

- Figure 2-1: Finger concept A – linkage system
- Figure 2-2: Finger concept B – lead screw design, cable system
- Figure 2-3: Finger concept C – worm gear design, cable system
- Figure 2-4: Wrist concept A – twin-bone system
- Figure 2-5: Wrist concept B – telescopic system
- Figure 2-6: Upper limb actuation concept A – artificial muscle system
- Figure 2-7: Upper limb actuation concept B – motor and pulley system
- Figure 2-8: Final design of the hand

Figure 2-9: Final design of the wrist and forearm

Figure 2-10: Final design of the upper limb actuation

Figure 2-11: Complete prosthetic arm final design

Figure 2-12: Stress analysis of hand

Figure 2-13: Stress analysis of forearm

Figure 2-14: Overview of the final design prosthetic arm system

Figure 2-15: Joint and link diagram of the hand

Figure 2-16: Kinematic model of the finger (units in mm)

Figure 2-17: Kinematic model of the thumb (units in mm)

Figure 2-18: Kinematic model of the hand (units in mm)

Figure 2-19: Joint and link diagram of the arm

Figure 2-20: Kinematic model of the arm (units in mm)

Figure 2-21: Prosthetic hand development process overview

Figure 2-22: Working zone illustrated by red box

Figure 2-23: (a) CAD render of distal (b) 3D printed distal (c) CAD render of middle (d) 3D printed middle (e) CAD render of proximal (f) 3D printed proximal (g) CAD render of thumb base (h) 3D printed thumb base

Figure 2-24: Assembled finger

Figure 2-25: Elastic bands used for extension of the fingers

Figure 2-26: 3D printed palm chassis

Figure 2-27: Example of complete finger joined to the palm

Figure 2-28: Complete hand with dimensions

Figure 2-29: Nylon non-slip covering to improve grip stability

Figure 2-30: Polulu 6V DC motor with 50:1 gear ratio

Figure 2-31: A mounted motor used for thumb flexion and 4 finger motors.

Figure 2-32: Worm secured on motor shaft.

Figure 2-33: Complete assembly of worm wheel and cable pulley

Figure 2-34: Two views illustrating complete finger actuation system

Figure 2-35: Anatomic motions of the wrist; (a) extension/flexion (b) ulnar/radial deviation (c) supination/pronation

Figure 2-36: Servo motor: (a) Autodesk Inventor picture and (b) MG945 servo motor

Figure 2-37: Mounting disc made from clear perspex material

Figure 2-38: Mounting disc and servo horn being machined on milling machine

Figure 2-39: 3D printed wrist housing from ABS plastic

Figure 2-40: Components of the wrist housing

Figure 2-41: Amputee's current prosthetic hand with cable and hook end effector

Figure 2-42: Fabrication stages of prosthetic socket

Figure 2-43: Fitting of the socket and end effector angle

Figure 2-44: Socket and end effector

Figure 2-45: Prosthetic harness

Figure 2-46: Amputee wearing prosthesis

Figure 2-47: Transradial; model on the left and actual on the right

Figure 2-48: Exploded view of the forearm components

Figure 2-49: Assembled view of the forearm components

Figure 2-50: Transradial prosthetic arm

Figure 2-51: Transhumeral prosthetic arm

Figure 2-52: Transhumeral connection with air muscles and elbow joint

Figure 2-53: Chassis plate

Figure 2-54: Fluidic air muscle

Figure 2-55: Muscle female adapter

Figure 2-56: Crescent shaped mount.

Figure 2-57: Transhumeral socket connector

Figure 2-58: Redirection pulleys.

Figure 2-59: Main pulley

Figure 2-60: Shaft

Figure 2-61: Rigid link

Figure 2-62: Servo motorised valve unit.

Figure 2-63: Catalytic material (manganese dioxide)

Figure 2-64: The evolution of steam and oxygen

### **3. Electrical design**

Figure 3-1: Overview of the electrical system

Figure 3-2: Arduino Mega (blue) and the Seeeduino Mega (red) size comparison

Figure 3-3: Overview of the electrical system

Figure 3-4: FSR 400 force sensors (a) 8 mm diameter (b) 18 mm diameter

Figure 3-5: Voltage divider circuit with 22 k $\Omega$

Figure 3-6: Voltage vs force relationship for the 4.7 k $\Omega$  and 22 k $\Omega$  resistors

Figure 3-7: 18 mm force sensor output voltage, trend line:  $y = 0.625 \ln(x) + 3.052$

Figure 3-8: 8 mm force sensor output voltage, trend line:  $y = 0.6511 \ln(x) + 3.0222$

Figure 3-9: Temperature reading from the LM35 for direct and indirect contact

Figure 3-10: (a) Object temperature readings; (b) best fit linear equations for the initial 5 seconds

Figure 3-11: Final object temperature against gradient of temperature vs time

Figure 3-12: Average gradient example

Figure 3-13: Predicted temperatures with standard deviation

Figure 3-14: MiniSense 100 vibration sensor

Figure 3-15: Vibration signal at the start of slip

Figure 3-16: Sensor noise resulting from jerk motion

Figure 3-17: Sensor noise from collision 1

Figure 3-18: Sensor noise from collision 2

Figure 3-19: Sensor noise from collision 3

Figure 3-20: Texture vibration signal for smooth varnished wood

Figure 3-21: Texture vibration signal for semi-smooth plastic

Figure 3-22: Texture vibration signal for smooth ridged plastic

Figure 3-23: Texture vibration signal for smooth metal mesh

Figure 3-24: Texture vibration signal for Velcro, soft side

Figure 3-25: Texture vibration signal for Velcro, rough side

Figure 3-26: Texture vibration signal for bumpy plastic

Figure 3-27: Texture vibration signal for a keyboard

Figure 3-28: Myoelectric sensors

Figure 3-29: Surface mounted electrodes on forearm

Figure 3-30: Circuit design for the haptic feedback armband

Figure 3-31: The vibrotactile armband

Figure 3-32: Haptic feedback placement on transradial amputee

Figure 3-33: Haptic feedback placement on transradial amputee

Figure 3-34: TB6612FNG Dual motor driver

Figure 3-35: Multiple layers involved in assembling the hand

Figure 3-36: Custom wire ribbon used to connect electronic components

Figure 3-37: 4.5" Flex sensors used for position control of the fingers

Figure 3-38: Complete electronics layer

Figure 3-39: Complete assembly of the hand incorporating both actuation and electronic layers

#### **4. Control**

Figure 4-1: Flow diagram example of HUI menu navigation

Figure 4-2: Overview of HUI menu

Figure 4-3: Flow diagram of HUI menu navigation

Figure 4-4: Logic flow diagram of pulse counting loop

Figure 4-5: Flow diagram for single grasp controlled by muscle flexion or extension

Figure 4-6: Functionality vs smoothing window size for accuracy and response time

Figure 4-7: Execution methods to be implemented in motor control algorithm

Figure 4-8: User's closed loop control of hand grip

Figure 4-9: Example of the vibrotactile communication protocol

## 5. Tests and results

Figure 5-1: Expected temperature versus actual temperature for a period of 20 seconds

Figure 5-2: Expected temperature versus actual temperature for extreme temperatures

Figure 5-3: Force distribution for tripod grip

Figure 5-4: Test subject wearing the armband

Figure 5-5: Spatial discrimination accuracy percentage ( $\pm$  standard deviation)

Figure 5-6: Intensity discrimination accuracy percentage ( $\pm$  standard deviation)

Figure 5-7: Intensity variation accuracy percentage ( $\pm$  standard deviation)

Figure 5-8: Haptic feedback accuracy comparison ( $\pm$  standard deviation)

Figure 5-9: Time taken to select a grip with the HUI system

Figure 5-10: Number of commands versus time for the HUI system

Figure 5-11: Grip force test results

Figure 5-12: Fingertip slip during grip

Figure 5-13: 250ml graduated water bottle

Figure 5-14: Nylon non-slip covering to increase grip strength

Figure 5-15: Graph showing how secure a grip felt as weight of water bottle increases

Figure 5-16: Joint paths tracked and velocities measured using Kinovea kinematic analysis software

Figure 5-17: Joint paths and velocities tracked of the prosthetic hand

Figure 5-18: Graph of joint velocities for both human and prosthetic hands

Figure 5-19: Comparison between kinematic behaviour using joint displacements

Figure 5-20: Hand gripping bag for passive load testing

Figure 5-21: Weakest point under passive loading test – worm wheel and cable pulley coupling

Figure 5-22: Hand gripping square objects

Figure 5-23: Hand gripping unusually shaped bottle and a 2 litre bottle

Figure 5-24: Hand gripping a spherical object

Figure 5-25: Amputee training with EMG control of the prosthetic hand

Figure 5-26: Sequence of the amputee grasping and drinking out of a cup with the prosthetic hand

## NOMENCLATURE

---

|      |                                      |
|------|--------------------------------------|
| 3D   | 3-Dimensionally                      |
| ABS  | Acrylonitrile Butadiene Styrene      |
| AI   | Artificial Intelligence              |
| D-H  | Denavit–Hartenberg                   |
| DIP  | Distal Interphalangeal               |
| DOF  | Degrees Of Freedom                   |
| EDFS | Event Driven Finite-State            |
| EEG  | Electroencephalography               |
| EMG  | Electromyography/myoelectric         |
| FEA  | Finite Element Analysis              |
| HUI  | Haptic User Interfacing              |
| MBC  | Multiple Binary Classification       |
| MCU  | Microcontroller Unit                 |
| NMES | Neuromuscular Electrical Stimulation |
| PIP  | Proximal Interphalangeal             |
| PLP  | Phantom Limb Pain                    |
| PWM  | Pulse Width Modulation               |
| RMS  | Root Mean Square                     |
| SANS | South African National Standards     |
| SMA  | Shape Memory Alloy                   |



## 1. INTRODUCTION

---

A classic example of upper extremity prostheses can be seen worn by Captain Hook in the childhood story of Peter Pan (Barrie, 1904). Prosthetics have come a long way from simple hooks. Advancements have been made steadily bring hooks closer and closer towards the ultimate goal of a full and lifelike replacement for the human hand. That stage hasn't arrived yet. There are still several large engineering problems to overcome before reaching this goal as well as the practical consideration of keeping the costs low.

A normal human hand has three basic functions; gripping objects, manipulating them and exploring the surrounding environment (Carrozza et al., 2003). Most rudimentary prosthetics restore the ability to grip and manipulate to some degree. If full restoration is to be achieved through prosthetics, the prosthetic hand must restore the ability to explore as well. Full restoration requires the prosthesis to have proprioceptive (a sense of one's body's positioning) and exteroceptive (touch) sensors, and for this information to be communicated back to the amputee.

### 1.1 An overview of contemporary prostheses

In order for progress to be made in the field of prosthetics, it is important to review the current state of prosthetics and to identify the areas needed to be focused on to further improve a system. This section reviews current prostheses available in the market as well as the latest research being conducted around the world. It highlights the weaknesses in these prostheses and makes suggestions for the direction of future work.

#### 1.1.1 Contemporary commercial hand prostheses

The three main competitors in the market of myoelectric prosthetics are OttoBock®, Touch Bionics® and RSLSteeper®. Touch Bionics®'s latest myoelectric hand, the i-limb ultra, can be seen in Figure 1-1 (Touch Bionics, 2013). In 2011, comparisons were done between OttoBock®'s DMC plus and older versions of Touch Bionics®'s i-limb ultra, the i-limb pulse and the i-limb (van der Niet et al., 2011). The DMC plus and i-limb pulse were found to be about equal in grip strength, with the i-limb being weaker. The DMC plus was much stronger than either of the i-limbs in tripod grip strength. The pulse had the highest scores for posture and movement. The pulse also had the highest client satisfaction, although it must be mentioned that only one test subject was used.



Figure 1-1: i-limb ultra from Touch Bionics© has multi-fingered grip resulting in more realistic movement and a variety of grips.

The BeBionic3 from RSLSteeper© (RSLSteeper, 2013) uses a state machine to control the prosthesis, this state machine relies on manually selected thumb position (opposed or non-opposed) as well as a toggle button allowing a second group of positions. The user simply has two degrees of freedom (DOFs) in control: open and close commands. Although this is currently advertised as the most advanced commercially available prosthesis, it is still using a very old system of control.

### 1.1.2 Shortcomings of commercial hand prostheses

It has been found that the grip strength of commercial prosthetic hands is much lower than that of an able-bodied individual (van der Niet et al., 2010). Hand control and motion is also very clumsy and requires manual correction of thumb positions. Dexterity of fingers is extremely limited. Previous research (van der Niet et al., 2011) emphasized that at least 4 months of daily training was needed to be able to use a multifunctional myoelectric prosthetic hand.

One of the major drawbacks in the use of these state-of-the-art prosthetic hands is the high cost involved. An example of this is the Robohand (Van As and Owen, 2013), a purely mechanical prosthetic hand that works on a cable/leverage actuated system. It was released in 2013 and costs around US\$ 150. This device is very simple and has only one grip position (the tripod grip) in comparison to the multi-grip commercial prosthetic hands mentioned above. Despite this, the Robohand has received a large amount of popularity due to its cheap design.

### 1.1.3 Research and development of hand prostheses

There have been several multi-grasp prosthetic hands developed in recent years (Dalley et al., 2010). These hands range between one and six actuators working independently which control a varying number of fingers from just the index and thumb in a “claw” style to each

finger individually. Vanderbilt University's (Dalley et al., 2010) prosthetic hand can be seen in Figure 1-2, demonstrating its 8 different hand positions.

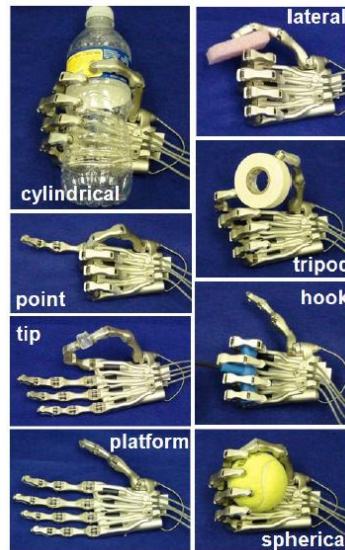


Figure 1-2: Eight different grips/hand postures made by a prosthetic hand.

State-of-the-art myoelectric prosthetics are highly complex and challenging to design. This is because they have to be entirely independent, relying on self-actuation, internal power, built-in intelligent control and sensory feedback while also remaining compact and light-weight to resemble a human hand. They need to be highly functional allowing the user a full range of actions as well as sensory feedback and also have a good battery life. This is a difficult task for a device that is the size of a human hand. Researchers have come a long way in obtaining these goals, as can be seen in the MARCUS (Kyberd et al., 1995) and Southampton Hand (Cotton et al., 2006), earlier attempts at improving the state of upper extremity prosthetics. The progression showed favour to improving the number of degrees of freedom and the control needed to obtain these positions.

A notable research-based prosthetic hand currently being developed is the SmartHand by the ARTS Lab of Scuola Superiore Sant' Anna, Pontedera, Italy (Cipriani et al., 2009, 2012). This research showcases the use of 4 DC motors to control 16 DOFs, proprioceptive and exteroceptive sensors with 5 vibrotactile feedback displays. Vibrotactile (haptic) displays are a medium to communicate information to the user through haptics (the sense of touch) in the same way as a visual display communicates information through the sense of sight. The SmartHand's weight was considered to be a small problem, 520 g in comparison to an adult male average of 400 g (Cipriani et al., 2011). Its size is 1.3 times larger than the same average adult male statistic. There remains no adequate method of transmitting detailed haptic feedback

to the user. It is also stated that the mechanical architecture contains a compromise of mechanical efficiency and the lack of an extension grip, used to grip a book or a plate (Cipriani et al., 2010), for adaptive gripping fingers and more strength in power and precision grips. It has also been highlighted that power consumption should be kept to an absolute minimum to extend the battery life of the prosthesis.

## **1.2 Haptic feedback**

Many different forms of feedback are available with contemporary technology. The term “haptic”, refers to the sense of touch. Within the field of prosthetics, feedback normally serves as a replacement of the sensory system lost with amputation. These senses communicate with the brain through the nervous system. However, this connection is severed in the case of amputation. Haptic feedback is non-invasive method of communicating with the nervous system through its natural receptive fields in the skin.

### **1.2.1 The role of senses in the hand**

The human body has more than the classically believed 5 senses, the clear 6th sense is the vestibular system, or the sense of balance which is located in the ears. Depending on how one defines senses, touch can be broken down into 4 separate senses; physical touch, temperature, proprioception and pain (which can be separate from touch as humans sense internal pains as well as pains induced through touch). Henshaw (2012) suggests that these 9 senses (vision, hearing, smell, taste, touch, balance, temperature, proprioception and pain) should be considered as the fundamental senses. A broader definition can break each of these senses down into more specialised fields, but it is felt that this is of no further aid in understanding senses.

Using the above definition, the classical definition of touch is associated 4 senses, touch/tactile (types of surfaces, i.e. rough, smooth or wet as well as pressure and force), temperature, proprioception and pain (a warning of danger). These four senses are all sensed by ones hand and arm and play a large role in both communicating and exploring one’s environment (Maclean, 2000). It is therefore important to restore not only the motion and physical function of a lost arm or hand through prosthesis but also these 4 senses. Achieving this will create a holistic prosthesis capable of fully restoring the amputee to normal function.

It has been found that haptic feedback reduces fatigue in myoelectric prosthetics users. This is because users without haptic feedback tend to use excessive force for excessive periods of time in order to successfully complete tasks (Kim and Colgate, 2012). It has also been shown that the use of haptic feedback in prostheses reduces phantom limb pain (PLP) in amputees

(Dietrich et al., 2012). One of the challenges in haptic feedback systems is the fact that touch, which can be classified as a form of communication, hasn't had the rules and symbols to define it explicitly created (Maclean, 2000). Without these rules it is impossible for a computer system to recognize and process this language. A language of communication needs to be established if these senses are to be restored through haptic feedback.

### **1.2.2 Contemporary haptic feedback systems**

Haptic feedback systems focus on two areas, tactile (touch) and force feedback (Okamura, 2004). Within the tactile feedback area, there are currently two main subdivisions; pressure displays and vibrotactile stimulation (Hayward and Cruz-Hernandez, 2000). Force feedback systems are found commercially in joysticks and gaming steering wheels, as well as other devices but are not generally implemented in prosthesis as the prosthetic arm itself transfers forces to the amputee's residual limb directly. It has been found that both vibration and pressure feedback systems in addition to visual feedback improved task completion over visual alone (Tejeiro et al., 2012). Previous research performed by comparing vibration and pressure feedback systems found that pressure systems are slightly easier to recognize than vibration systems (Antfolk et al., 2013). Haptic feedback is clearly important in the future development of prosthetics in contrast to the high level of dependence on visually aided control in contemporary prosthetic arms.

### **1.2.3 Novel haptic feedback research**

A more recent development in haptic feedback is the use of skin stretching devices. These devices use a mechanical mechanism to stretch the skin of the user in either a lateral (Hayward and Cruz-Hernandez, 2000) or rotational (Bark et al., 2009) manner in order to display signals. Previous research suggested that the lateral stretch could be used to signal textures (Hayward and Cruz-Hernandez, 2000). The lateral stretch technique shown in Figure 1-3 (Hayward and Cruz-Hernandez, 2000), shows how the vertical actuators move the crown laterally. A rotational stretch device, as shown in Figure 1-4 (Bark et al., 2009), could be used for proprioceptive sensing. Natural proprioceptive sensing uses skin stretch on the joints and so using this rotation skin stretch display is a more natural and thus easily understandable medium for signalling. Tests done using the rotational stretch showed promising results, improving the accuracy of users over no-feedback conditions (Wheeler et al., 2010). This method could be developed further as a proprioceptive feedback device. The proprioceptive sense is significantly more useful than visual positioning when controlling a prosthetic arm. However, there are no current proprioceptive feedback devices commercially available for use in prosthetic arms (Gurari et al., 2013).

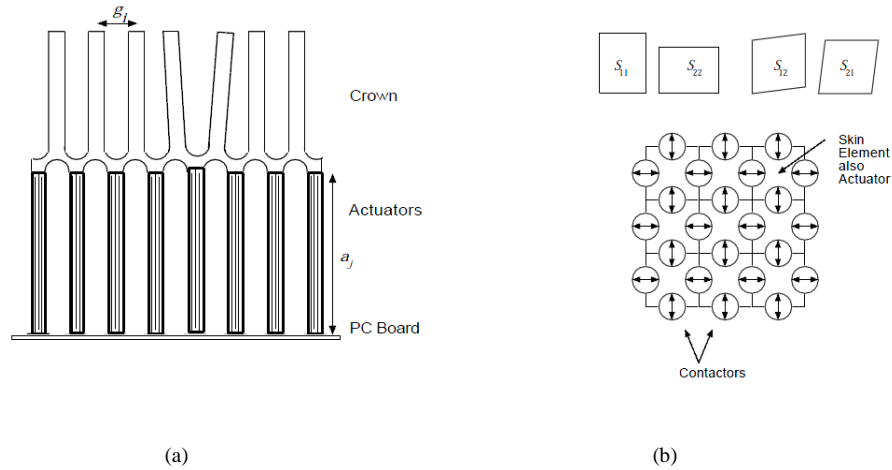


Figure 1-3: Lateral stretch idea shown from side (a) and top-down (b) views. The crowns swing laterally when the actuators move up and down.

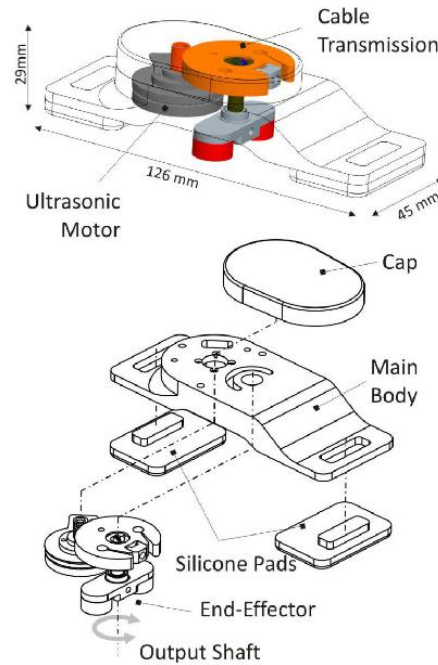


Figure 1-4: Rotational skin stretch device.

One of the major problems found with prosthetic hands is the lack of reliable grip strength. Problems occur with either the grip being too strong and damaging a fragile object or too weak and a heavy object slipping out of the prosthetic hand. There are two possible solutions to this problem; robotic control of grip strength or discernible haptic feedback allowing users to accurately control the grip strength themselves. Experiments have shown successful application of both grip strength and object slip tactile displays (Damian et al., 2012). These experiments used a vibrator to indicate grip strength and a stroking belt, as shown in Figure 1-5 (Damian et al., 2012), to indicate slippage. The stroking belt is a new approach to haptic feedback, however, it was found to be both less comfortable and more difficult to

interpret than the vibrator. Both displays were stepped into 4 stages and the experiments were done in an individual manner. Further work can be done to investigate the combined effect of the sensors in a real-world situation.

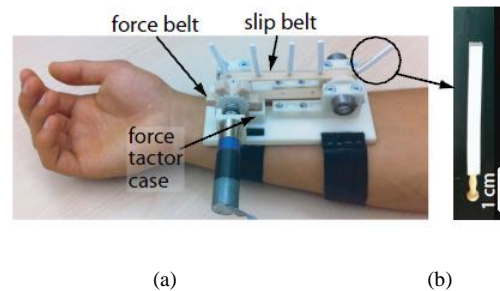


Figure 1-5: (a) Grip strength and object slip display using a vibrator and (b) stroking belt.

A previous research study was done by using three miniature vibrotactile devices placed in different locations on the forearm simultaneously (Cipriani et al., 2012). They concluded that the subjects were able to sense the different locations being stimulated with great accuracy and were also able to discern between 6 unique patterns created by the 3 devices with lesser accuracy but still greater than 75%. It was suggested that three basic types of information are essential in communicating with the amputee; contact touch, contact position (where on the prosthesis) and contact force.

There are few studies on Neuromuscular Electrical Stimulation (NMES) as a form of haptic feedback. NMES works by providing small stimulating electric shocks to the user. These shocks can vary in amplitude, pulse width and frequency. A study was done on the comfort and effectiveness of using it as haptic feedback for a video game and had mostly positive results (Kruijff et al., 2006). It was found that most subjects thought the stimulation to be informative and exciting (adding to the video game experience) although a few found it uncomfortable and irritating. Previous research analysed the different types of stimulation that can be induced by NMES (Geng et al., 2012). It was found that touch, vibration, pinprick and movement were the most frequently reported stimulations. The type of stimulation felt was controlled to a degree depending on site location of the NMES, type of pulse and number of channels. The magnitude of the sensation was also variable. It is proposed that due to NMES's variety in stimulation it is an appropriate feedback for myoelectric prosthetic hands.

### 1.3 Myoelectric control

The one of the highest priorities when designing prostheses is the ability for it to be controlled by the amputee. Traditionally prostheses were controlled by mechanical cables and levers attached to the amputees body, allowing the amputee to drive the prosthesis. In most



modern prostheses, the focus is to restore full function to the amputee. The amputee can control his/her prosthesis simply by using his mind, as he controls any other limb in his body. This approach can be carried out through invasive nerve connectors which read signals directly from the nerves or through an electroencephalography (EEG) headset. Another method is for the signals to be read directly from the muscles through electromyography (EMG). This method is generally a non-invasive technique and is preferred in upper extremity prosthetics because of its simplicity to connect the EMG sensors to the patient along with the rest of the prosthesis. It has also had the most success in upper prosthetic control (Matrone et al., 2012).

### 1.3.1 Problems in electromyography

The main challenge of EMG control is mapping the myoelectric input signals to the output actuators of the prosthetic hand. This is particularly challenging when the number of input channels is significantly less than the number of output channels. There are several other challenges faced with all EMG signal extraction (Castellini and van der Smagt, 2009):

- a) everybody's arm produces different electrical signals, and so the EMG controller needs to be configured for each user individually
- b) a change in arm position results in a change in EMG signals even if the hand grip did not change
- c) the EMG signal will vary according to the placement of the electrode
- d) fatigue of the muscles being read reduces the root mean square (RMS) value of the signal

### 1.3.2 Approaches to myoelectric control

Different experiments have been done with the number of EMG sensors ranging from 2 to 32 sensors (Khushaba et al., 2012). Results have been found to be better with a larger number of sensors, but not drastically, and the large increase in cost in the use of multiple EMG sensors motivates the use of less electrodes. There are two main fields of EMG control, pattern recognition and non-pattern recognition (Matrone et al., 2012). Pattern recognition is the most common method for EMG signal processing in research literature (Khushaba et al., 2012). Algorithms have been developed to be able to recognize multiple finger movements both individual and paired, with roughly 90% accuracy. The problems with contemporary pattern recognition systems are that they are limited in the number of patterns to select from, which means that the prosthesis has limited positions and lacks the freedom of a natural hand (Jiang et al., 2009). Increasing the number of patterns means that the classification error will worsen and the training time will be extended. Also, only one pattern can be selected at a time further reducing the flexibility and creating a sequential control scheme. There has been recent work done to allow for multiple DOFs control simultaneously (Jiang et al., 2009). Non-pattern recognition is more commonly used in clinical practice as it is more reliable and offers



simplified open/close or proportional control (Matrone et al., 2012). This control method can be simply used to control the grip strength (a high priority in modern prostheses) of a single DOF prosthesis such as ones used clinically like OttoBock®'s DMC plus (OttoBock<sup>a</sup>, 2013).

The main reasons why pattern recognition hasn't been used in clinical applications yet is due to the lack of an easy user interface, uncertainty that good classification relates to good control of a prosthesis and that muscle patterns change over time making long term accuracy more questionable. One of the reasons for poor control through pattern recognition despite the high accuracy of classification is that there is also a high level of false activation movements (an unintended activation of movement). A method to reduce this is a multiple check classification system that uses all the classes to agree on a decision before activating a movement. A multiple binary classification (MBC) algorithm has been developed in previous research using this method. It was found that the MBC system, compared to a conventional pattern recognition system, had lower false activation and better control of a virtual prosthesis despite an increased classification error. (Hangrove et al., 2010)

One of the approaches to non-pattern recognition control is an array selection technique (Matrone et al, 2012). An array consisting of a 5x5 grid was used to represent three grip types; power, precision and lateral and a variety of intermediate positions between an open hand state and the stated closed grip positions. The user could navigate through this 2-dimensional array by either flexing (x-axis) or twisting (y-axis) his wrist. The maximum and minimum myoelectric signals would be collected from the user to calibrate the system before use. The systems major shortcomings are the lack of grip strength control and a relatively long time required to grip objects correctly (approximately 5 seconds). The time taken to grip objects could be improved through prolonged practice with the device. Another non-pattern recognition control technique is the use of an event driven finite-state (EDFS) algorithm (Dalley et al., 2012). This approach only uses the state of flexion on the wrist as an input, requiring only a single pair of EMG sensors. The sensors read 4 states; flexion, extension, joint flexion-extension (co-contraction) and rest. Using these command inputs it is possible to navigate through a bi-linear map corresponding to all the different grip types in a sequential order. Flexion and extension signals were used to progress forwards and backwards through the different stages of the map and co-contraction as a toggle between linear maps (Dalley et al., 2012). Power, tip, pinch and hook grips were achieved in this manner as well as a point and open hand position. These grips were achieved faster than the previously mentioned method (the average time taken to select a position was around 2 seconds) and also improved with practice.

## 1.4 Comparative results

It is necessary to compare the various available prostheses in order to fully understand the scope of work that has been achieved and what can be implemented in the future to further improve this area. The comparison was done by using available information. Comparisons were done with 3 commercially available dexterous prosthetic hands and a state-of-the-art researched based prosthetic hand, which can be seen in Table 1-1 and Table 1-2 (van der Riet et al., 2013a). Only relevant and comparable data was used in the tables.

TABLE 1-1: CONTEMPORARY UPPER EXTREMITY PROSTHESES

|  | <b>i-limb ultra (Touch Bionics, 2013)</b> | <b>BeBionic3 (RSLSteeper, 2013)</b> | <b>Michelangelo (OttoBock<sup>b</sup>, 2013)</b> | <b>SmartHand (Cipriani et al., 2011)</b> |
|--|---|-------------------------------------|--|--|
| <b>Grip Strength (N):</b>                            |   |                                     |  |  |
| <b>Power Grip<sup>**</sup></b>                       | 136                                       | 140                                 | 70   | 36                                       |
| <b>Lateral Grip<sup>***</sup></b>                    | 34  | 27                                  | 60   | 8  |
| <b>Passive Load (kg) - Hook Grip (Suitcase Hold)</b> | 90  | 45                                  | - <sup>*</sup>                                   | 10                                       |
| <b>Closing Speed - Power Grip (sec)</b>              | 1.2                                       | 1.0                                 | - <sup>*</sup>                                   | 1.5                                      |
| <b>Grip and Hand Positions</b>                       | 11  | 14                                  | 7  | - <sup>*</sup>                           |
| <b>Control</b>                                       | 2 Channel Myoelectric                     | 2 Channel Myoelectric               | 2 Channel Myoelectric                            | Myoelectric                              |
| <b>Actuators</b>                                     | DC Motors                                 | DC Motors                           | DC Motors  | DC Motors                                |
| <b>Touch Sensors</b>                                 | No  | No                                  | No   | pressure                                 |
| <b>Feedback Displays</b>                             | No  | No                                  | No   | 5 vibrotactile displays                  |
| <b>Weight (g)</b>                                    | 479                                       | 598                                 | 600  | 530                                      |
| <b>Cost (US\$)<sup>****</sup></b>                    | 40'000                                    | 35'000                              | 75'000   | - <sup>*</sup>                           |

<sup>\*</sup>data unavailable <sup>\*\*</sup>this grip uses all the fingers and the palm with the thumb is in the opposed position and its used to grip objects such as a bottle

<sup>\*\*\*</sup>this grip is between the thumb and the side of the finger with the thumb in the non-opposed position and its used to grip objects such as a key

<sup>\*\*\*\*</sup>cost is approximate and varies greatly according to the amputation

TABLE 1-2: RESEARCH BASED UPPER EXTREMITY PROSTHESES

|  | <b>SmartHand (Cipriani et al., 2011)</b> | <b>Vanderbilt University Hand (Dalley et al., 2010)</b> | <b>Southampton Hand (Cotton et al., 2006)</b> | <b>MARCUS (Kyberd et al., 1995)</b> |
|--|--|---|---|-------------------------------------|
| <b>Grip Strength – Power Grip<sup>**</sup> (N)</b> | 36                                       | 50  | - <sup>*</sup>                                | - <sup>*</sup>                      |
| <b>Degrees of Freedom</b>                          | 16                                       | - <sup>*</sup>  | 6   | 2                                   |
| <b>Closing Speed - Power Grip (sec)</b>            | 1.5                                      | 0.3   | - <sup>*</sup>                                | - <sup>*</sup>                      |
| <b>Grip and Hand Positions</b>                     | - <sup>*</sup>                           | 8   | 6   | 3                                   |
| <b>Control</b>                                     | Myoelectric                              | Myoelectric   | Myoelectric                                   | Myoelectric                         |
| <b>Actuators</b>                                   | DC Motors                                | DC Motors   | DC Motors                                     | DC Motors                           |
| <b>Touch Sensors</b>                               | pressure                                 | No  | pressure, slip, temperature                   | pressure, slip                      |
| <b>Feedback Displays</b>                           | 5 vibrotactile displays                  | No  | No  | No                                  |

<sup>\*</sup>data unavailable <sup>\*\*</sup>this grip uses all the fingers and the palm with the thumb in the opposed position and it's used to grip objects such as a bottle

Table 1-2 compares the prosthetic hands developed through research based institutions. Some of the more notable hands have been compared here and Table 1-2 also shows the development of the upper extremity prostheses over time with older versions also included.

From these tables, graphs have been drawn up to compare various aspects. Figure 1-6 (van der Riet et al., 2013a), shows a comparison of grip strength of the prostheses in power and lateral grip positions. Not all of the prostheses compared in this section had test results for measured grip strength. It was found that power and lateral grips were the best for comparison as they were the most commonly measured grip strengths. The passive load limit of the prostheses is shown in Figure 1-7 (van der Riet et al., 2013a). Again only some prostheses had data available on passive force test and the hook grip was the most common of these tests. Most of the prostheses compared in this study had a high DOF, allowing for a large combination of grip types. The limiting factor in grip types is the control algorithm used. The MARCUS (Kyberd et al., 1995) and Southampton Hand (Cotton et al., 2006) both used state machine control methodologies. Generally the prostheses developed in research are capable of a high level of dexterity and are limited only by the current technology available to control the prosthesis. The possible grip and hand positions are shown in Figure 1-8 (van der Riet et al., 2013a). The total weight of the complete prostheses including the wrist is shown in Figure 1-9 (van der Riet et al., 2013a).

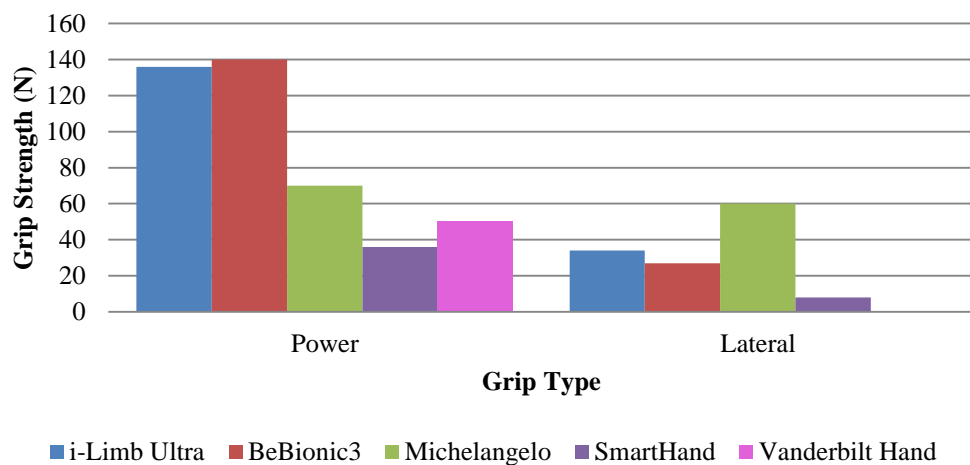


Figure 1-6: Grip strength (in Newtons) of prosthesis in power and lateral grip types.

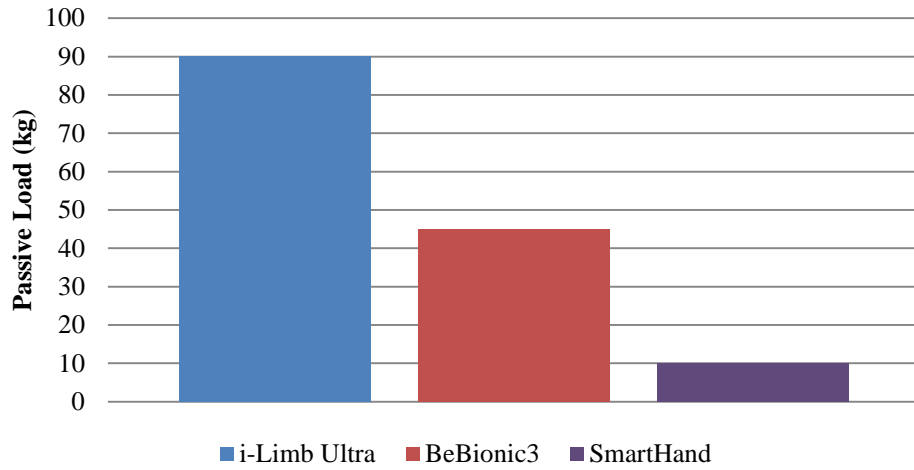


Figure 1-7: Passive load (in kilograms) of prosthesis in the hook grip position.

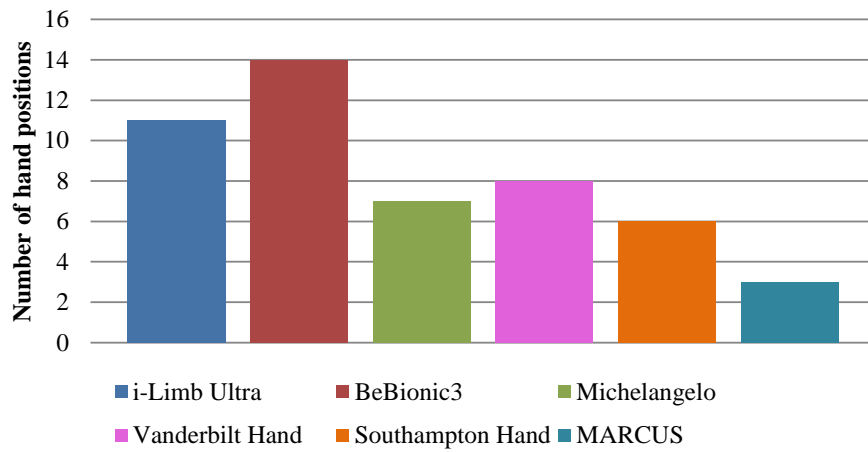


Figure 1-8: The number of available grip and hand positions the prosthesis is able to form.

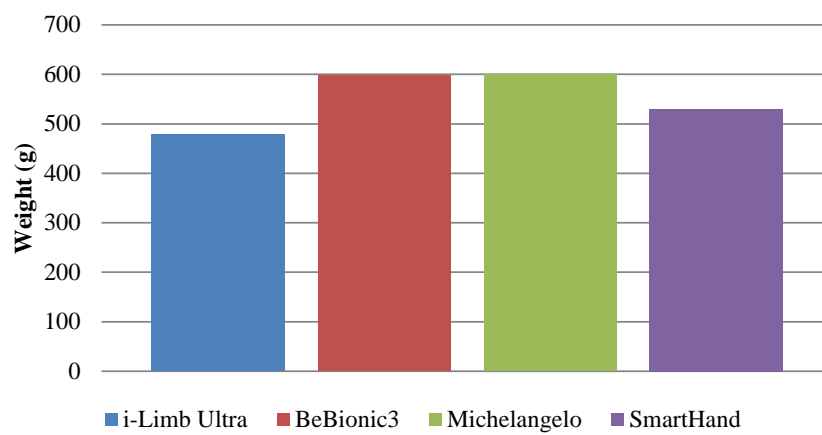


Figure 1-9: Complete system weight (in grams) of prosthesis including the wrist.

## 1.5 Discussion

From the initial study, various observations can be made. These observations include the grip and load force performance of the prosthetic hands; their weight; their control methodology and hand positions; their haptic feedback methods and their cost.

### 1.5.1 Grip and load force

Grip strength, although improving, is still considerably lower than that of an unimpaired hand. The i-Limb Ultra and the BeBionic3 have the best grip strength from the comparison, and this is still 4 times less than an unimpaired adult hand. The motor size is the limiting factor in this area. Most prostheses are designed with 4-5 motors which are all situated in the hand itself, thus the space is very small. Since a motor's power is related to its size, this proves a difficult challenge that has yet to be properly solved. Possibly redesigning the entire system would be needed to improve the grip strength as a cable/tendon system has high losses due to force angles. Further work should be done into mechanical designs of the finger as well as consideration into alternative actuators to improve this problem. The passive load limit ranges greatly between the 3 prostheses compared in Figure 1-7. i-Limb Ultra's performance in this area is remarkable and definitely adequate for daily life, even BeBionic3's passive force limit would be sufficient to lift daily items. The extent and thoroughness of this test is unknown and no tests with amputees have been done in this area to the author's knowledge.

### 1.5.2 Weight

Considering that a normal adult male's hand weighs around 400 g, the weights of the prostheses seen in Figure 1-9, are still too heavy. Weight is another trade-off criteria and this area will improve slowly as the development of micro-electronics continues. The major contributors to weight are the motors. The ratio of motor weight and grip force is difficult to balance as it was also stated that the grip strength was lower than that of a normal hand. Thus it can be seen that the designers have taken both these factors into consideration and probably placed more importance on keeping the weight down, as the weights are only 25% – 50% off the mark. It is notable that an overly heavy prosthesis would be unusable but an underpowered prosthesis is merely limiting. Future work needs to be done in the use of lighter materials and using alternative actuators to reduce the weight of the system.

### 1.5.3 Hand positions and myoelectric control

The number of grip types available to the prosthesis is very important. This plays a big role in how useful a prosthetic hand is practically. One must consider the number of daily tasks that can be achieved with the prosthesis and which tasks cannot. In the first versions of the

myoelectric upper extremity prosthetic they would have only 1 grip type, a precision grip, similar to that of the hand of a manufacturing robot. MARCUS was one of the first adaptations to this idea bringing in a second DOF to allow for both precision and power grips. A progression of grip types is seen in Figure 1-8 from MARCUS (Kyberd et al., 1995) to the Southampton Hand (Cotton et al., 2006) and then the Vanderbilt Hand (Dalley et al., 2010) showing the progress research has made in fifteen years. The number of grips these prostheses are able to perform is limited by the myoelectric control algorithm. There are several different methods of control divided into two main fields; pattern recognition and non-pattern recognition. It is interesting to note also that all the commercial prostheses use very simply non-pattern recognition control. The simple control is probably used because of the low level of training needed to learn how to use these state driven control algorithms, the prosthesis doesn't need to be trained or personally configured. However the drawback of such systems is the time taken to select the required grip. As the number of grips increases this method will become cumbersome and slow, thus industry will need to adapt to the newly developed control systems in the near future. The current commercial prostheses could be improved through implementing an advanced pattern recognition algorithm. However, current state-of-the-art myoelectric control algorithms such as pattern recognition have flaws such as the fact that the EMG signals vary over time. These flaws limit the development of pattern recognition as a long term solution. Future work needs to be done to develop a control algorithm that successfully allows the user to control all fingers of the prosthesis separately, proportionately and simultaneously.

#### **1.5.4 Haptic feedback**

Haptic feedback has been largely neglected in current prostheses. The only prosthesis out of the comparison using haptic feedback is the SmartHand. This research could be incorporated into current commercial prostheses to improve grip control and create a more realistic feel of the prosthesis for the amputee. Haptic feedback technology still remains very rudimentary. Pressure and vibration are the only two well-developed feedback systems. More attention needs to be paid in future work to improve the haptic display of information allowing for multiple dimensions to be displayed simultaneously such as pressure and proprioception. Existing devices such as the rotational stretch and the NMES should also be investigated in actual prosthesis application.

#### **1.5.5 Cost**

The commercially available prostheses are all very expensive (US\$ 20'000+). The Michelangelo is significantly more expensive (~US\$ 70'000) than the other devices, however this large price difference doesn't reflect in any performance improvements over the other hands. The large cost associated with all the myoelectric prosthetic limbs is one of the main

reasons preventing these devices becoming widely used in the prosthetic community. Future work should focus on the development of cheaper myoelectric controlled upper extremity prostheses.

## 1.6 Biological anatomy of hand and arm

It is important to understand the structure and function of the human hand and arm in the design of a prosthetic upper extremity limb. This allows the designer to both consider the human limb and be inspired by it in the designs. The result of such considerations is that the design is both aesthetically and functionally natural, helping the amputee's life to be restored to its daily norms.

### 1.6.1 Hand skeletal structure

Bone is a complex array of canals and blood vessels (Skeletal System, 2013). Each hand consists of 27 bones; these are divided into 3 regions, the carpals, metacarpals and the phalanges. Muscles connect to the bones allowing the motions of the limbs including the fingers. They form a structural base in which all other biological components are secured.

Bone is relatively hard and lightweight and made of calcium phosphate (Skeletal System, 2013). The three groups of bones in the hand can be seen in Figure 1-10 (Richards and Loudon, 2013).

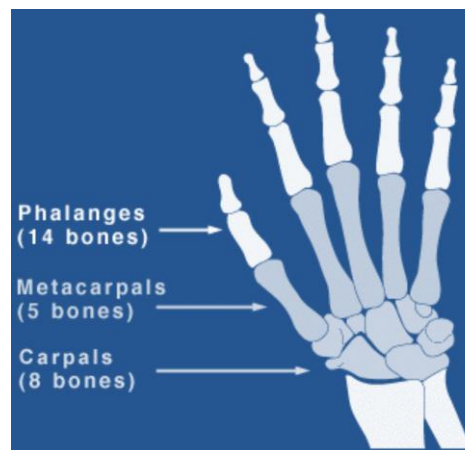


Figure 1-10: Three groups of bones in the hand

#### 1.6.1.1 Finger joint anatomy

Joints facilitate movement between bones by providing a meeting point between the bones and providing lubrication. There are three bones in each finger called the proximal phalanx, the middle phalanx and the distal phalanx. Each finger has three joints. The first is the connection between the finger and the hand. This is where the bones that form the palm of the hand, the metacarpals, join with the first bone of the finger, the proximal phalanx. The second

joint is the proximal interphalangeal (PIP) joint and the last is the distal interphalangeal (DIP) joint. These joints can be seen in Figure 1-11 (Artificial Joint Replacement of the Finger, 2013). Each of these joints is covered with articular cartilage. Articular cartilage is a smooth, spongy material that covers the end of bones that make up a joint. The cartilage allows the bones to slide easily against one another as the joint moves through its range of motion. (Finger Joint Anatomy, 2013)



Figure 1-11: Finger joints

#### 1.6.1.2 Finger ligaments and tendons

The fingers of the human hand possess several biological features that are hard to mimic simultaneously. The bones have unique shapes at the knuckles, which determine the degrees of freedom at those joints. The joint capsules are made up of fine ligaments, which control the range of motion for the joints. Cartilage and synovial fluid is found in the joints, enabling low-friction contact between the two articulated surfaces (Zhe Xu et al., 2012).

### 1.6.2 Upper extremity skeletal anatomy

The human body is a dynamic organic system. The arm consists of three bones; the humerus, ulna and radius. Figure 1-12 (Science Kids, 2013), shows the skeletal structure of the upper extremity limbs. The humerus is the longest and largest bone in the upper extremity; it is connected to the scapular through the humeral head forming the shoulder joint.



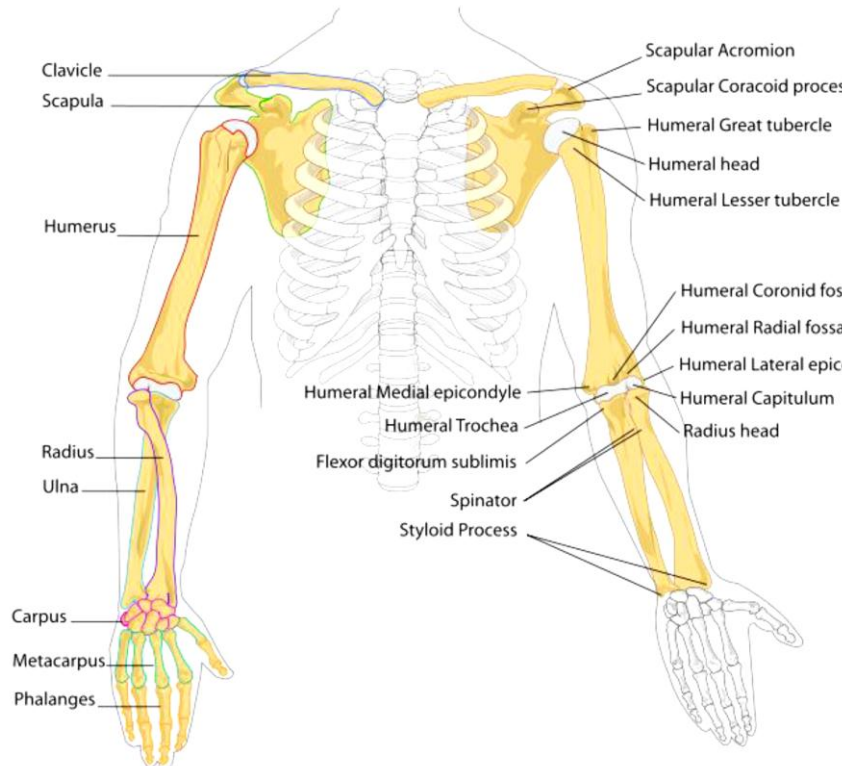


Figure 1-12: Bones of the human arm

The elbow joins the humerus and the forearm bones (ulna and radius). The average human elbow flexion/extension range of motion is shown in Figure 1-13 (Docstoc, 2013). In some cases hyperextension is possible where the elbow can extend passed the neutral.

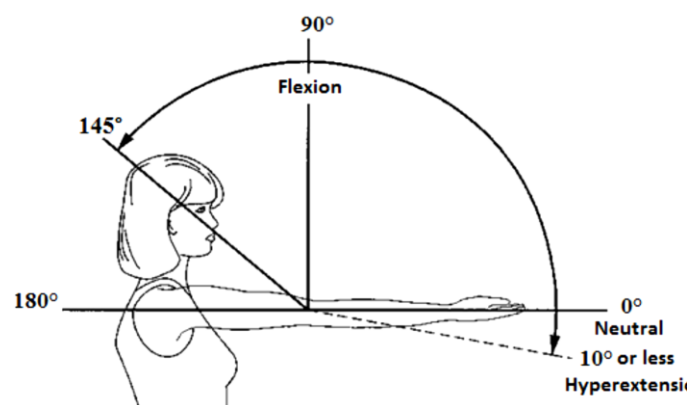


Figure 1-13: Elbow flexion/extension

The elbow also allows for the ulna and radius to twist about each other causing a rotation of the forearm and wrist. These movements are termed supination and pronation, as shown in Figure 1-14 (Docstoc, 2013).

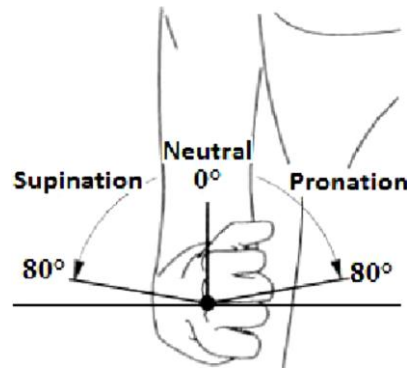


Figure 1-14:-Forearm supination/pronation

Another important part of the forearm is at the distal end where the wrist is situated. The wrist connects the hand to the forearm. The wrist is formed of eight bones together called the carpus which is the wrist biological term. Its can flexion/extension and abduction/adduction to a limited range of about 80°/70° and 20°/30° respectively as shown in Figure 1-15 and Figure 1-16 (Docstoc, 2013). Flexion/extension of the wrist being the ability of the hand to bend downward and upwards in reference to Figure 1-15 and abduction/adduction being of wrist being the hands ability deviate sideways in reference to Figure 1-16. These movement motions assist humans to perform their day to day basic activities with fewer worries.

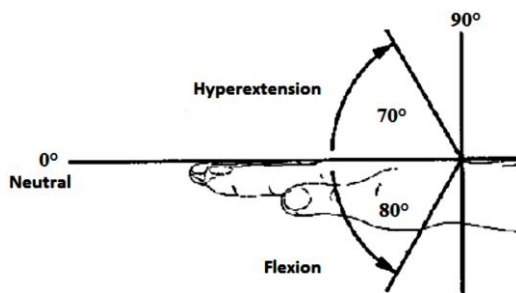


Figure 1-15: Wrist flexion/extension

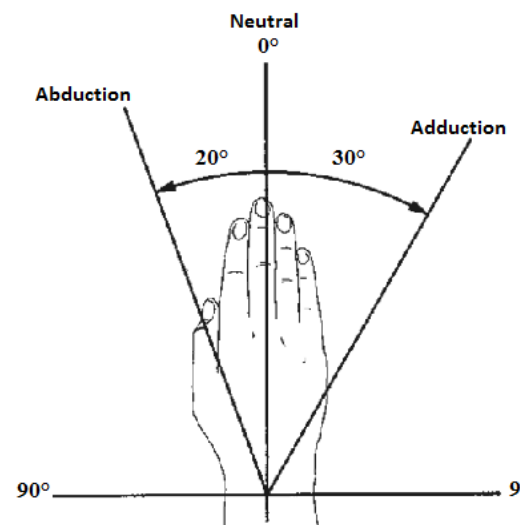


Figure 1-16: Wrist abduction/adduction

### 1.6.3 Upper extremity amputation

Amputation is the removal of a body part when a person has suffered a particular trauma (machine accidents), having disease/infection (diabetes) or when a person has a deformed limb. Upper extremity amputations are divided into four main categories as seen in Figure 1-17 (Otto Bock Healthcare, 2013). These are classified according to the level at which they are performed.

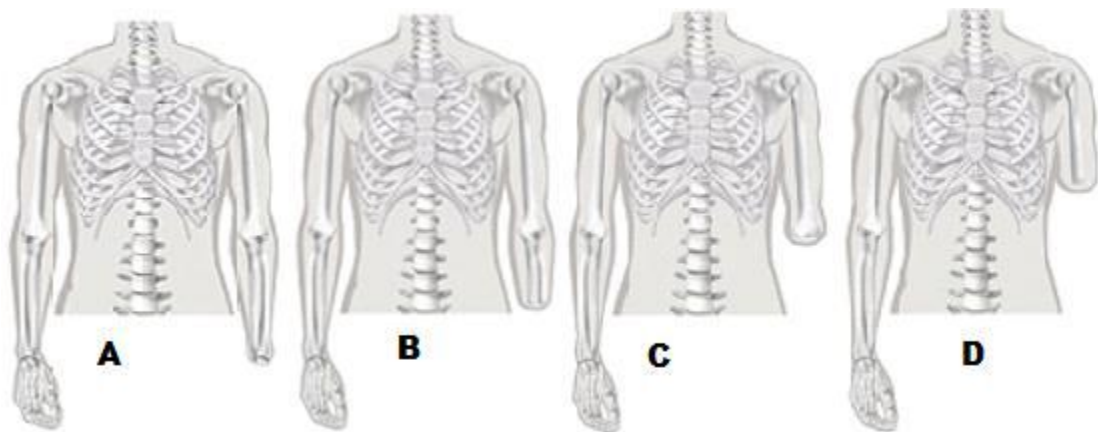


Figure 1-17: Types of amputation (a) wrist disarticulation, (b) transradial, (c) elbow disarticulation (d) transhumeral

#### 1.6.3.1 Wrist disarticulation

Wrist disarticulations include the removal of the radius and ulna. That is the amputee loses the wrist movements, Figure 1-17(a) shows the shape of a residual stump which is bulging thus permitting prosthetic suspension. As the forearm is unaffected by the amputation pronation and supination of the wrist is still possible.

Several innovations in prosthetic socket design have emerged for application at the transradial and wrist disarticulation amputation levels. The introduction of flexible socket materials in contact with the residuum and secured within a rigid framework significantly increases the potential for improved outcomes.

#### 1.6.3.2 Transradial

Transradial prosthetic devices are created for patients who have been amputated through their forearm as shown in Figure 1-17(b). Depending on the percentage of the forearm removed, the residual can still pose rotation motion. These prostheses can be operated by a simple harness system (also termed “body-power”) or electronic parts (Myoelectric). The harness is fitted to allow the user control of the prosthetic hand through other motions like moving the elbow forward.

#### 1.6.3.3 Elbow disarticulation

This is when the whole of the forearm is removed at the elbow; the amputee loses elbow motion including forearm rotation as seen in Figure 1-17(c). Amputation at this level is performed for a variety of reasons. The primary rationale being that this can be a less disruptive procedure since the surgery is through a joint and therefore creates less disruption of the bone and tissue. Due to the length of the elbow-dis-articulation residual, the elbow-locking mechanism is normally fitted on the outside part of the socket. Other than that, the prosthesis and harnessing methods are identical to those applied to the above-elbow case.

#### **1.6.3.4 Transhumeral**

Figure 1-17(d) shows amputation above elbow which is termed transhumeral amputation. Residual limbs are usually embedded to encompass the shoulder joint. Long upper arm residual limbs require a socket that encompasses the residual limb in order to achieve success with the right technique and while leaving the joint (elbow) exposed. The use of silicone liners, custom-made in some cases, offer new possibilities; encompassing the shoulder can also be omitted for upper arm residual limbs of medium length. The use of straps, harnesses or belts to secure the prostheses is a must since there is not much room in the upper arm to do this.

#### **1.6.4 Muscles in the human arm**

The purpose of muscles is to convert energy into motion and thus propel the body. Muscles are long lasting, self-healing and are able to grow stronger. They have a range of functions to perform from allowing speech to keeping blood flowing. Skeletal muscle is the most easily visible muscle type. They are attached to the skeleton in pairs. Such that one muscle can move the bone in one direction and the other to move it back the other way. They contract voluntarily. Body muscles are arranged in such a way that they work either together or in opposition to achieve movement. (Arnould-taylor, 1998)

Muscles can only pull but they can never push. As a muscle shortens its insertion moves towards its origin. Therefore whatever one group of muscles does another group undoes. Muscles are a band of fibrous tissue that can contract in order to produce movement in or maintaining the position of a body part. The muscles in the arm are skeletal muscles under the control of the somatic nervous system where contraction is stimulated by electrical impulses transmitted by the nerves through motor neurons. Tendons, which are bundles of collagen fibres, link the skeletal muscles to the bones. This movement is produced by flexion, extension, abduction, supination, pronation and circumduction (Arnould-taylor, 1998).

##### **1.6.4.1 Biceps Brachii**

This muscles consists of two bundles of muscle, they have different origins but share the same insertion point. The main function of biceps is to supinate the forearm and to flex the elbow. The bicep is an important flexor of the elbow joint, and power supinator of the forearm. The maximum power of both flexion and supination is achieved at (Arnould-taylor, 1998). This muscle can be seen in Figure 1-18(a) (Anatomy Universe, 2013)

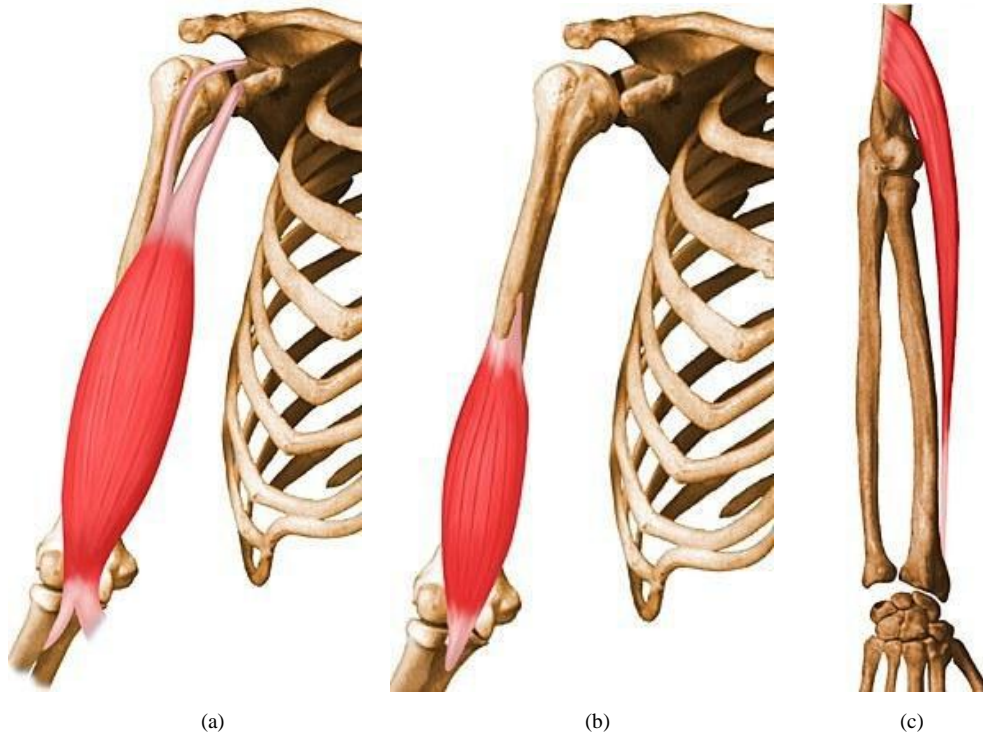


Figure 1-18: The biceps brachii (a), the brachialis (b) and the brachioradialis (c)

#### 1.6.4.2 Brachialis

The brachialis, seen in Figure 1-18(b) (Anatomy Universe, 2013) lies under the cover of the biceps brachii in the lower half of the anterior aspect of the arm. The brachialis is the main flexor of the elbow joint it is also important in controlling extension produced by gravity, the flexors of the elbow control the movement by an eccentric contraction. This muscle lies just deeper than the biceps brachii, and is a synergist that assists the biceps in flexing the elbow. It is the strongest flexor of the elbow.

#### 1.6.4.3 Brachioradialis

This is a superficial muscle found on the lateral side of the forearm extending almost as far as the wrist as seen in Figure 1-18(c) (Anatomy Universe, 2013). The fibres of this muscle run more or less parallel to the radius and it is used primarily to maintain the integrity of the elbow (Arnould-taylor, 1998).

#### 1.6.4.4 Triceps brachii

This muscle is situated on the back of the arm on arises from three heads, two of which arise from the humerus and are separated by the spiral groove whilst the third arises from the scapula. The three heads are the long lateral and medial heads. This muscle attaches via a tendon to the ulna. The triceps brachii is the extensor of the elbow joint the long head can also abduct the arm and extend it from a flexed position. When the elbow is flexed, gravity often provides the necessary force for extension, with the elbow flexors working eccentrically to control the movement (Anatomy Universe, 2013).

#### 1.6.4.5 Anconeus

This is a small triangular muscle situated immediately behind the elbow joint it appears to be almost part of the triceps brachii. This muscle assists in the extension of the elbow joint. Because it is attached to the ulna, it is thought that it produces abduction of the ulna and the extension of the bone at its distal end. These movements occur during pronation and are essential in actions such as using a screw driver (Arnould-taylor, 1998).

#### 1.6.4.6 Muscles in the forearm

The muscles of the forearm act on the elbow and wrist joints and on those of the phalanges. These muscles can be divided into flexor-pronator and extensor-supinator groups (Arnould-taylor, 1998). Figure 1-19 and Figure 1-20 (Anatomy Universe, 2013) show all the muscles in the forearm.

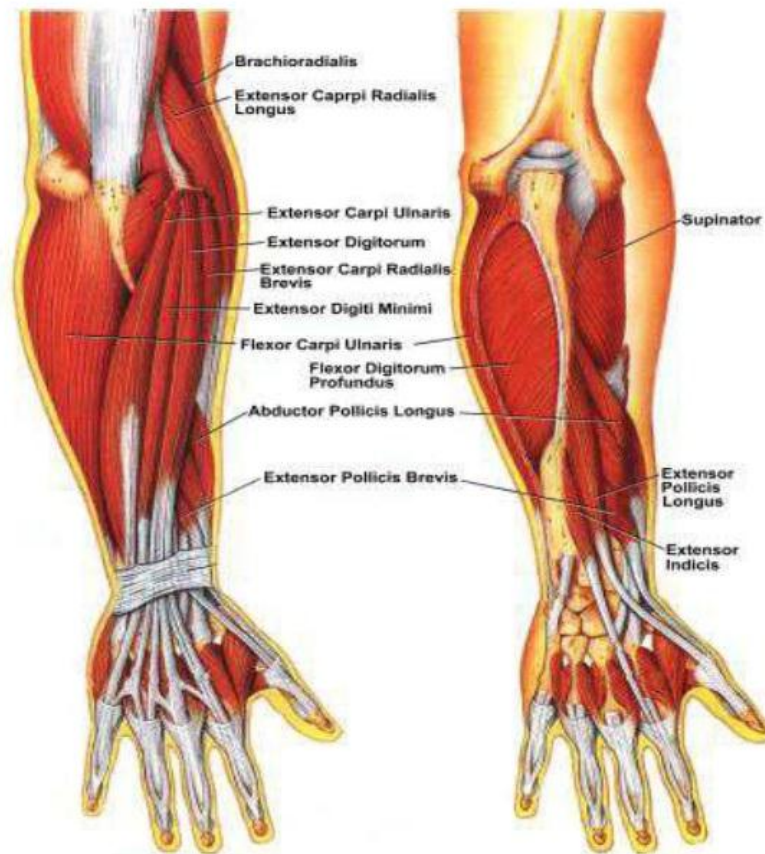


Figure 1-19: Anterior of the forearm



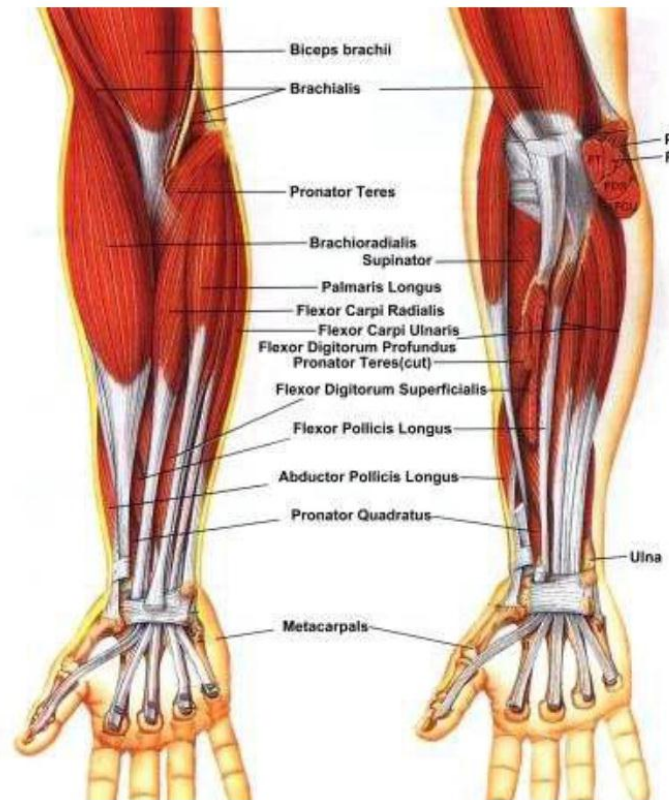


Figure 1-20: Posterior of the forearm

The muscles to consider here which are of great importance are the supinator and pronator muscles since they cause the primary rotation of the forearm.

### 1.7 Research objectives and specifications

The research conducted under this dissertation aims to develop a prosthetic hand with objectives in several categories. The hand must meet certain mechanical, electrical, control and general objectives. The objectives of the prosthetic hand are:

- grip with a force of 15 N using a power/cylindrical grip type and to grip with a force of 3 N using a lateral/key grip (only using the thumb)
- hold 4 kg in a static (motors off) hook grip
- fully close the hand in 3 seconds
- a multi-dexterous design, with individual actuation of each finger
- sense the grip force of the hand
- measure the temperature of objects being touched
- a novel sensory feedback system to communicate all sensory information simultaneously to the user
- be controllable using only two EMG channels

- introduce a novel method of control, allowing for more than 14 grip-type and hand gesture options
- a modular design allowing for use with a transradial or transhumeral amputee
- a low-cost design with the total material cost under US\$ 3'000

## 1.8 Contributions

This dissertation will explore three new areas of research within the field of myoelectric upper extremity prosthetics.

- a) An alternative control method for EMG based prostheses will be developed. The new approach will investigate whether the number of controllable grip types can be increased above 14. Also the ability for a control method to allow for free form motion of the fingers and wrist to allow for hand gestures will be investigated.
- b) A novel haptic feedback display will be developed to allow for various types of sensory information to be communicated to the user simultaneously. This will be tested to verify the ability of the user to receive multi-sensory information simultaneously.
- c) An inexpensive modular prosthetic arm will be designed to allow for different upper extremity amputation types and at a fraction of the cost of contemporary prosthetic arms. The prosthetic hand will be built for as inexpensive as possible while still meeting the objectives stated in this section, with a goal of keeping the material cost of the prosthetic hand under US\$ 3'000.

## 1.9 Publications

The following publications were produced as part of the research attributed to this dissertation:

- van der Riet, D., Stopforth, R., Bright, G. and Diegel, O., "An overview and comparison of upper limb prosthetics," IEEE AFRICON Conference, Mauritius, September 2013.
- van der Riet, D., Stopforth, R., Bright, G. and Diegel, O., "Simultaneous vibrotactile feedback for multi-sensory upper limb prosthetics," 6<sup>th</sup> IEEE Robotics and Mechatronics Conference of South Africa, Durban, October 2013.



- van der Riet, D., Stopforth, R., Bright, G. and Diegel, O., “The low cost design of a 3D printed multi-fingered myoelectric prosthetic hand,” *Mechatronics: Principles, Technologies and Applications*, Nova Science Publishers Inc., submitted.
- van der Riet, D. and Stopforth, R., “A low cost, extendable prosthetic leg for trans-femoral amputees,” *Mechatronics: Principles, Technologies and Applications*, Nova Science Publishers Inc., submitted.

### 1.10 Chapter summary

Upper extremity prosthetics has improved greatly over the last 10 years. This chapter has reviewed the state of contemporary prostheses as well as the progress made to get there. Current work on haptic feedback systems for use with prosthetic hands was investigated and it was found that there are few systems available for use in prostheses. Work still needs to be done to improve the quality of haptic displays. Current commercial prostheses could benefit from the incorporation of haptic feedback into their grip strength control allowing the user to regulate the applicable grip accurately.

Myoelectric control has had the most success in controlling upper extremity prosthetics and is commonly found in commercial prosthetics. There are currently a variety of different EMG control techniques but all with many limitations. These limitations are in the number of hand positions the prosthesis is able to make. Improvement in the field of myoelectric control is the most direct way to improve current upper extremity prostheses. During comparisons it was found that the i-limb Ultra and the BeBionic3 were tied as far as performance as the best currently available prosthesis. But both systems could benefit immediately with the incorporation of haptic feedback displays.

Replicating the design of the human hand and arm are extremely challenging engineering tasks. The design of a fully functional robotic hand needs to be more complex than its human original. The human hand takes power from the heart, control from the brain and the muscles actuating the hand are in the forearm. A prosthetic arm needs to have internally its own power supply, control system and actuators, while still weighing the same and providing the same dexterity and grip strength as a human hand.

All test subjects that participated in the research done in this dissertation did so voluntarily. The volunteers were informed that they may refuse to participate or withdraw from participation at any time with no negative consequences. There was no monetary gain for volunteers. All volunteers' identities have been kept confidential and anonymous.

## **2. MECHANICAL DESIGN**

---

The mechanical design process will be discussed in detail in this chapter. The manufacturing process and the final prosthetic hand and arm prototype will be shown and its strengths and weaknesses will be discussed. The mechanical design objectives for the prosthesis were low-cost, modularity for both transradial and transhumeral use and simplicity in design, manufacturing and use. The success of these design objectives will be outlined in the course of this chapter.

### **2.1 Considered designs**

Before manufacturing can commence, a design needs to be drawn up and selected. In order to arrive at the best design, several different concepts were considered. In this section these concept designs will be highlighted and analysed according to their respective strengths and weaknesses in reference to the overall mechanical design objectives of low-cost, modularity and simplicity. The concept designs were broken into three categories: finger, wrist/forearm and upper limb.

#### **2.1.1 Finger designs**

There are two main approaches to finger designs in prosthetics, linkage and cable driven systems. Both of these approaches have advantages as a linkage system has a better force transfer efficiency and a cable system has a better adaptability. A concept sketch of the first linkage system is shown in Figure 2-1. This system sees the finger open and close in response to a single actuator, two which it would be directly coupled. This would mean that all forces on the fingers would be transmitted directly on the actuator.



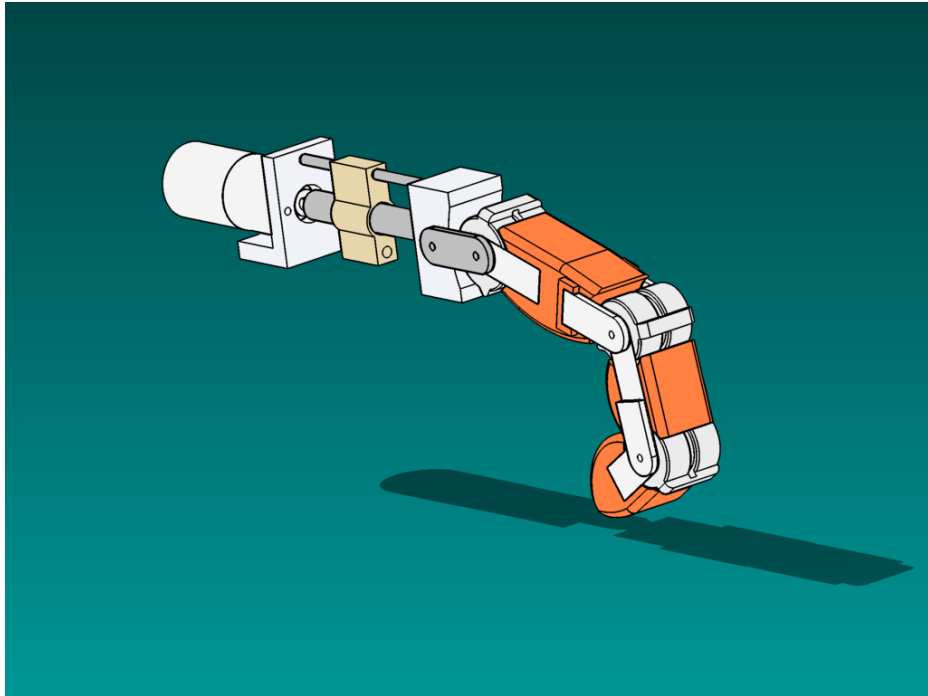


Figure 2-2: Finger concept B – lead screw design, cable system

A worm gear coupled with a pulley, shown in Figure 2-3, is considered as an alternative design to that of the lead screw actuated cable system. The worm gear concept also retains the self-locking feature of the lead screw. Another advantage of the worm gear over the lead screw is that it doesn't require the physical space of the linear displacement of the cable as the cable is wound onto the pulley. The worm gear is thus seen as a superior design to the lead screw with the cable system.

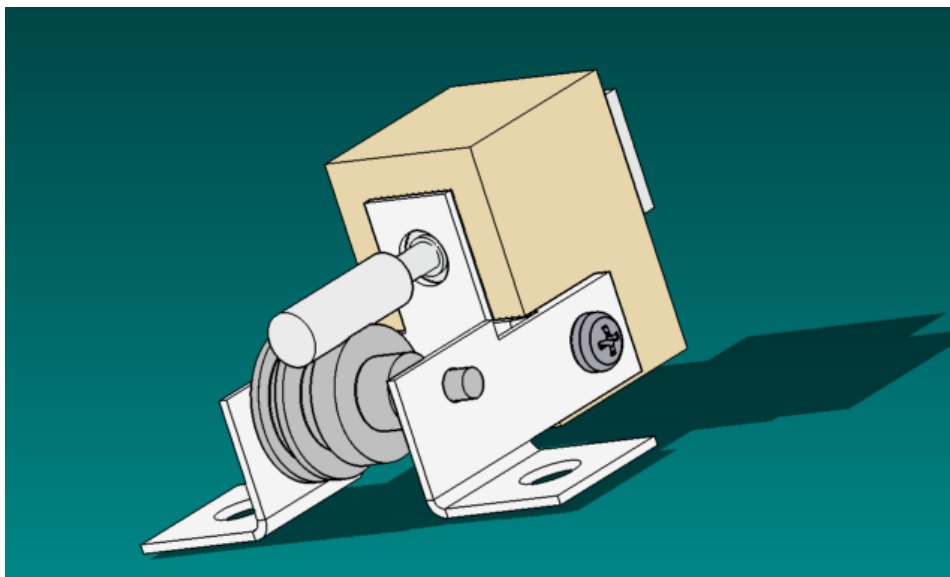


Figure 2-3: Finger concept C – worm gear design, cable system

Out of the three concepts shown, the worm gear design, cable system concept is selected as the final design. The cable system is seen as being more beneficial as it provides adaptable grasping and also provides a more energy efficient design. The fingers will also be more life-like as they will be “soft” or movable when the hand is open and will close completely around objects. The linkage system would lock up once one section of the finger had tightened on the object, preventing the rest of the finger to close.

### 2.1.2 Wrist and forearm design

The wrist and forearm design brings the first aspect of the modular design into the design of the prosthesis. The prosthesis needs to be able to work with both transradial and transhumeral amputees. In order for this objective to be met, the hand and wrist needs to be able to connect directly to the socket of a transradial amputee as well as to the prosthetic arm used by a transhumeral amputee. The human wrist has 3 DOFs, rotation, flexion/extension and abduction/adduction. However, including all 3 DOFs would increase the cost and weight of the prosthetic hand, therefore a tradeoff decision was made to only use a single DOF (rotation) as this is the most critical DOF in the wrist. The first concept takes inspiration of the natural biology of the human arm with the twin-bone design. A motor placed in the wrist rotates the centre bone and the off-center bone rotates around it. The concept design is shown in Figure 2-4.

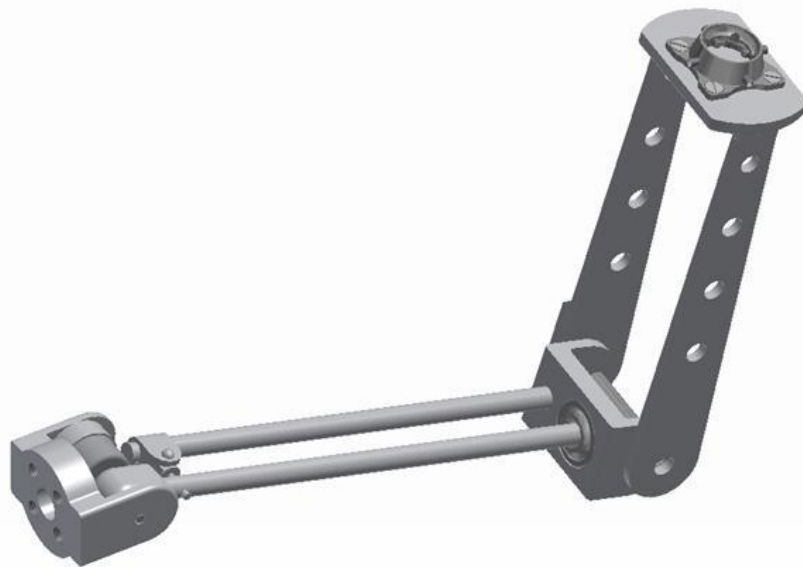


Figure 2-4: Wrist concept A – twin-bone system

Not all people are the same size. Therefore it is ideal if the prosthetic arm's length could be adjustable to suit the length of each amputee easily, without manufacturing different sizes. To solve this problem, a telescopic concept design was proposed, shown in Figure 2-5. The telescopic system replaces the twin-bone system with a telescopic arm that can be easily

adjusted according to the required length. The wrist motor is situated in the housing and attaches easily to the forearm with the same adapter as used to connect to the transradial socket.

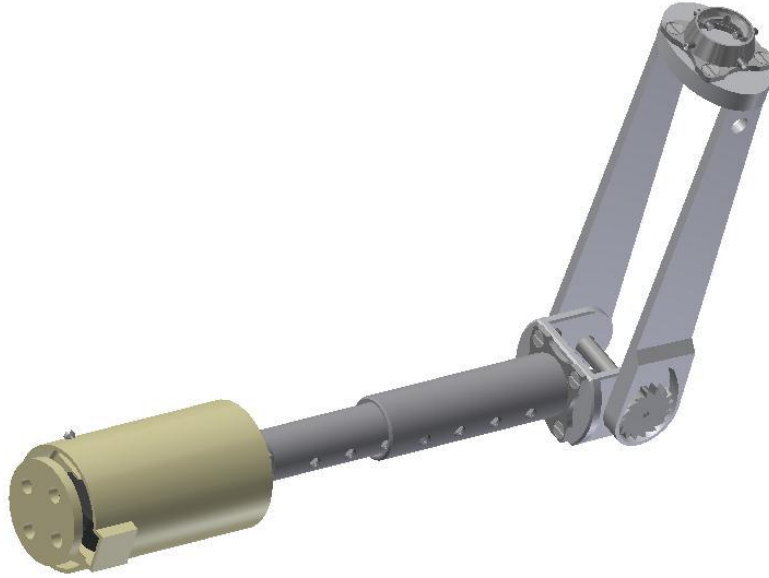


Figure 2-5: Wrist concept B – telescopic system

Out of the two concepts discussed in this section, the telescopic design was selected as the final design. The telescopic design is significantly simpler than the twin-bone concept and includes an easily modular solution to connecting the wrist to both transradial and transhumeral amputees. The adjustable arm length is another feature that is beneficial in the prosthetic arm.

### 2.1.3 Upper limb actuation design

The upper limb actuation is needed to rotate the elbow joint of the transhumeral prosthesis. The first concept design uses an artificial muscle made up of an array of shape memory alloys (SMAs) coupled with a spring and pulley system. The artificial muscle acts as the bicep and the spring acts as the triceps as shown in Figure 2-6. This bio-inspired design mimics the human arm closely.

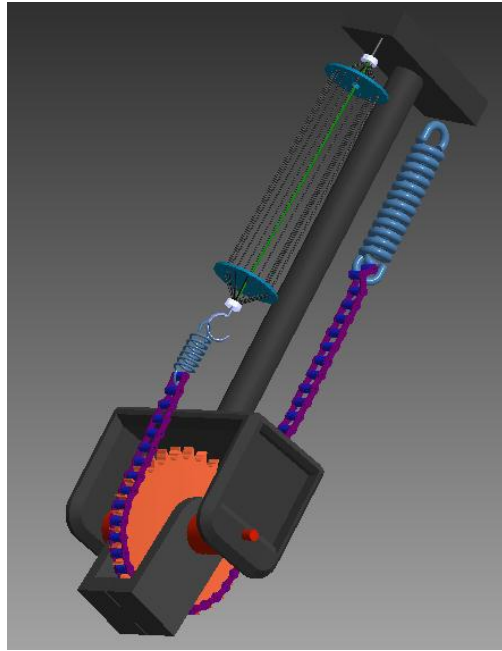


Figure 2-6: Upper limb actuation concept A – artificial muscle system

The second concept, shown in Figure 2-7, uses two motorised pulleys to generate both elbow flexion/extension and forearm rotation, as an alternative to wrist rotation. The motorised pulleys provide quick, high torque actuation to the elbow and forearm. This concept has a higher force transfer efficiency than the artificial muscle concept which loses force in overcoming the spring.

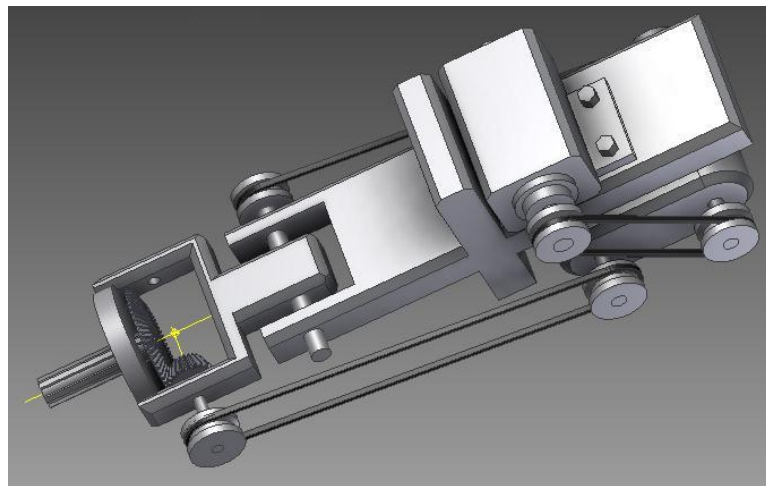


Figure 2-7: Upper limb actuation concept B – motor and pulley system

The SMAs are not ideal as a prosthetic actuator as they operate at around 500 °C. Although they have a good response time to heating, they have a long cool-down time and would not be capable of quick movements. An alternative to SMAs are air muscles. These work much like the proposed SMA artificial muscle system but with a quick response time. A pair of

air muscles can replace the muscle-spring system in the first concept. The proposed dual air muscle concept system is selected as the final design. The motorised pulley system is much simpler than the air muscle system. However, the air muscles are selected as an investigation of air muscles as a possible actuator for prosthetics.

## 2.2 Final design

The final mechanical design of the prosthetic arm was decided on based on the concepts discussed in the previous section. The hand contains six motor and worm gear pairs for the fingers (1 DOF each) and thumb (2 DOFs). The wrist (1 DOF) houses the servo motor for wrist rotation and has a connection that can be attached to the socket of transradial amputees. The telescopic forearm is adjustable to allow for different arm lengths. The elbow (1 DOF) is actuated by the air muscles located around the transhumeral socket connection and coupled with a pulley rigidly connected to the elbow joint. Close ups of the three systems are shown in Figure 2-8, Figure 2-9 and Figure 2-10.

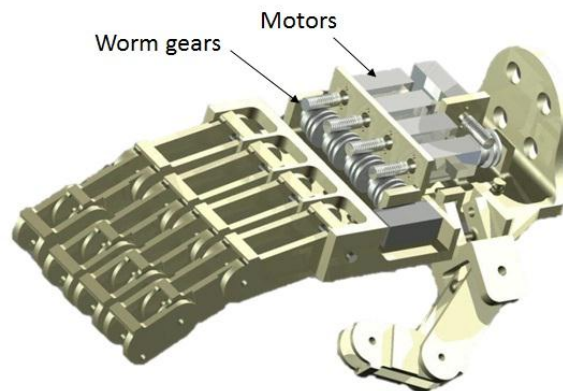


Figure 2-8: Final design of the hand

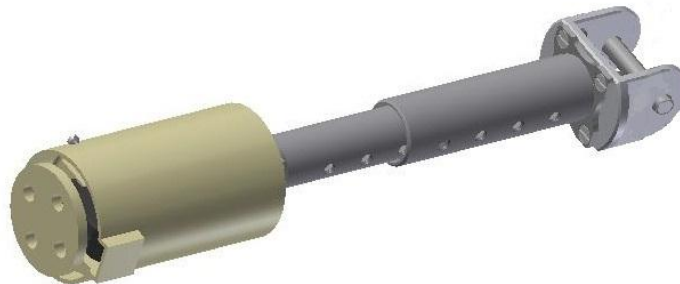


Figure 2-9: Final design of the wrist and forearm



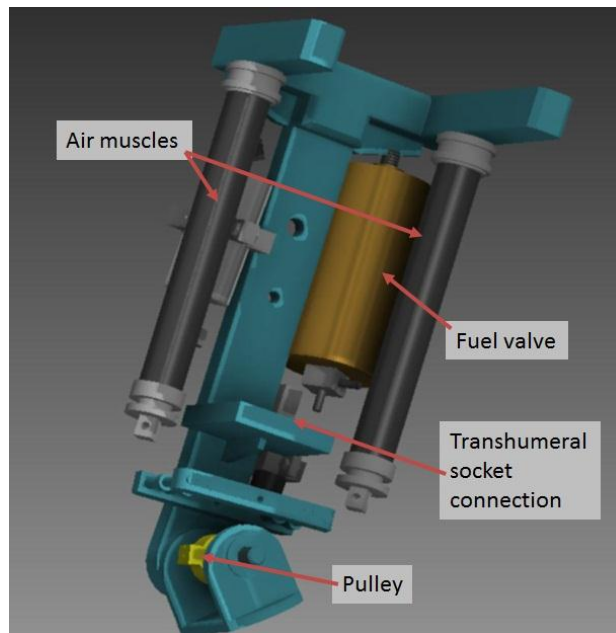


Figure 2-10: Final design of the upper limb actuation

The mechanical design will contribute an inexpensive modular upper extremity prosthetic arm. The hand and wrist are 3-Dimensionally (3D) printed with acrylonitrile butadiene styrene (ABS) plastic allowing a quick and inexpensive manufacturing process. Only the elbow and transhumeral socket connection were machined from aluminum. The full transhumeral arm design is shown in Figure 2-11.

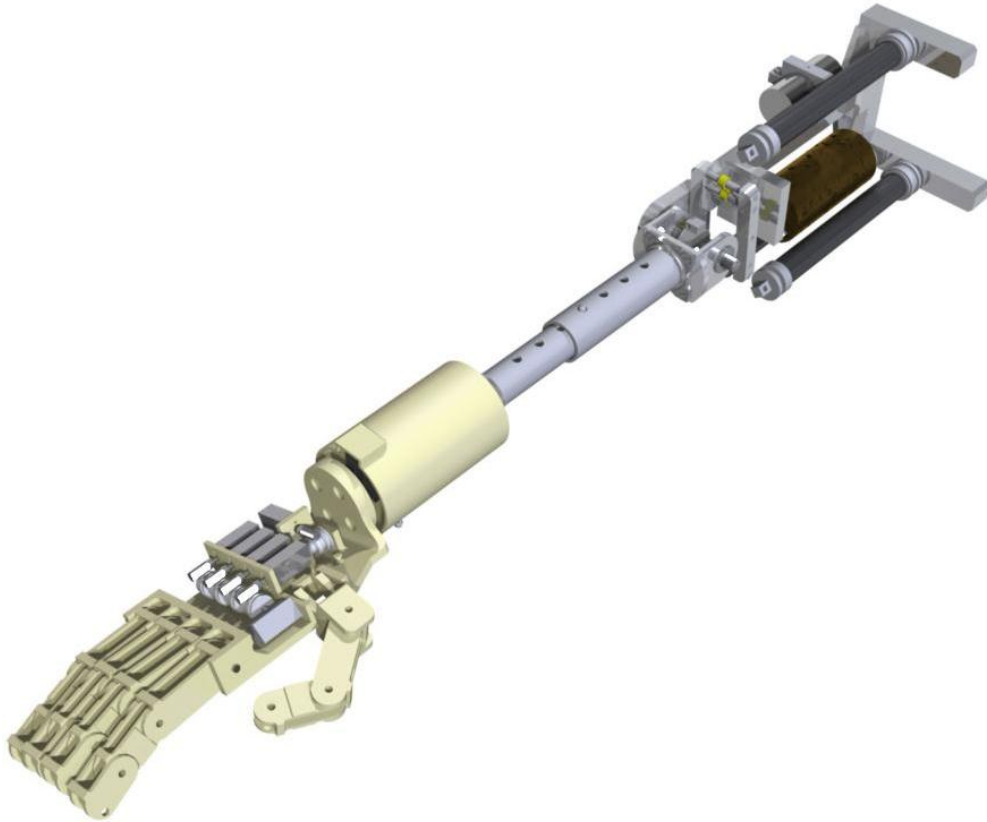


Figure 2-11: Complete prosthetic arm final design

### 2.2.1 Stress analysis

Finite Element Analysis (FEA) was used to perform stress analysis on the prosthetic hand and arm to test the design for possible weak spots. The deflection analysis was not performed as small deflections in the hand and arm will not affect the performance of the prosthesis in any way. The simulation was run assuming the hand was using a power/column grip to lift a 3 kg weight. As can be seen in Figure 2-12, the hand experiences a maximum stress of 35.98 MPa at the hinge connection with the wrist. This stress is within the yield stress of ABS plastic which is 42.5 MPa.

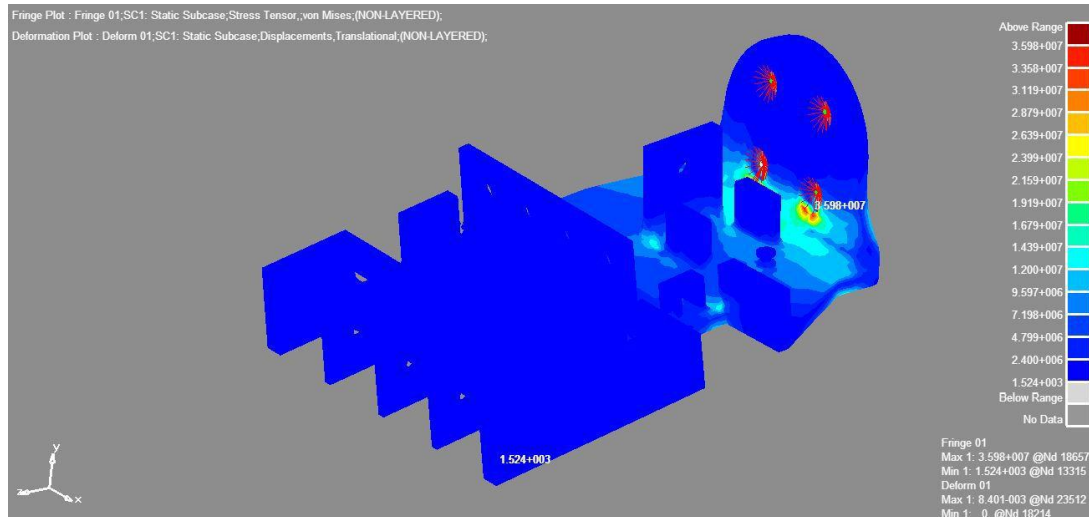


Figure 2-12: Stress analysis of hand

The forearm was tested with a load force of 30 N on the wrist adapter end. The forearm is held in place at the elbow by the two opposing air muscles which are each capable of lifting 110 N. The results of this stress analysis test, shown in Figure 2-13, revealed a maximum yield stress of 69.2 MPa which is safely under the 200 MPa yield strength of aluminium.

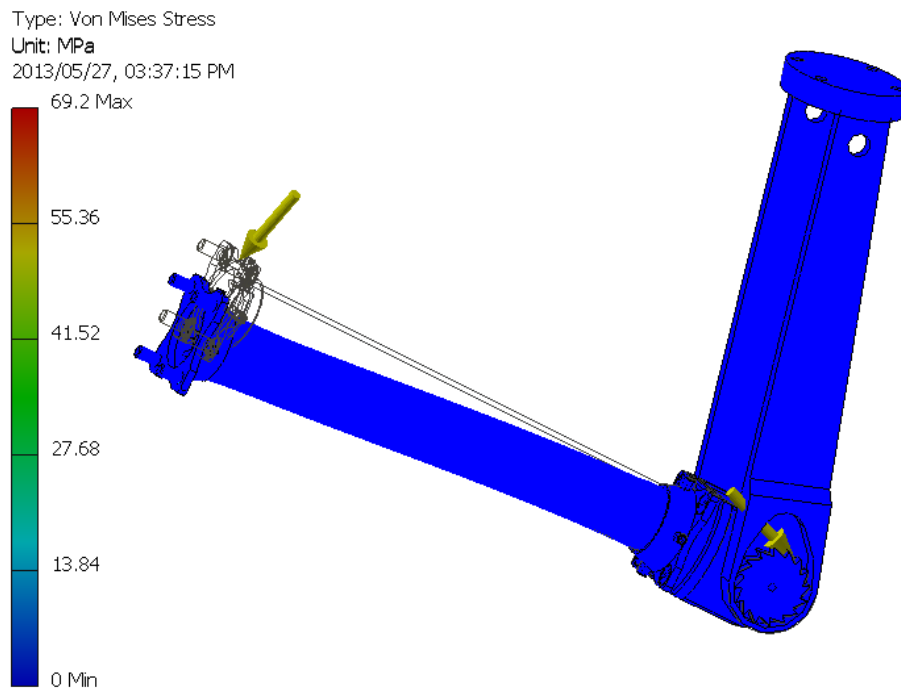


Figure 2-13: Stress analysis of forearm

## 2.3 Kinematic models

The range of motion of the prosthetic arm can be described through kinematics. This section covers the kinematic equations used to plot the range of motion graphs. The Denavit–

Hartenberg (D-H) convention is used to generate the kinematic equations. The base equation is shown in Equation 2-1, describing motion from joint 0 to joint 1.

$$A_{01} = \begin{bmatrix} c_\theta & -s_\theta c_\alpha & s_\theta s_\alpha & ac_\theta \\ s_\theta & c_\theta c_\alpha & -c_\theta s_\alpha & as_\theta \\ 0 & s_\alpha & c_\alpha & d \\ 0 & 0 & 0 & 1 \end{bmatrix} \quad (2-1)$$

The arm can be divided into two parts in order to analyse its range of motion as shown in Figure 2-14. The hand is the effective end effector of the prosthetic arm. However, beyond merely gripping objects, the prosthetic hand is designed to mimic the natural motion of the human hand. The hand has been given six DOFs (four fingers and two DOFs in the thumb). Each digit on the hand can be treated as a robotic arm in order to apply kinematic modelling to predict the fingers' range of motion. The prosthetic arm is considered as a standard robotic arm with two DOFs, with the hand as a standard end effector to predict the full range of motion of the prosthetic arm.

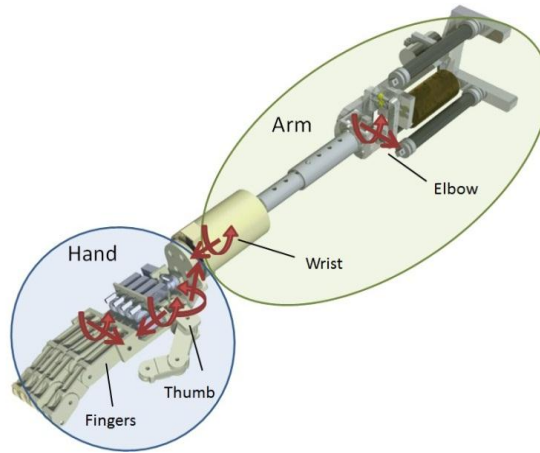


Figure 2-14: Overview of the final design prosthetic arm system

### 2.3.1 Hand

Each finger is identical in the hand, and so only one equation is necessary to describe all of them. All three joints in the finger are in the same frame of reference and are all actuated by the same motor. The thumb is slightly different as it has two motors actuating it. The first controls the rotation of the thumb between the opposed and non-opposed positions. The second closes the thumbs two additional joints in the same way as the fingers. The hand is simplified to joints and links as seen in Figure 2-15.

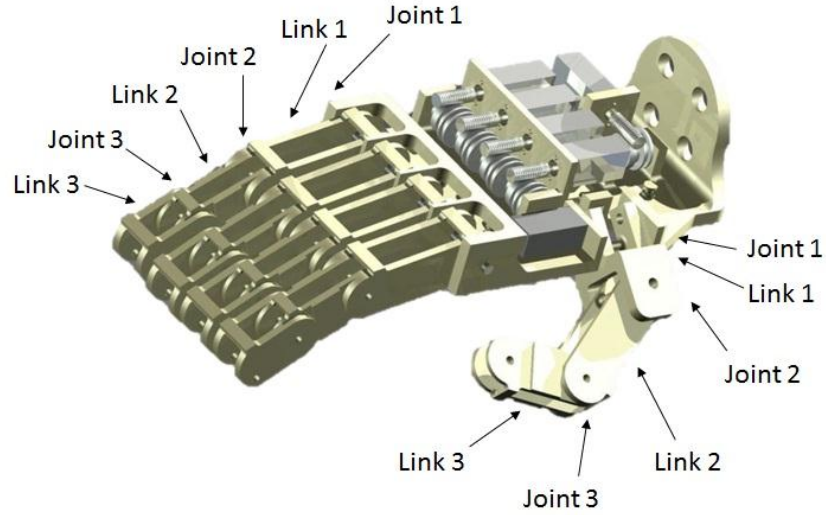


Figure 2-15: Joint and link diagram of the hand

The kinematic models derived from the hand for the finger are shown in Equation 2-2, Equation 2-3 and Equation 2-4. Using these D-H equations, a plot of the range of motion of the finger is given in Figure 2-16 which includes the 120 mm long hand.

$$A_{01} = \begin{bmatrix} c_1 & -s_1 & 0 & a_1 c_1 \\ s_1 & c_1 & 0 & a_1 s_1 \\ 0 & 0 & 1 & 0 \\ 0 & 0 & 0 & 1 \end{bmatrix} \quad (2-2)$$

$$A_{12} = \begin{bmatrix} c_2 & -s_2 & 0 & a_2 c_2 \\ s_2 & c_2 & 0 & a_2 s_2 \\ 0 & 0 & 1 & 0 \\ 0 & 0 & 0 & 1 \end{bmatrix} \quad (2-3)$$

$$A_{23} = \begin{bmatrix} c_3 & -s_3 & 0 & a_3 c_3 \\ s_3 & c_3 & 0 & a_3 s_3 \\ 0 & 0 & 1 & 0 \\ 0 & 0 & 0 & 1 \end{bmatrix} \quad (2-4)$$

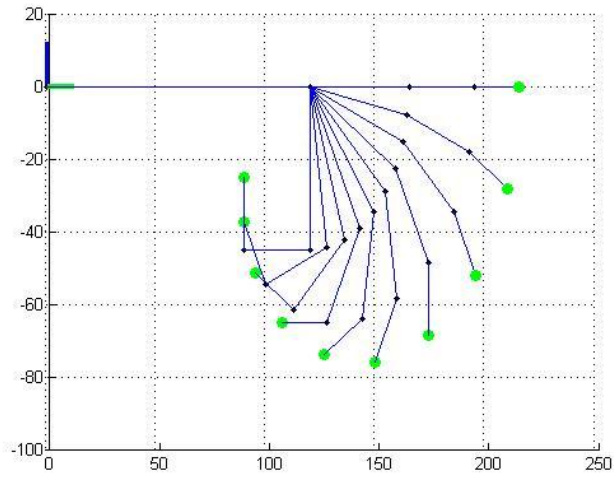


Figure 2-16: Kinematic model of the finger (units in mm)

The kinematic models derived from the hand for the thumb are shown in Equation 2-5, Equation 2-6 and Equation 2-7. Using these D-H equations, a plot of the range of motion of the thumb is given in Figure 2-17. In Figure 2-18, all the fingers and thumb are then combined for a full plot of the hand.

$$A_{01} = \begin{bmatrix} c_1 & 0 & -s_1 & a_1 c_1 \\ s_1 & 0 & c_1 & a_1 s_1 \\ 0 & -1 & 0 & 0 \\ 0 & 0 & 0 & 1 \end{bmatrix} \quad (2-5)$$

$$A_{12} = \begin{bmatrix} c_2 & -s_2 & 0 & a_2 c_2 \\ s_2 & c_2 & 0 & a_2 s_2 \\ 0 & 0 & 1 & 0 \\ 0 & 0 & 0 & 1 \end{bmatrix} \quad (2-6)$$

$$A_{23} = \begin{bmatrix} c_3 & -s_3 & 0 & a_3 c_3 \\ s_3 & c_3 & 0 & a_3 s_3 \\ 0 & 0 & 1 & 0 \\ 0 & 0 & 0 & 1 \end{bmatrix} \quad (2-7)$$

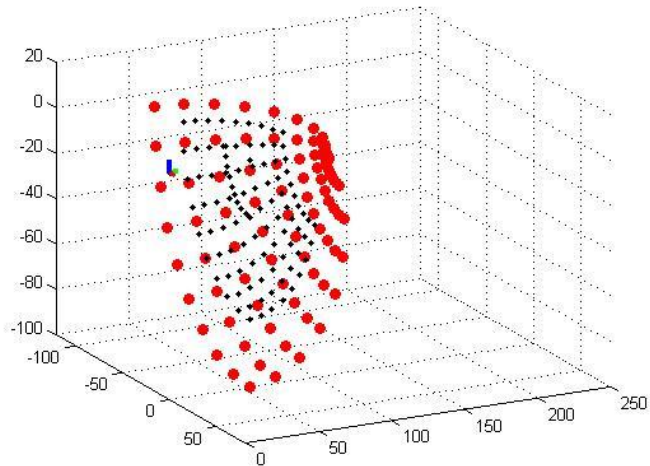


Figure 2-17: Kinematic model of the thumb (units in mm)

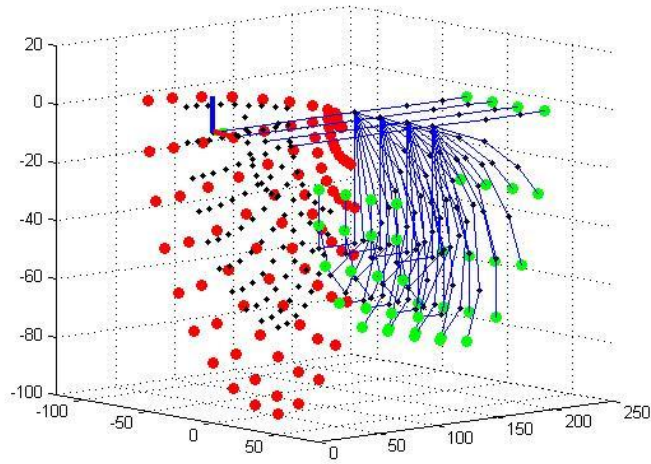


Figure 2-18: Kinematic model of the hand (units in mm)

### 2.3.2 Arm

The full prosthetic arm with the transhumeral socket connection is then considered as the robot arm. The arm uses two air muscles to flex and extend the elbow. A servo motor capable of 180 degrees of rotation is used to rotate the wrist. The prosthetic arm is simplified into joints and links as shown in Figure 2-19.

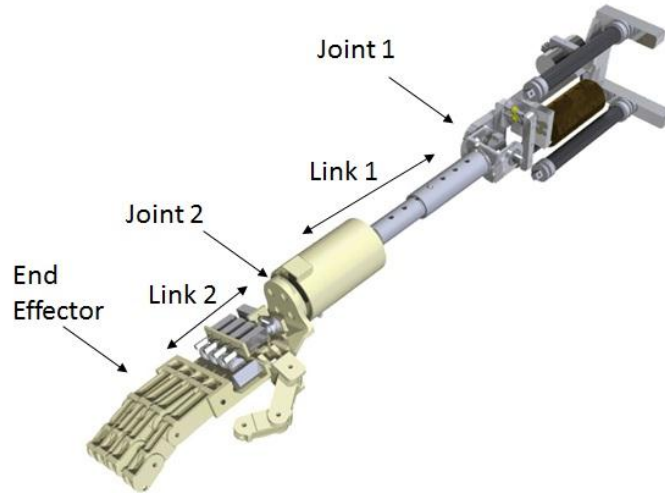


Figure 2-19: Joint and link diagram of the arm

The kinematic models derived from the arm are shown in Equation 2-8 and Equation 2-9. Using these D-H equations, a plot of the range of motion of the arm is given in Figure 2-20. The red dots in Figure 2-20 represent the thumb as it rotates around the index finger (green dot).

$$A_{01} = \begin{bmatrix} c_1 & 0 & -s_1 & a_1 c_1 \\ s_1 & 0 & c_1 & a_1 s_1 \\ 0 & -1 & 0 & 0 \\ 0 & 0 & 0 & 1 \end{bmatrix} \quad (2-8)$$

$$A_{12} = \begin{bmatrix} c_2 & -s_2 & 0 & 0 \\ s_2 & c_2 & 0 & 0 \\ 0 & 0 & 1 & d_2 \\ 0 & 0 & 0 & 1 \end{bmatrix} \quad (2-9)$$

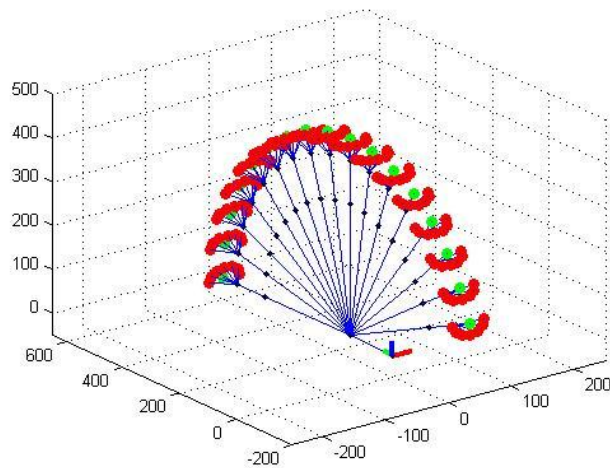


Figure 2-20: Kinematic model of the arm (units in mm)



## 2.4 Hand manufacturing process

Current commercial prosthetic arms involve sophisticated and expensive actuators, electronics and materials. It has been shown that a functional grasping end effector can be achieved using suitable materials, off-the-shelf electronic components and open-source coding architecture. The advent of advanced 3D printing as a manufacturing medium allowed for complex design features whilst accommodating the short time frame in which to manufacture and assemble the complete hand. The design of the hand incorporates only the basic degrees of freedom that enable functional operation and grasping abilities whilst allowing ease of control for the amputee.

A final design concept was chosen after reviewing various concept designs. The conceptual components chosen are compared with their respective manufactured versions. After comparisons are made, the various amendments that either improved performance, functionality or made assembly simpler are stated. Many challenges were encountered during the design and manufacturing processes, this section will explain the solutions posed and illustrate the processes in which these solutions were formulated. Figure 2-21 shows an overview of the overall process from concept to final prototype. Only the right hand prosthetic arm was designed and manufactured. A left-hand prosthesis would simply be the mirror image of the right hand prosthesis.

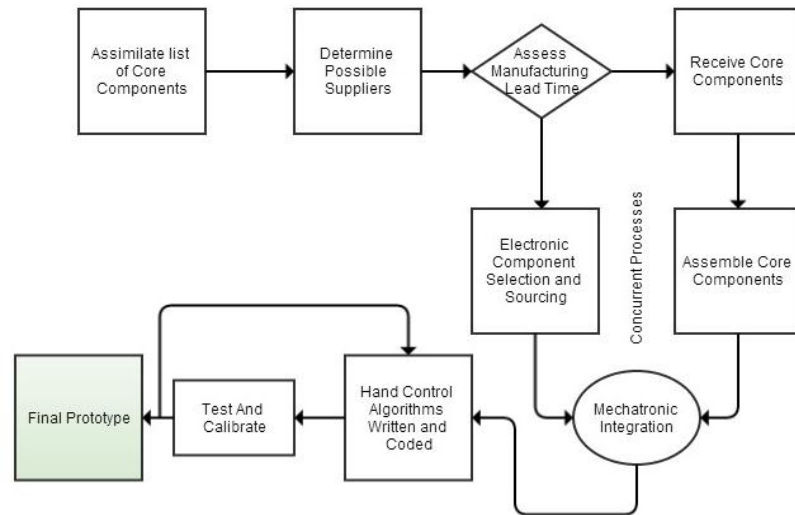


Figure 2-21: Prosthetic hand development process overview

### 2.4.1 The working zone

The hand design had to meet certain core specifications. In implementing the final concept into a working prototype, a ‘work-zone’ needed to be established. This working zone is

the space available in which an anthropomorphic and functional end effector can be implemented. The working zone (illustrated by the red box shown in Figure 2-22) is a function of the level of amputation. As the client is double amputated, it is not clear exactly how long the prosthesis should be, as he has no human arm length to compare it too.



Figure 2-22: Working zone illustrated by red box

The working zone must start at the point of amputation and terminate at the point where a human arm of typical length would end. This gives a good idea of the dimension and size of components needed. A length of 350 mm was agreed upon as the desired length of the prosthesis. This working zone indicated that all actuators and electronic components were to be housed inside the hand itself. This posed many practical challenges ranging from sourcing inexpensive components of the required dimension to assembling the hand itself. The final concept chosen was one that met these specifications within an allowable tolerance at a length of 410 mm, 17% longer than desired. This compromise was acceptable as this design is only a proof-of-concept prototype. Future streamlining of the electrical and mechanical components would result in a smaller hand design.

#### 2.4.2 Manufacture of fingers and thumb

This section presents the construction processes undertaken to take the hand from concept to prototype. It also highlights the challenges in constructing the mechanical components, assembly and how these challenges were overcome. The finger is divided into three segments (phalanges). All of the four fingers are identical which results in simpler manufacturing and assembly. A computer simulated kinematic analysis was carried out to attain dimensions that matched the motion of the human finger as close as possible.

All core structural components were 3D printed at the Massey University. Three dimensional printing allowed for an accelerated manufacturing process without limitations

being imposed on the complexity of the design. The three printed phalanges along with their respective 3D printed versions are shown in Figure 2-23.

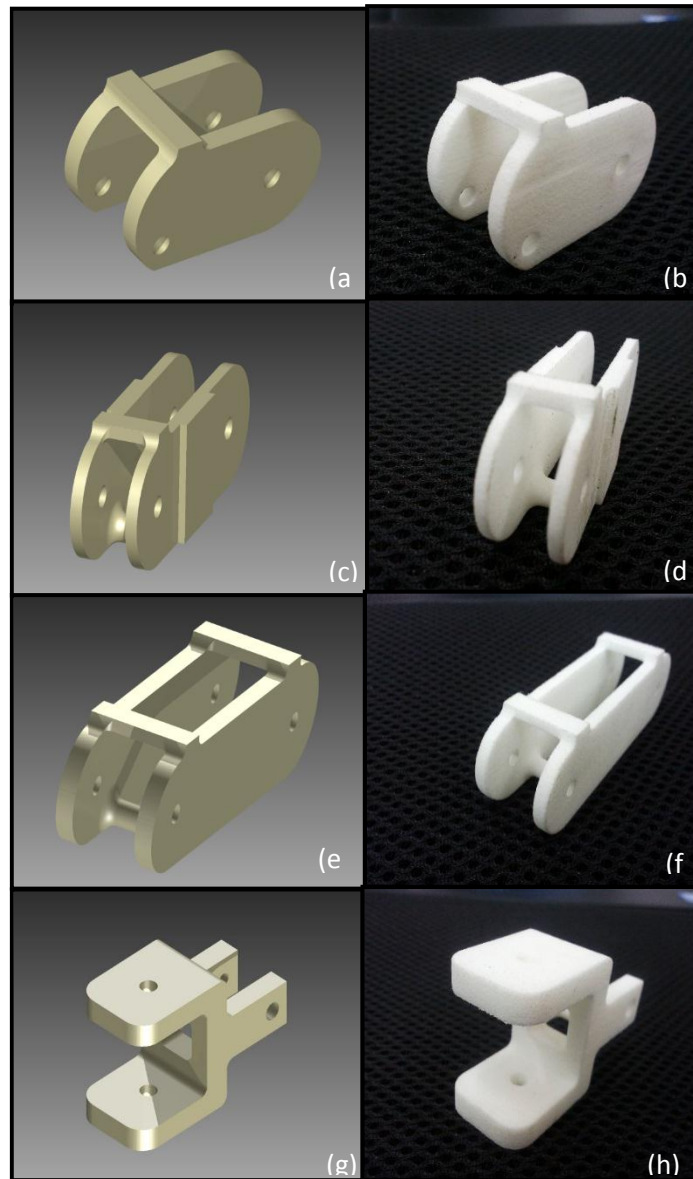


Figure 2-23: (a) CAD render of distal (b) 3D printed distal (c) CAD render of middle (d) 3D printed middle (e) CAD render of proximal (f) 3D printed proximal (g) CAD render of thumb base (h) 3D printed thumb base

It can be seen that the CAD model of each component was accurately realized by the 3D printer. Holes for joint pins were added as features to be printed. The accuracy of the printing process seemed to be a disadvantage when it came to inserting pins into the holes. The stainless steel pins were 3 mm in diameter. The dimensional accuracy of the pins was at a lower degree than that of the printed holes thus causing inconsistencies in the fit. A solution to this was to enlarge the diameter by drilling through the pre-existing holes with a 3.1 mm drill bit. A fine fit

was achieved allowing for minimal friction between the mating surfaces. ABS plastic lends itself to a self-lubricating property thus a further decrease in surface friction was achieved.

Assembly of the fingers began by sliding the ends of the distal and proximal phalanges onto the corresponding ends of the middle phalanx. The middle phalanx acts as the core pivot frame for the entire finger. The stainless steel pins are inserted into each phalanx, creating revolute joints between each segment of the finger. Figure 2-24 shows a complete assembled finger. Each of the four assembled fingers are identical.



Figure 2-24: Assembled finger

The thumb consists of the middle and proximal phalange only. This simplification made manufacture of all the fingers simple and time effective. Approximately one week had been dedicated to the fabrication of steels pins and assimilation of the finger components.

The fingers are actuated using a cable which would only actuate flexion of the fingers. It was decided that an elastic element would be utilized to actuate the extension of the fingers. Elastic bands, shown in Figure 2-25, were attached across the top of the fingers to produce the necessary joint torque for extension.



Figure 2-25: Elastic bands used for extension of the fingers

### 2.4.3 Finger and palm assemble

Once the fingers had been assembled they could be married to the palm unit. The palm unit, pictured in Figure 2-26, was designed with the required holes and features that would facilitate a secure mechanical hand assembly in which all electromechanical and electronic components were to be mounted.

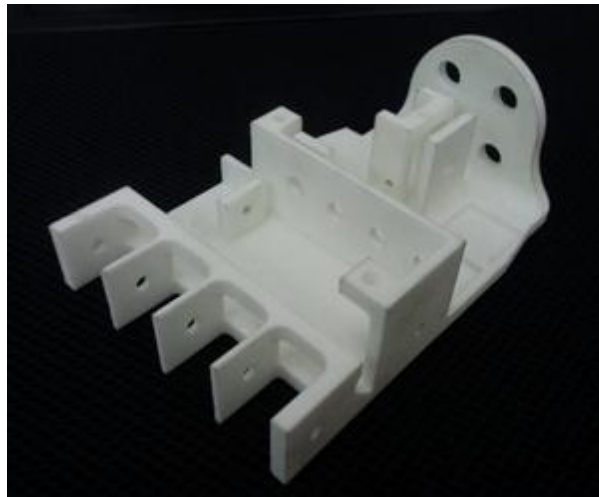


Figure 2-26: 3D printed palm chassis

The palm was 3D printed utilizing the same printing technique as the fingers. The palm has a high dimensional accuracy and is extremely light weight. Minimal effort was needed to ensure a clearance of 1 mm between the fingers and the palm due to this high dimensional accuracy. A single 3 mm stainless steel pin was used to create the revolute joint between the palm and proximal phalanges. Figure 2-27 shows an example of a complete finger married to the palm.

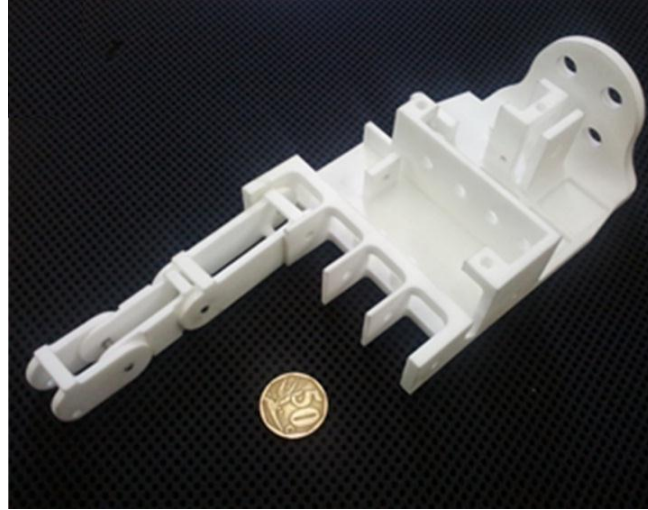


Figure 2-27: Example of complete finger joined to the palm

The assembled hand with all components attach was 220 mm in length, 120 mm in width at thumb, 90 mm in width at knuckles, 70 mm in height at palm (including electronics) and 25 mm in height at knuckles. These dimensions can be seen on the hand in Figure 2-28. The weight of the hand and wrist with all electrical components (excluding the battery) was measured at 540 g.

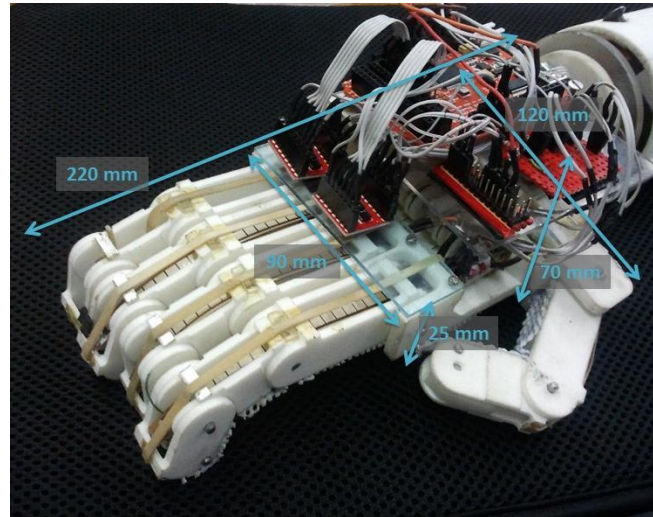


Figure 2-28: Complete hand with dimensions

A non-slip nylon covering was used on the palm of the hand and fingers to greatly reduce object slip. This covering is shown in Figure 2-29.





Figure 2-29: Nylon non-slip covering to improve grip stability

#### 2.4.4 Assembly of actuator and drive system

Actuating the fingers posed a significant challenge as quantized by the working zone. The space allowed for installation of the actuation system was one of the key criteria for motor selection. Suitable calculation and selection tools were utilized to choose the most effective actuator for the purposes of this project. A 6 V Polulu Motor with a 50:1 gear ratio was chosen because of its compact size and low-cost. The motor was rectangular with rounded edges having dimensions of 12 mm x 10 mm x 24 mm and a stall torque of 0.1 N.m. Figure 2-30 (Pololu, 2013) shows the motor that was used.



Figure 2-30: Polulu 6V DC motor with 50:1 gear ratio

The motors were securely mounted to their respective positions, as seen in Figure 2-31. The mounting of these motors was critical as it directly impacted the reliability and accuracy of the drive gear mesh.



Figure 2-31: A mounted motor used for thumb flexion and 4 finger motors.

A worm gear system was chosen to transfer torque from the motor shaft to the cable pulley. The worm was securely fitted to the motor shaft using a D-shaped shaft and gear bore, as shown in Figure 2-32. Epoxy was then applied onto the inner and outer surfaces of the worm and motor shaft respectively. This ensured a tight and immovable coupling of the gear to the shaft.



Figure 2-32: Worm secured on motor shaft.

The cable pulley and worm gear were optimized from their initial concept. The worm gear drive system allowed grips to be held without having to continually power the motors due to its self-locking property, thus increasing battery life. The worm wheels were secured to the palm using a single 3 mm diameter shaft. A 3D printed cable pulley was designed to feed or retract the actuating cable (tendon). Shown in Figure 2-33 is the complete worm wheel and pulley assembly.





Figure 2-33: Complete assembly of worm wheel and cable pulley

The worm and cable pulley are coupled using epoxy. The actuating cable is slotted in a 1 mm diameter hole drilled through the pulley walls. This configuration showed the smoothest winding and unwinding of the cable of all the configurations attempted. The core components were assembled individually. It was then possible to assemble the entire actuation system to the palm. Motor mounts and worm gear positions needed to be meshed with a very fine level of tolerance. Shown in Figure 2-34 is the full drive system assembly. Slight adjustments were made through the assembly process as it was found that tool placement and accessibility was a critical aspect of easy maintenance and repair.

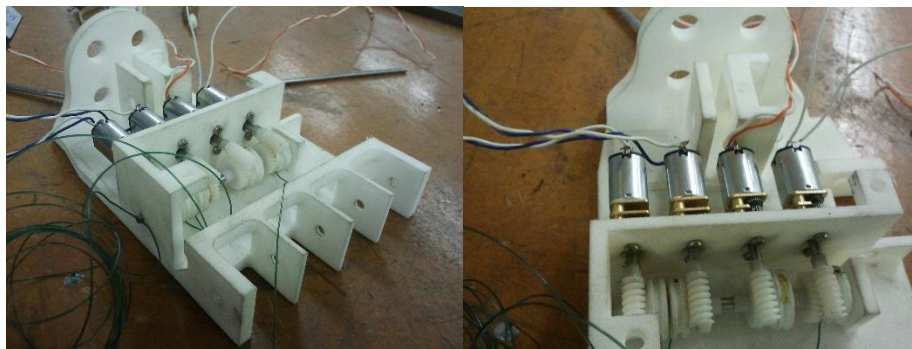


Figure 2-34: Two views illustrating complete finger actuation system

## 2.5 Arm and socket manufacturing process

In this section, the manufacturing process of the prosthetic forearm will be discussed in detail. The forearm acts as the connection of the hand and the upper arm as the prosthesis was designed to cater for transradial and transhumeral amputees. The wrist design and fabrication will be explained first, followed by the prosthetic socket and modulation of the prostheses. The safety procedures are also discussed in this section as they are implemented when operating power tools.

### 2.5.1 Wrist

This section introduces the development of the wrist design and its components fabrication. The wrist is a joint found between the hand and the distal end of the forearm. Its purpose is to couple the two so that they work in harmony when one is using his/her hand. The biological wrist like the one shown in Figure 2-35 has three DOFs; that is flexion or extension, abduction or adduction and pronation or supination (American Society for Surgery of the Hand, 2013). The wrist was designed with one DOF, pronation and supination (rotation). This degree of freedom was based on one of many requirements of the client and is seen as the most critical of the wrist's three DOFs.

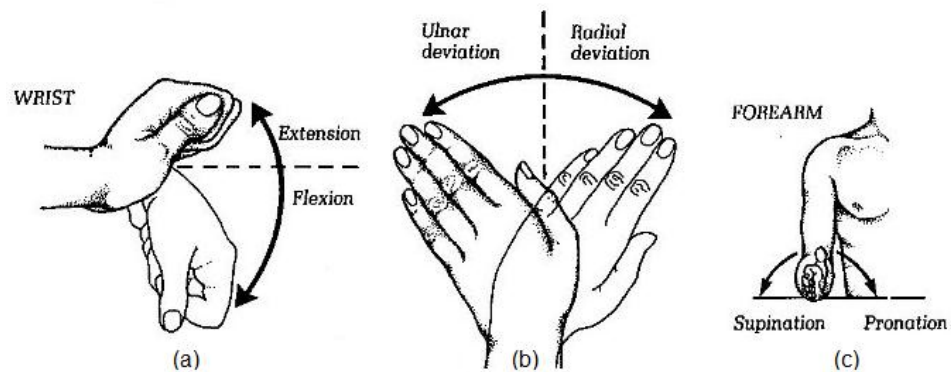


Figure 2-35: Anatomic motions of the wrist; (a) extension/flexion (b) ulnar/radial deviation (c) supination/pronation

The pronation and supination of the wrist is produced with a servo motor (MG945). This motor has a speed of 0.22 seconds per 60 degrees. It has a range of motion from 0° to 180°. Figure 2-36 shows an Autodesk Inventor picture simulating picture used for the design and the actual servo motor model that is used for the wrist respectively. As the wrist must be able to withstand and rotate a mass of 2 kg, the motor produces a torque force of 1.2 N.m at 4.8 V. The metal output shaft of the servo motor is splined to make a perfect fit with a black thermoplastic polymer servo horn attachment and has a mounting hole to secure it.

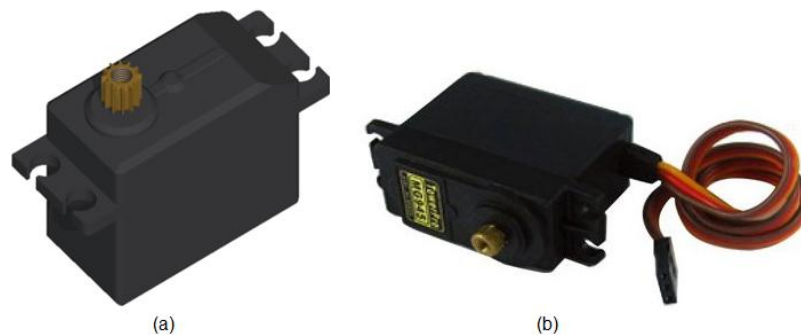


Figure 2-36: Servo motor: (a) Autodesk Inventor picture and (b) MG945 servo motor

The servo horn allows for output shaft to mechanically link to the rest of the mechanism. In this case, it was bonded to the mounting disc of the hand to transmit rotation (pronation and supination) of the hand. The mounting disc is 64 mm in diameter, 5 mm in thickness and made from clear perspex material as shown in Figure 2-37. It has four 8 mm holes drilled into it using a vertical drilling machine, which are used for coupling the wrist to the hand. The centre hole of 15 mm diameter in the disc is for placing circular part of the servo horn to attach it to the servo motor metal splined shaft.



Figure 2-37: Mounting disc made from clear perspex material

The vertical milling machine was used to clean and machine a slot to place a servo horn attachment as shown in Figure 2-38. Then the mounting disc and the servo horn were bonded together using epoxy bonding material. This was done to prevent the servo horn from skidding within the centre hole of the mounting disc when the servo shaft was rotating, as the shaft will be subjected to the load of the object being carried and the load of the hand.



Figure 2-38: Mounting disc and servo horn being machined on milling machine

As part of the prototype evaluation of the wrist the servo motor is mounted in a 3D printed semi-circle housing by four M4 socket cap head bolts high tensile black. The housing is made of ABS plastic material. The housing and servo motor are shown in Figure 2-39. As the

name states, this material comprises of 50% styrene and the balance is divided between butadiene and acrylonitrile (Celanese, 2013). It can be processed by any of the standard thermoplastic processing method. Its disadvantage, that could be more fatal to prosthetic use, is that it is flammable in the range of 110 °C to 125 °C with high smoke generation (Rutkowski and Levin, 1986). The prosthetic wearer must be alert of open flames as the material may catch on fire. It is thus recommended that ABS plastic is not used for commercial use.

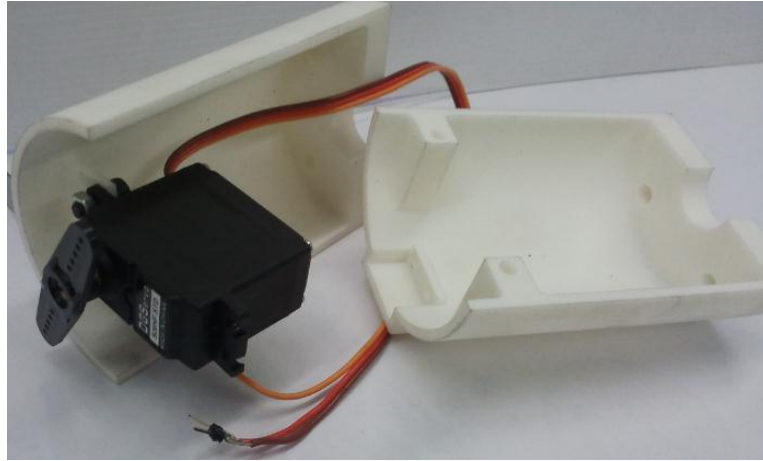


Figure 2-39: 3D printed wrist housing from ABS plastic

The housing is 70 mm in diameter and 100 mm in length. At the front end where the motor fits, the inner shell was extended in a rectangular shape so that the motor shaft is centralised in the middle of the housing. This was done to eliminate the eccentric positioning design of the servo motor shaft. It also has two 6 mm diameter holes which are in line with the two holes of the outer shell. The disc has two M10 counter sink bolts fixed on it, to easily mount the hand. Two bolts were used because of the small space clearance on the palm monocoque and also to reduce the loading on the servo motor shaft. The full labelled components of the wrist are shown in Figure 2-40; this was before the two M10 bolts were fused to the mounting disc using epoxy.

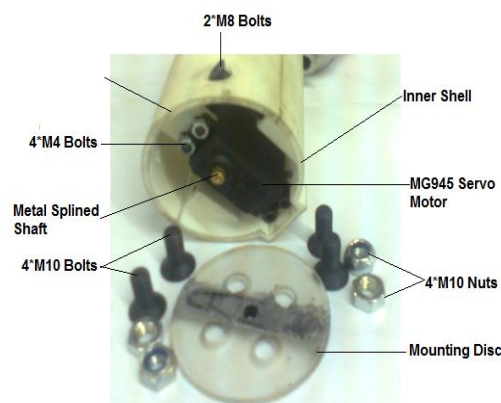


Figure 2-40: Components of the wrist housing

## 2.5.2 Prosthetic socket

The socket is the most critical element of the whole prosthesis because it forms the mechanical interface between the amputee and the prosthesis. As the socket transmits forces from the prosthetic device to the amputee's residual stump, the socket must be precisely fitted to limb. This ensures that the amputee does not get skin irritation or damage. The prosthesis can be state-of-the-art but if the prosthetic socket is uncomfortable to the wearer, he/she will reject it. Another factor which may lead to rejection of the prosthesis is the ease of attaching and detaching the device.

In this section the fabrication of the prosthetic sockets and the suspension system will be discussed. It must be stated that the prosthetic socket was not designed but a new pair was fabricated to fit the amputee, according to his existing socket specifications, on whom the prosthetic hand was tested on.

### 2.5.2.1 Socket fabrication

For this prosthetic arm to come to life a prosthetic socket was needed for the amputee to wear so that the functionality of the hand could be put on the test. All the works of producing the prosthetic sockets was done at the Wentworth Hospital, Durban, South Africa.

As the amputee was already the patient of the hospital, his measurements of the remaining residual limbs were already available. Since the hand that has been designed was to be myoelectrically controlled, the sockets differ from that of body-powered prosthetics socket. Figure 2-41 shows the current prosthetic hand being used by the amputee. The cable mounting parts and end effectors (hooks) were eliminated in order to accommodate myoelectric parts.



Figure 2-41: Amputee's current prosthetic hand with cable and hook end effector



There were three main stages implemented to obtain the final prosthetic sockets; measurement and casting, rectification and fabrication. Plaster wrap was used to cover the limbs of the amputee. For easy removal of the cast, the plaster wrapped limb was coated in a separator. The plaster of paris was then used to make the plaster cast of the limb which is termed a negative mold. The negative mold was then used for creating positive mold by filling it with Gypsum plaster. Figures 2-42 shows the stump of the amputee ready for measurements and wrap casting. Figure 2-42 also depicts white Gypsum plaster positive mold stumps.



Figure 2-42: Fabrication stages of prosthetic socket

In rectification, the measurements of the positive mold and residual limb of the amputee were compared for any indifference. All the molds were found to be in perfect length dimensions with respect to the amputee limbs. The modifications made on the mold differ for each amputee as their requirements and needs are unique. The customisation process of the socket involves adding and removing of the Gypsum plaster on the mold. This is done to ensure that the amputee will bear the load ideally according to his/her stumps pressure tolerances.

After the adjustment of socket shape was done and agreed by the amputee, the alignment marks were made to indicate how the prosthesis should hang on the arm in order to reach the amputee's mouth. The final socket was produced from the adjusted socket shape mold by laminating plastic resin with fiberglass as reinforcement material on the mold. The socket was then fitted to the amputee to check the comfort and placement of the end effector connection. The angle of the end effector was found to be 45 degrees; it was from the amputee's current prosthetic socket as shown in Figure 2-43.



Figure 2-43: Fitting of the socket and end effector angle

The prosthetic socket was then bonded to a steel pyramid using molten thermoplastic for connecting to the wrist housing female adapter. This is shown in two different angles in Figure 2-44 below when the client was fitting the device.



Figure 2-44: Socket and end effector

#### 2.5.2.2 Suspension system

The method of keeping the socket attached to the residual limb (the method of suspension) is also important. Upper-extremity prostheses must be suspended throughout the entire range of motion and be able to tolerate loading during normal use. Suspension of the socket was gained using a figure of eight harness. It was made from 25 mm wide nylon webbing belt. The finished harness mounted to the socket is shown in Figure 2-45.

This harness is different from that of the current used prosthetic harness as this was made for one arm which is myoelectric controlled. It does not have the paddings for protecting the amputee from moving cables. It was made following the South African National Standards (SANS) specification to account for safety.



Figure 2-45: Prosthetic harness

The fitting of the prosthetic harness is shown on Figure 2-46 where the amputee was wearing the transradial prosthetic arm for the first time.



Figure 2-46: Amputee wearing prosthesis

### 2.5.3 Device modulation

This section deals with modulation of the prosthetic arm. It will introduce the technique used to integrate the upper arm to the forearm. The client that participated in this research was a transradial amputee. It was the intention of the research, however, to design a prosthetic hand that could be used both for transradial and transhumeral amputees. By designing the prosthetic arm in a modular way the hand can be attached to a forearm and elbow system for transhumeral amputees.

#### 2.5.3.1 Transradial

The wrist housing forms the base of this prosthetic hand. When the housing is connected to the socket, the prosthesis is transradial. Any type of transradial amputee would be able to wear it as long their sockets are fitted with a pyramid adapter at the distal end. Its components include a stainless steel female adapter which is mounted by 4 M6 bolts and nuts to the back of a 3D printed housing. Figure 2-47 shows an Autodesk Inventor picture of the final design transradial model which is seen next to the actual transradial prosthetic hand.



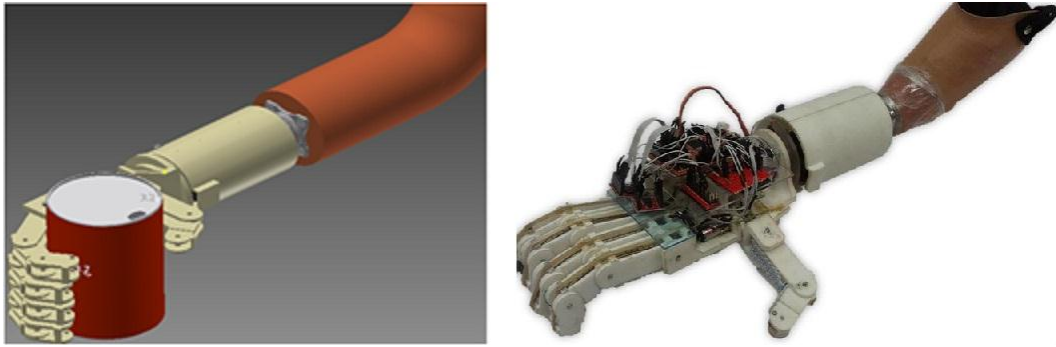


Figure 2-47: Transradial; model on the left and actual on the right

### 2.5.3.2 Transhumeral

In transhumeral amputations, the whole forearm is missing including the elbow. To aid such amputees, the artificial forearm was designed and implemented. It connects the base (wrist housing) at the distal end and connects the upper arm to the aluminium bracket at the dorsal end. The bracket forms the elbow of the arm.

An aluminium round billet was machined in a CNC machine to produce the bracket. This material was used because it is lightweight and was easily available. The exploded view and assembly of the forearm components, excluding the wrist housing are shown in Figure 2-48 and Figure 2-49. Starting from left to right of Figure 2-48; (1) Aluminium bracket, (2) 4-Hole male adapter (3) 30 mm female pyramid tube clamp (4) Caps (5) 30 mm aluminium tube (6) 30 mm male pyramid tube clamp.

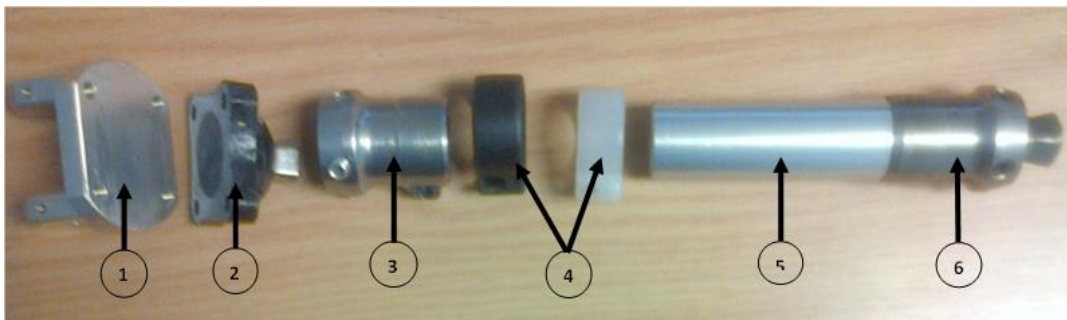


Figure 2-48: Exploded view of the forearm components



Figure 2-49: Assembled view of the forearm components

The aluminium tube used was 50 mm in length and depending on the length of the forearm a shorter or longer tube would be used, though making the forearm part adjustable. All the components excluding the bracket are according to SANS specifications.

The full assemblies of the transradial and transhumeral are shown in Figure 2-50 and Figure 2-51 respectively.

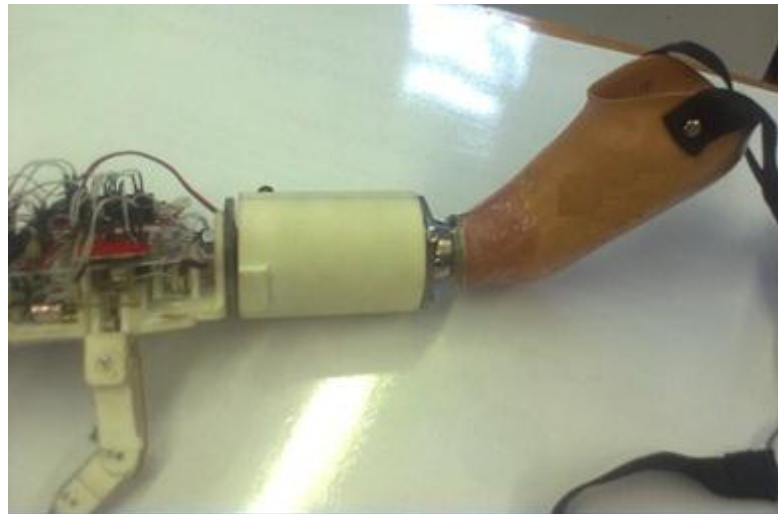


Figure 2-50: Transradial prosthetic arm

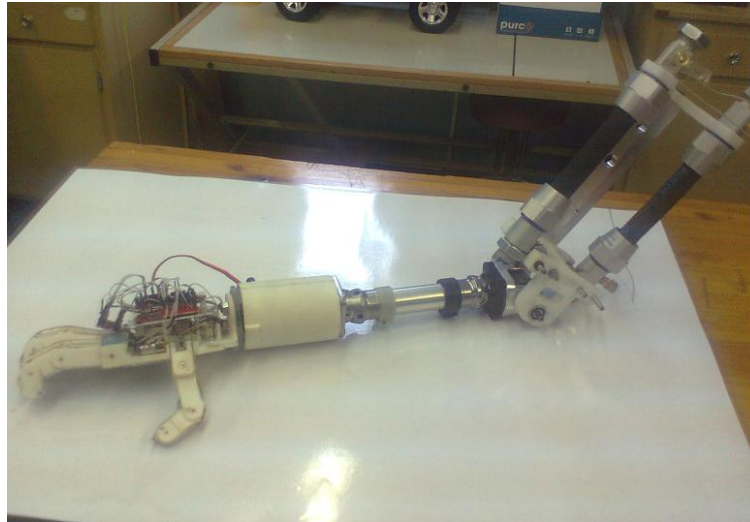


Figure 2-51: Transhumeral prosthetic arm

## 2.5.4 Upper limb

The mechanical components were made from two manufacturing methods. The first being subtractive manufacturing in the form of CNC machining, lathe work, milling etc. The second manufacturing technique used was additive manufacturing in the form of ABS plastic 3D printing. Both approaches were used in order to explore the material selection capacities of each of these materials. Subtractive and additive manufacturing each have their own strengths and weakness. A combination of manufacturing techniques was used so that they would complement each other functionally. Figure 2-52 shows the combination of the materials used in the upper arm coupled to the forearm.

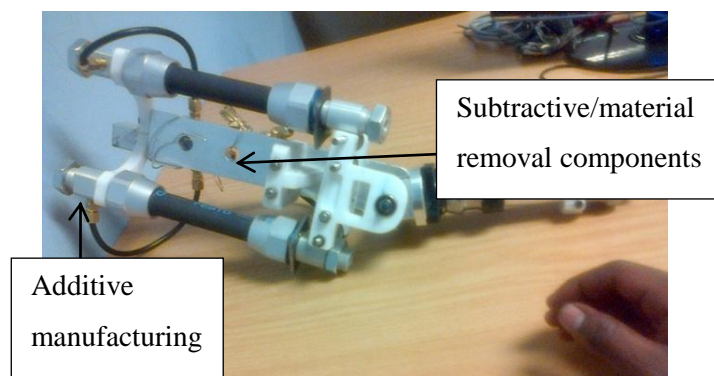


Figure 2-52: Transhumeral connection with air muscles and elbow joint

### 2.5.4.1 The chassis plate

The chassis support plate, shown in Figure 2-53, is the essential component in the structure of the upper arm because it acts as the chassis to which all of the other components are fastened. Due to the fact that the support bracket has all of the components fastened to it, it

means that it will have many holes, varying from drilled holes to tapped holes. This contributes to the reason why aluminium was used. The drilled holes would have more zones of potential failure under bending. The chassis plate has a bearing to allow for the rotation of the elbow and has a thickness of 12 mm. The elbow joint bearing had an inner diameter of 7 mm and an outer diameter of 19 mm.

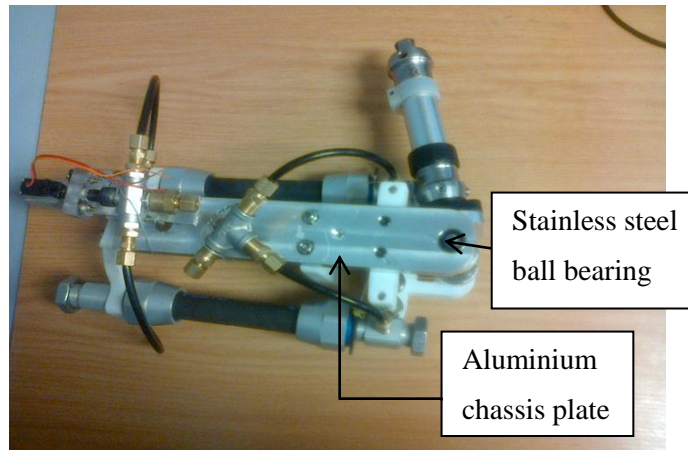


Figure 2-53: Chassis plate

#### 2.5.4.2 Fluidic muscle

A Festo fluidic artificial muscle was used as the actuator (Figure 2-54); this is because of its high level of bio-mimicry. The fluid muscle works according to the hill muscle model because it expands similar to the contractile element. It stops itself from over expanding similar to the parallel element of the hill muscle model. The muscle has an unexpanded diameter of 20 mm, it is rated at a maximum of 6 bars of pressure and the pulling force the muscle is 102 N. The muscle consists of seven parts that make up the composite bladder. These parts are two bladder attachments, two threaded attachments and nuts on either end. The bladder attachment has a female tread shown in Figure 2-55. The muscle adapter has a 3.175 mm female thread and valves used were 6.35 mm valves therefore 3.175 mm to 6.35 mm adapters were used. The tubing used was 3.175 mm in diameter.



Figure 2-54: Fluidic air muscle



Figure 2-55: Muscle female adapter

#### 2.5.4.3 Muscle support structure

The muscle support was made of 3D printed ABS plastic and was designed as 'C' shape consisting of two sections. This allowed for the width between muscles to be adjusted according to the diameter amputee's arm stump. The circular crescent shape is designed to fit comfortably around the stump of the amputee. The end of the mount was bolted to the chassis plate by two M6 bolts. Figure 2-56 shows the two ABS crescent shaped adjustable muscle mounts. One end was made rectangular to fit against the chassis plate and the other end circular to allow for the muscle to fit into it. With 3D printing this shape was easily obtained.

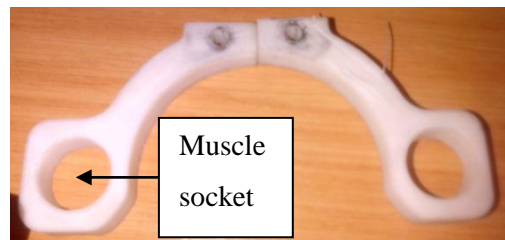


Figure 2-56: Crescent shaped mount.

#### 2.5.4.4 Transhumeral socket connector

The purpose of the transhumeral socket connector is to act as the connecting link between the prosthetic socket and the mechanical upper arm. The prosthetic socket adapter is to be mounted on the upper surface of the transhumeral socket connector which was made from ABS plastic to reduce the overall weight of the system. Two M6 threaded bars were used to connect the transhumeral socket connection to the chassis plate. The transhumeral socket connector is seen in Figure 2-57.



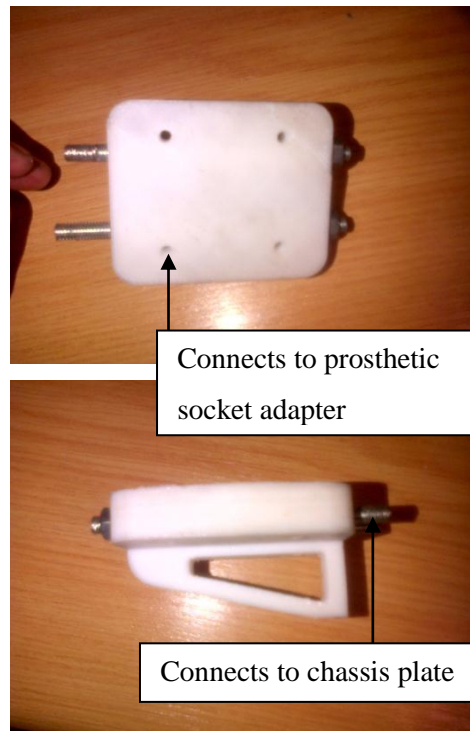


Figure 2-57: Transhumeral socket connector

#### 2.5.4.5 Pulley redirection system

The rigid pulley and air muscles were out of line as the air muscles needed to sit around the amputee's stump and the rigid pulley was located at the centre point of the elbow. The pulley redirection system was made to route the cable from the air muscle to the elbow's rigid pulley. The pulley redirection system consists of four steel bobbins, four threaded bars and four adjustment nuts, shown in Figure 2-58. The outer pulley allows the cable to go from the muscle under the first pulley then over the second pulley and then attached to the rigid pulley (shown in Figure 2-59 and Figure 2-61). Six nuts were used so that each pair can tighten itself. The chassis of the redirection system is made from ABS plastic, and the thread bars are made from steel. The redirection system chassis also has a press fitted bearing to allow the forearm to swing.



Figure 2-58: Redirection pulleys.

#### 2.5.4.6 The rigid pulley

The rigid pulley is the mechanical lever that converts the linear contractile motion of the muscle in to rotational motion. It is also the key component in the upper arm, where the energy is transferred to the forearm. The rigid pulley was made from steel. A grub screw was used to fix the rigid pulley to the shaft. An indentation was made in the shaft and a threaded hole was made in the steel pulley. Figure 2-59 shows the grub screw holes and the holes in which the tendons are to be attached. Figure 2-60 show the corresponding indentations on which the screws will sit. The critical linkage upon which the flexion and extension of the elbow depends on is shown in Figure 2-61. Furthermore vesconite stoppers were used to ensure that the forearm swings without any lateral movement which would result in improper alignment.

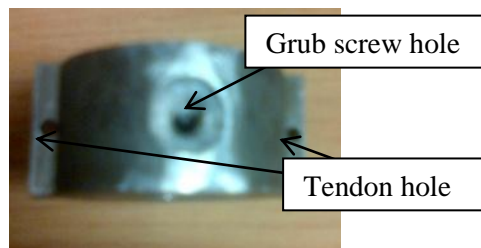


Figure 2-59: Main pulley

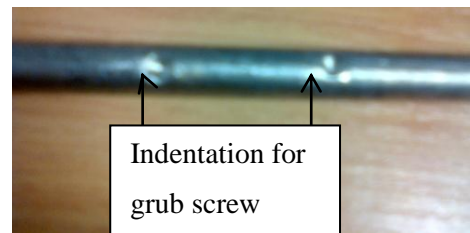


Figure 2-60: Shaft

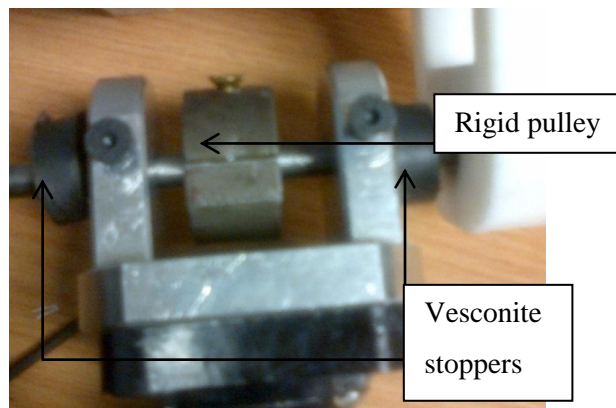


Figure 2-61: Rigid link

#### 2.5.4.7 The valves

The valve system was designed in such a way that it can implement the antagonistic movement. It was also designed for steam, although it can run off air. In order to achieve this opposing motion the timing of the valves needed to be synchronised. When the inlet valve of one muscle is open, the outlet of that valve needs to be closed to expand the air muscle. Simultaneously the inlet of the other muscle will be closed and its outlet opened. Table 2-1 shows the logic that was followed in the implementation of the system.

TABLE 2-1:

VALVE LOGIC

| Valve         | Flexion | Extension |
|---------------|---------|-----------|
| Bicep inlet   | 1       | 0         |
| Tricep inlet  | 0       | 1         |
| Bicep outlet  | 0       | 1         |
| Tricep outlet | 1       | 0         |

The system was designed for steam; however it was difficult to obtain steam valves in the solenoid ranges that would fit the upper arm because of the limited space on the prosthetic arm. 6.35 mm stainless steel manual ball valves were used. These valves are made of stainless steel and have PTFE seals. The Teflon seals and the stainless steel body provide good heat properties. The nuts were removed, the extension handle was ground off and the washer was removed in order to motorise the valves. The principle used to motorise the valve was the fact that a hexagonal nut can be opened by a flat head hexagonal bolt, provided that the bolt head fits perfectly onto the nut. The problem with this arises due to the fact that the bolt head will tighten the nut in one direction and open it in the opposite direction. The nut and bolt head were attached together using epoxy. Figure 2-62 shows the motorised valve that result from this process. The valve unit is mounted on the strip of aluminium flat bar. The flat bar is screwed onto the chassis plate by a 90 degree flange elbow attached to it. A perspex plate was used to couple the bolt and the servo motor. The bolts were cut to the smallest height that could fit in the space above the handle.

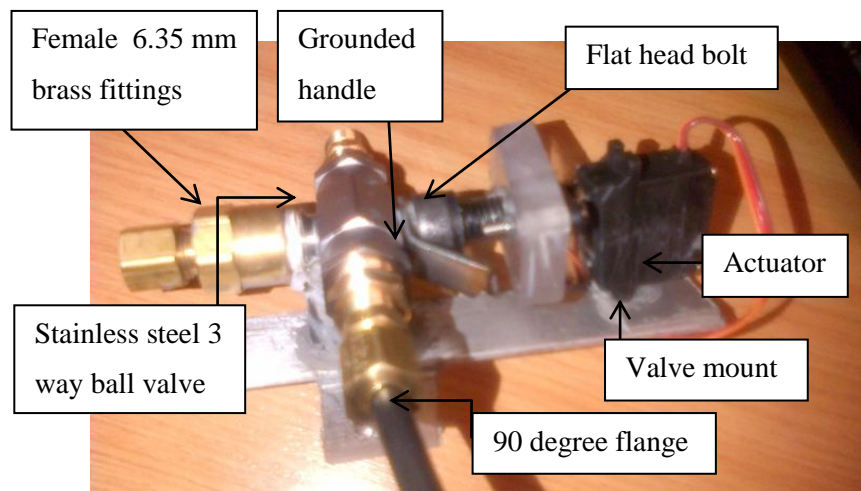
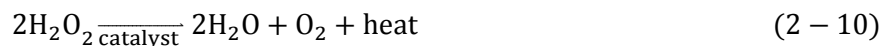


Figure 2-62: Servo motorised valve unit.



### 2.5.5 Chemical investigation

The catalytic decomposition of hydrogen peroxide is proposed as an actuating gas to be used to actuate the muscle. 30% hydrogen peroxide was used in the following experiment. The governing equation in the following operation is shown in Equation 2-10.



30% hydrogen peroxide, which is laboratory grade peroxide, was used. Higher concentrations may be used in the future. Manganese dioxide was used as the catalytic material as shown in Figure 2-63. It is an extremely fine, dark brown powder. A simple test was run to observe this reaction.



Figure 2-63: Catalytic material (manganese dioxide)

A can was used and the manganese dioxide was added with a spatula. Peroxide was poured over the material. It was noticed that the catalyst was most effective if the surface area exposed to the catalyst was maximized. The manganese never had to be replaced because a catalyst does not react. The sequence of the reaction can be seen in Figure 2-64. It should be noted that the reaction takes approximately 5 seconds to reach its maximum reaction rate.

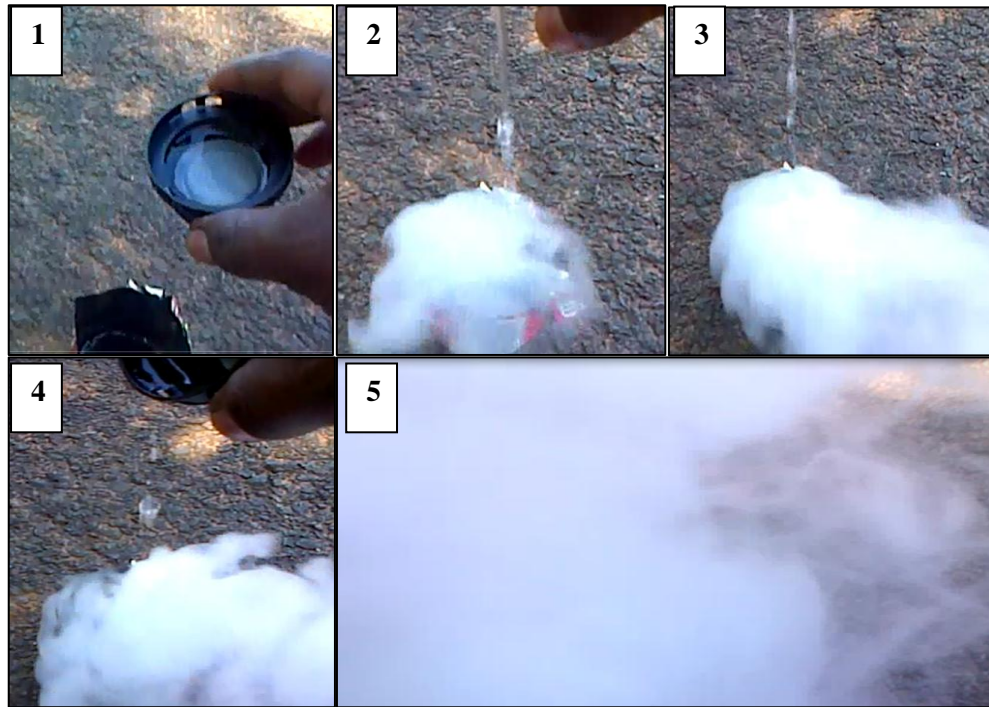


Figure 2-64: The evolution of steam and oxygen

## 2.6 Chapter summary

For future recommendations it is acknowledged that a more efficient system for actuation can be developed. It was noted that the actuation cables offered a significant resistance when sliding across the cable guides. The cables used can be substituted with less flexible ones. The monocoque design offered structural rigidity but there was no room for tools (such as screwdrivers) to reach in, making the assembly very time consuming. The design should be modified to allow for the easy installation of the mechanical and electrical components. Further consideration could be given to allowing the hand to have modular mechanical and electrical components. This would allow for a high degree of customizability and would allow the amputee to choose only the components he/she wants to be in his/her prosthetic hand.

As shown from the kinematics, the hand and fingers have a good range of motion, which cover the basic DOFs of a human hand. A more complex model allowing full DOFs would be actuator heavy, thus increasing the weight, size and cost of the prosthetic hand. For this reason the hand is optimized for weight, cost and function. The hand weighs 540 g which is 140 g more than the average adult male hand (Cipriani et al., 2011). The size of the hand is slightly larger than a human hand and its size should be reduced in future versions.

The wrist joint needs to be improved upon. The current design places the entire load of the hand on the servo motor shaft. A bearing needs to be incorporated into the wrist allowing for minimum force distribution across the motor shaft.

The wrist was designed with only a single DOF (rotation). However the flexion and extension movements are very important in daily life and inclusion of this second DOF would improve the overall function of the prosthetic hand. However, additional DOFs would bring added complexity, weight and cost to the hand. A modular approach could be taken here, allowing for the second DOF to be an attachable part to the prosthetic hand, allowing it to be used as necessary.

The socket was well fabricated but did not consider the placement of EMG sensors and haptic feedback displays. In future, a myoelectric prosthetic socket needs to be designed so that the wires of the electrodes pass from the microcontroller through the wrist housing and socket to the surface of the residual limb where the targeted muscles are located. The current design allows the haptic feedback displays to be attached anywhere on the upper body, in a modular fashion. The modular approach allows the user to choose the preferred area for haptic feedback. However, the socket could also be designed to accommodate the haptic feedback displays.

The connecting adapters were all made from stainless steel which increased the weight of the prosthesis. With the new technology of 3D printing they can be reproduced and be made from a much lighter material like carbon fibre.

The development of the artificial muscle showed positive results. Future work can be done to develop a fully portable artificial muscle system. The proposed artificial muscle system with hydrogen peroxide showed good potential. The fuel is compact and powerful enough to drive the air muscles to actuate the elbow in much the same way as in the human body. However, the designed pulley system was not suitable. A possible solution would be to use a belt and pulley system which would more effectively transfer the force from the air muscles to the elbow. The compact chemical reaction system needs to be designed to fit onto the arm, with replaceable fuel canisters. A custom designed system of tanks, electronic valves and air muscles can be designed to fit onto the upper limb of the prosthesis and would provide an alternative to motor actuated prosthetics.

### 3. ELECTRONIC DESIGN

The electrical design of the prosthetic arm is divided into four main areas:

1. Tactile sensors
2. Myoelectric (EMG) sensors
3. Haptic feedback and Haptic User Interfacing (HUI)
4. Actuating and position feedback circuitry

These areas are shown in Figure 3-1. It can be seen that each area interacts with the microcontroller unit (MCU). The MCU links all the different aspects of the prosthetic arm and collects the input signals from the EMG, tactile and position feedback sensors and then uses this data to control the HUI, haptic feedback, and actuating circuits.

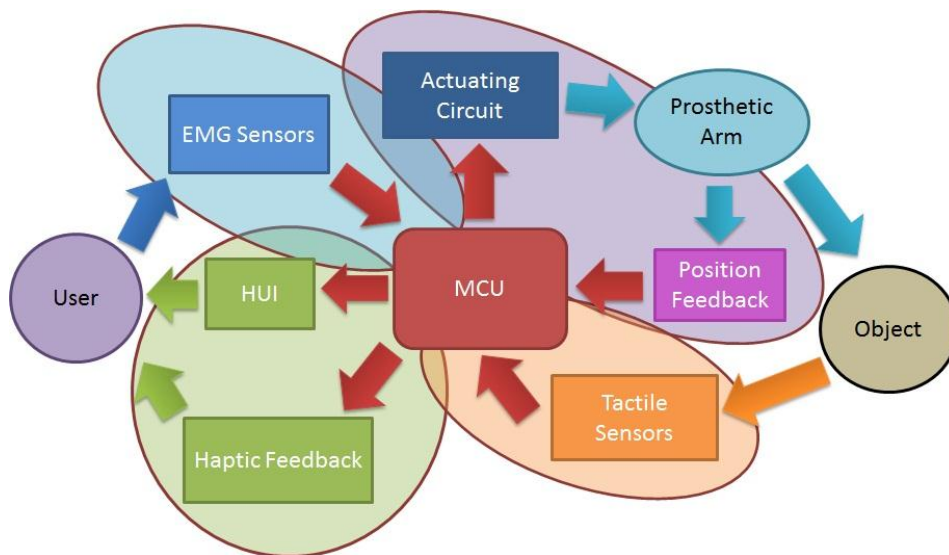


Figure 3-1: Overview of the electrical system

The MCU serves as the ‘brain’ of the prosthetic arm. The number of PWM and analog input pins that were required was determined so that an appropriate MCU could be selected. The two boards capable of meeting the performance requirements of the hand are shown in Figure 3-2. Size was a key criterion to be met when selecting the controller. The Arduino breakout board setup was used over the base MCU chip as this allowed for simple plug-and-play installation with the rest of the circuitry, allowing for ease of prototype development. Both boards use an Atmel ATmega 1280 MCU chip (Seeed Studio, 2014).

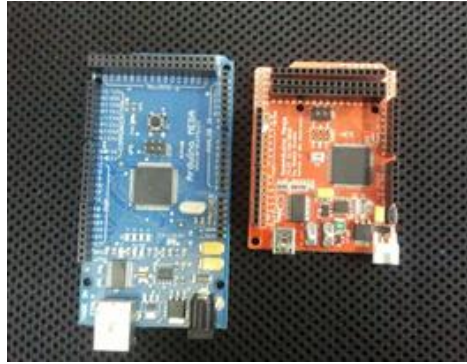


Figure 3-2: Arduino Mega (blue) and the Seeeduino Mega (red) size comparison

The Seeeduino Mega is thirty percent smaller in dimension than that of the Arduino Mega. Both boards are based on the Arduino open-source architecture and have the same processing power and number of I/O pins. The Seeeduino was chosen because of its compact form.

### 3.1 Tactile sensory system

The prosthetic hand is equipped with grip force and temperature sensors. An investigation was done to determine whether both object slip and texture could be detected with a single low-cost vibration sensor. The layout of the sensor positions in the hand is shown in Figure 3-3. This section doesn't include the flex sensors used to track the position of each finger, which is discussed in the actuation section of this chapter.

Grip force is measured between 2 N and 20 N using a force sensor placed on the tip of the index finger. Temperature is measured between 2 °C and 150 °C using a temperature sensor in the tip of the middle finger. Object slip is investigated by a vibration sensor located in the distal phalange of little finger. Texture is investigated by the same vibration sensor used for slippage in combination with a force sensor which is located on the tip of the little finger.

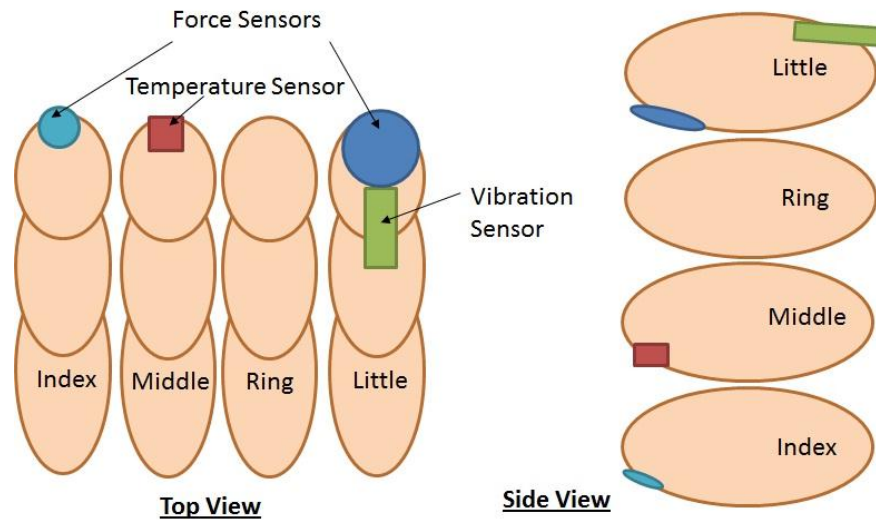


Figure 3-3: Overview of the electrical system

### 3.1.1 Grip force

The hand was equipped with two force sensors. The FSR 400 resistive force sensors were used for this purpose because of their low-cost and their force range. Two different sizes were used, as shown in Figure 3-4 (Interlink Electronics, 2014). Both sensors are capable of measuring between 0 N and 20 N of force (Interlink Electronics, 2014).

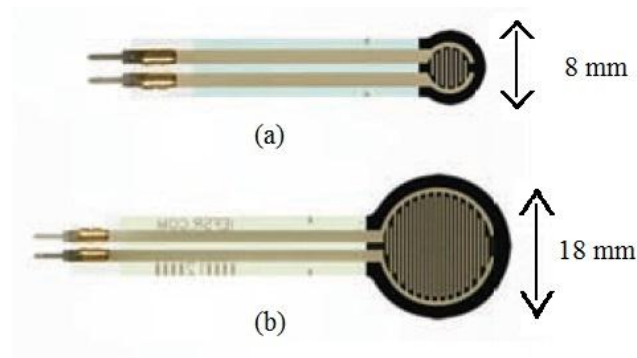


Figure 3-4: FSR 400 force sensors (a) 8 mm diameter (b) 18 mm diameter

These force sensors have identical force properties. However they perform differently due to their different surface areas as they require a constant pressure over their surface. As a result of this, it is found that the 8 mm force sensor gives more consistent results. The smaller 8 mm one was used for precision grip force measurements and was placed on the tip of the index finger. The 18 mm force sensor was used as a contact detection sensor to trigger the texture detection in the little finger and was placed on the tip of the little finger.

As these are resistive sensors it was necessary to determine the best voltage divider circuit to provide the best output voltage. The force sensors are an open circuit at no force and have a resistance of 1 k $\Omega$  at full load. Two voltage divider circuits were built with a 4.7 k $\Omega$  and a 22 k $\Omega$  resistor respectively, shown in Figure 3-5.

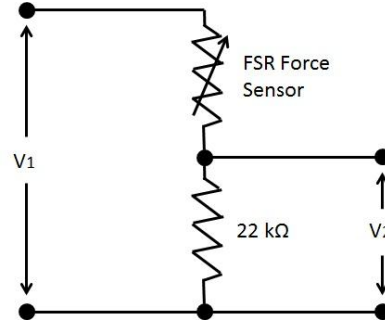


Figure 3-5: Voltage divider circuit with 22 k $\Omega$

A supply voltage of 7.2 V was used to test the two circuits with variable loads. The results, shown in Figure 3-6, indicate that the 22 k $\Omega$  resistor makes use of the full supply voltage and thus offers a better resolution of the grip force compared to the 4.7 k $\Omega$  resistor. Therefore a 22 k $\Omega$  resistor was selected for both force sensor circuits.

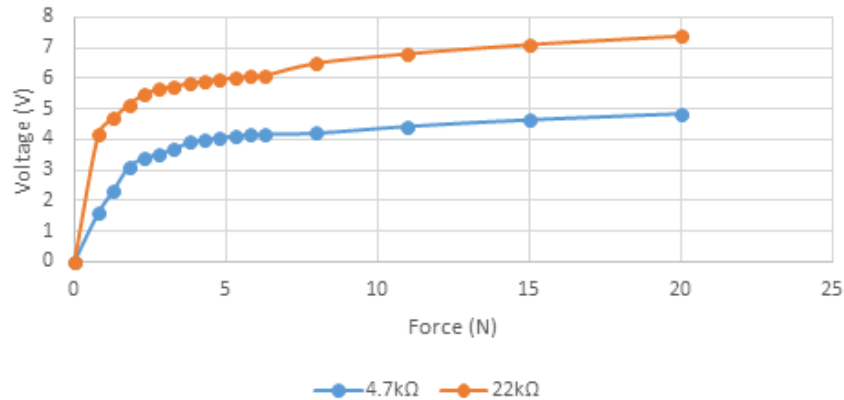


Figure 3-6: Voltage vs force relationship for the 4.7 k $\Omega$  and 22 k $\Omega$  resistors

The resistance of the force sensors for varying loads needed to be determined in order to calculate the force from the output voltage independent of the supply voltage. This was done by measuring the voltage over the 22 k $\Omega$  resistor and using the voltage divider Equation 3-1 to calculate the resistance of the force sensor, where  $V_1$  is the supply voltage,  $V_2$  is the measured voltage over the 22 k $\Omega$  resistor, and  $FSR$  is the force sensor resistance. This was done for varying loads up to 20 N.

$$V_2 = \frac{V_1 \times 22 \text{ k}\Omega}{FSR + 22 \text{ k}\Omega} \quad (3 - 1)$$

Once the resistances were calculated for each load point, Equation 3-1 was used to calculate the expected voltage for a 5 V supply, shown in Figure 3-7 and Figure 3-8 for the 18 mm and 8 mm force sensor respectively.

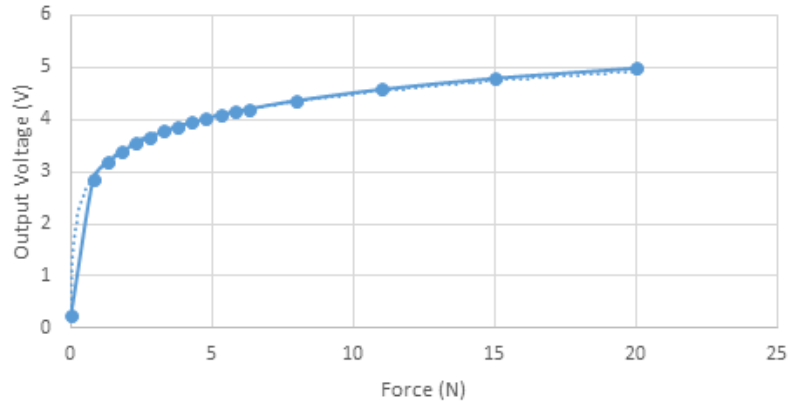


Figure 3-7: 18 mm force sensor output voltage, trend line:  $y = 0.625 \ln(x) + 3.052$

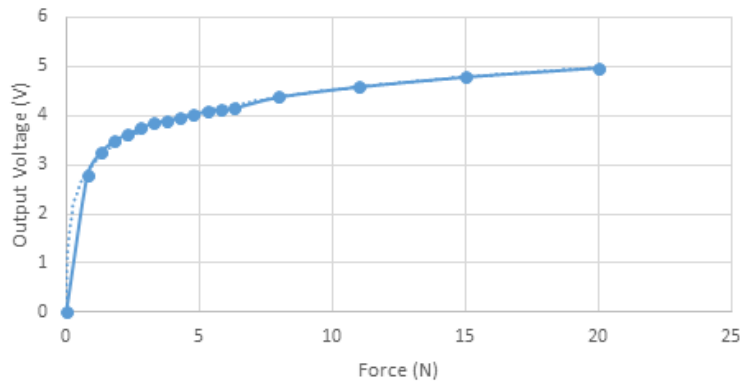


Figure 3-8: 8 mm force sensor output voltage, trend line:  $y = 0.6511 \ln(x) + 3.0222$

The trend lines of the force vs voltage graphs were then used to generate Equation 3-2 and Equation 3-3.

$$Force = e^{\frac{V_{out}-3.052}{0.625}} \quad (3-2)$$

$$Force = e^{\frac{V_{out}-3.0222}{0.6511}} \quad (3-3)$$

Where *Force* is in Newtons for the 18 mm and 8 mm force sensors respectively.

### 3.1.2 Object temperature

To give the hand the ability to sense temperature, a standard LM35 temperature sensor was used because of its low-cost and temperature range. The LM35 has a range of 2 °C to 150 °C (“LM35 precision centigrade temperature sensors,” 2000), which is suitable for



application in the hand, which needs to simply determine between hot and cold objects as well as dangerously hot objects (50 °C +). It needed to be determined how effective the temperature sensor would be if placed behind the nylon non-slip covering of the hand. The reason for a difference is explained through heat transfer theory, seen in Equation 3-4.

$$\frac{Q}{t} = \frac{\kappa A (T_{hot} - T_{cold})}{d} \quad (3 - 4)$$

Where  $Q$  is the heat transferred in time,  $t$ ,  $\kappa$  is the thermal conductivity of the barrier,  $A$  is the area,  $T$  is the temperature and  $d$  is the thickness of the barrier. The thermal conductivity of nylon is 0.25 W.m<sup>-1</sup>.K<sup>-1</sup> at 23 °C. The nylon non-slip covering acts as a barrier, slowing the heat transfer from the object to the LM35 temperature sensor. Therefore there will be a delay between the directly and indirectly detected temperatures caused by the nylon barrier.

Figure 3-9 shows the temperature detection difference of direct and indirect contact with the object. A mug with boiling water (mug temperature at 50 °C) and with warm water (mug temperature at 35 °C) was used for this test.

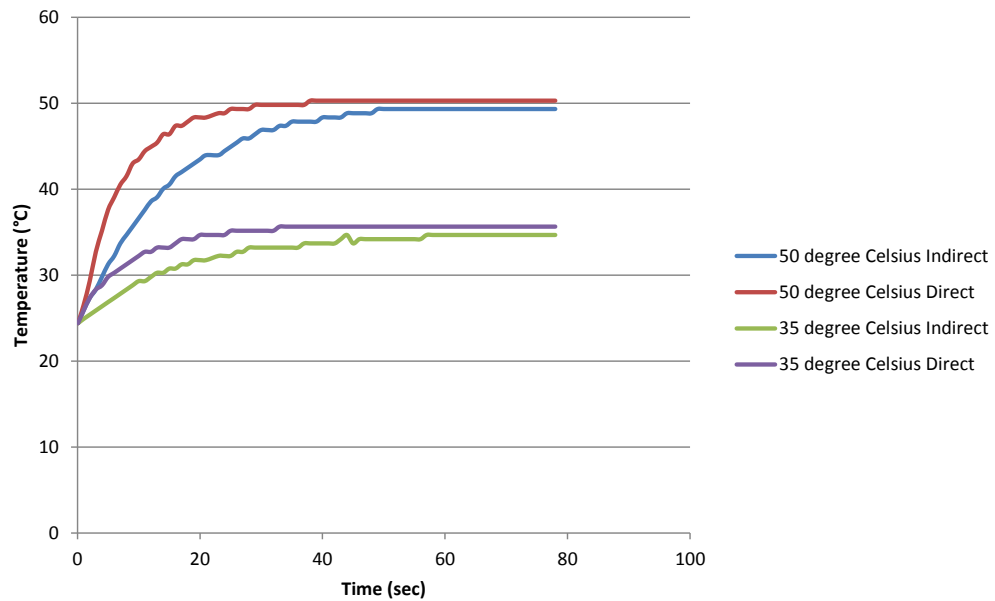
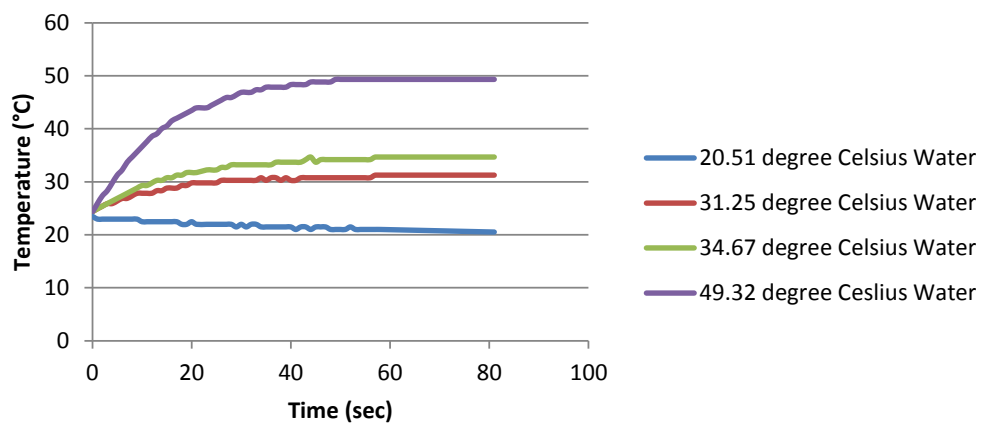


Figure 3-9: Temperature reading from the LM35 for direct and indirect contact

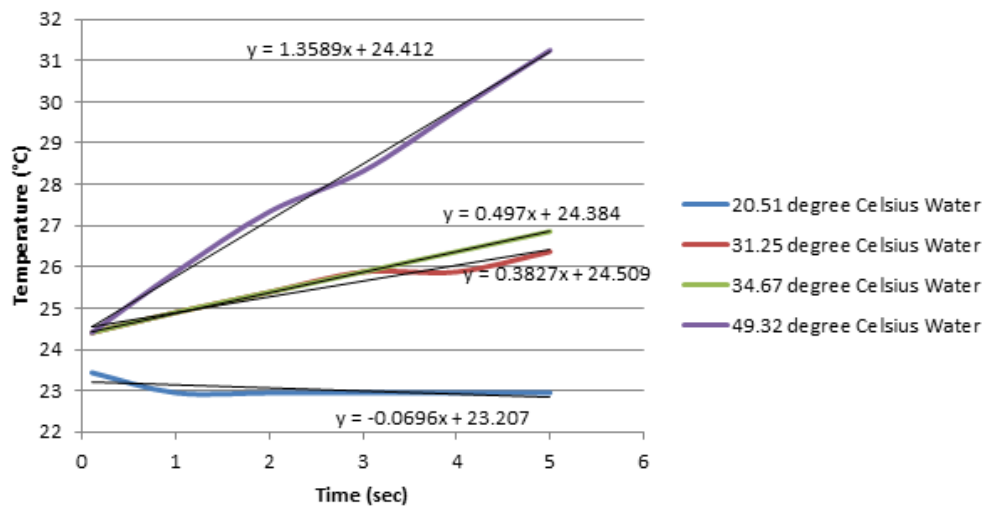
As can be seen in Figure 3-9, there is negligible difference between both detection rate and final detected temperature of the direct and indirect methods. It was therefore decided that the temperature sensor would be placed inside the tip of the middle finger, just behind the nylon non-slip covering. All further testing was done with this condition. These results also highlighted an important limitation of the LM35, this being that the sensor takes approximately 30 seconds to 40 seconds to determine the temperature of an object. This is slow and unhelpful

in daily living applications where the temperature of an object needs to be judged immediately, especially in dangerously hot scenarios.

It was observed that the rate of change in temperature differs proportionally according to the object temperature, according to Equation 3-4, where the temperature difference,  $T_{hot} - T_{cold}$  is directly proportional the rate of heat transfer. The object temperature ( $T_{hot}$ ) can be calculated using the measured rate of change in temperature (gradient) as the current temperature ( $T_{cold}$ ) of the hand is always known by the temperature sensor in the hand. Figure 3-10 shows the temperature readings of four different object temperature and then their corresponding initial 5 seconds with their best fitting linear equations.



(a)



(b)

Figure 3- 10: (a) Object temperature readings; (b) best fit linear equations for the initial 5 seconds

These results were then plotted together to see what the relationship between gradient and final temperature was, as shown in Figure 3-11. It was found that the gradient has a linear relationship with the final object temperature.

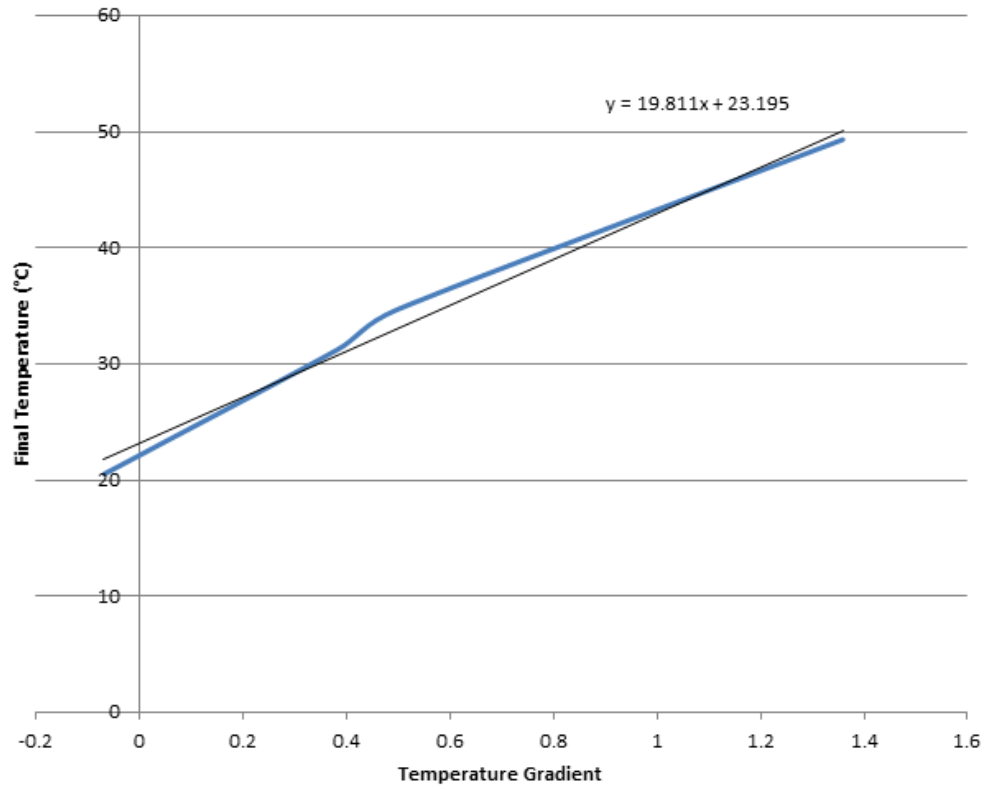


Figure 3-11: Final object temperature against gradient of temperature vs time

Using the best fit equation, Equation 3-5 was derived to predict the actual object temperature based on the rate of change of the temperature sensor.

$$T_p = 19.811 \times T_g + T_c \quad (3 - 5)$$

Where  $T_p$  is the predicted object temperature in °C,  $T_g$  is the temperature gradient and  $T_c$  is the current temperature in °C. The average gradient is calculated as the average of the consecutive gradients. Figure 3-12 shows an example graph with five data points. The gradient between each data point is calculated separately and the average is calculated from these gradients.

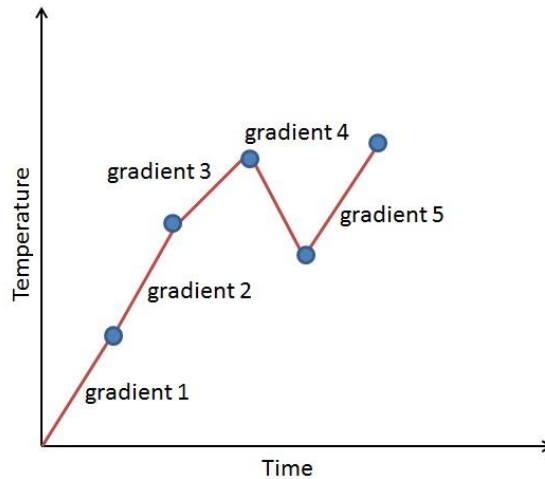


Figure 3-12: Average gradient example

In order to test Equation 3-5, a fixed temperature is used and the temperature sensor is programmed with Equation 3-5, with a varying number of samples using a one second period. These samples are used to determine the gradient of the temperature slope. The average of the predicted temperatures measured from the start until the temperature reaches its final temperature was taken. These predicted results are compared to those of the other sample numbers and the actual temperature, shown in Figure 3-13. These results show that the derived prediction over estimates by only 2 °C to 3 °C and that with an increase in samples, it has a reduced standard deviation of only  $\pm 1$  °C for five samples.

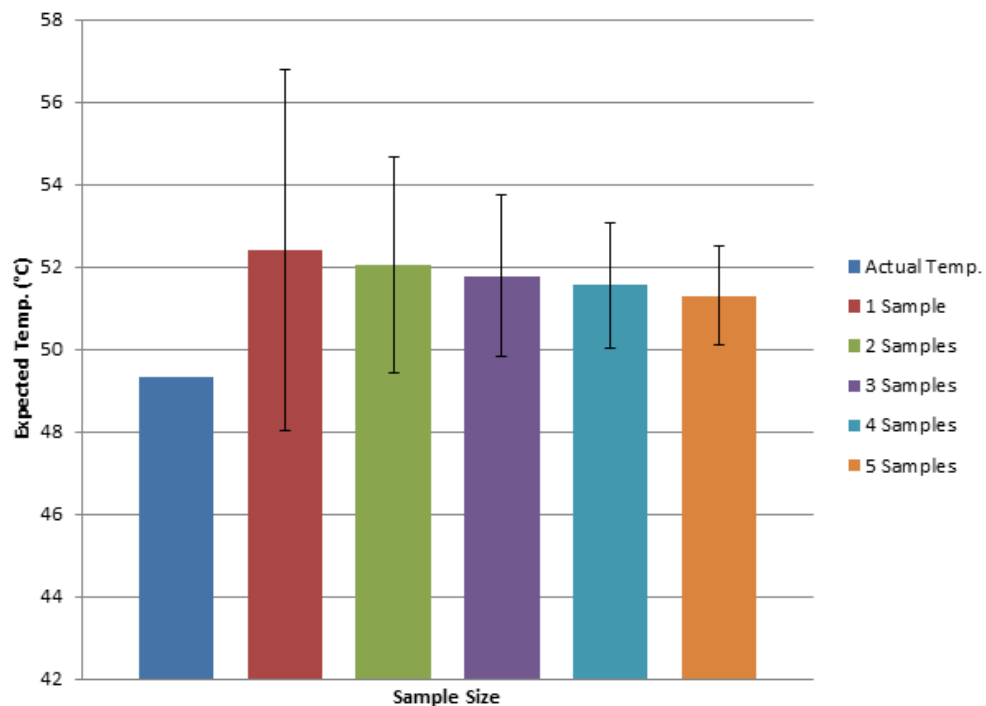


Figure 3-13: Predicted temperatures with standard deviation

The drawback of using a large number of samples is that the prediction is slower to react to change. In the daily application of a prosthetic hand, a quick response is seen as being more important than accuracy. This is especially the case as object temperature is merely an abstract indication, even with human touch. Therefore it is determined that the accuracy of the designed prediction method is satisfactory.

### 3.1.3 Object slippage

Object slip is the measure of when the object being grasped in the prosthesis' hand starts to involuntarily fall from the hand. Slippage occurs when not enough grip force is being applied to the object to generate enough friction to hold the object in place. The heavier the object, the more likely it is that the object will slip out of the hand.

In order to solve this problem a slip sensor is needed to detect the slippage immediately as it starts in order to increase the gripping force so that the object isn't dropped. When two objects slide across each other, as in the case during slippage, the friction in the system causes vibrations. The first sign of slippage or movement of the object can thus be detected with the aid of a vibration sensor. A low-cost piezo-electric vibration sensor is used to detect slippage. The MiniSense 100 vibration sensor from Measurement Specialties, as seen in Figure 3-14 (Measurement Specialties, 2014), was selected for this task which is capable of measuring between 40 Hz and 100 Hz and up to 1 g of acceleration (Measurement Specialties, 2014). The MiniSense 100 vibration sensor was selected because of its low-cost, compact size and frequency measurement range.

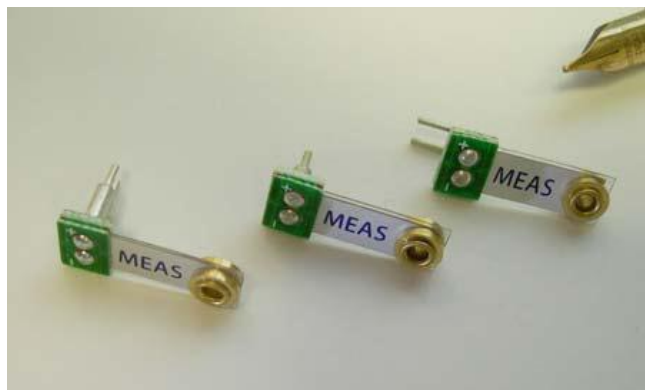


Figure 3-14: MiniSense 100 vibration sensor

This vibration sensor was placed inside the distal phalange of the little finger to investigate the effectiveness of such a sensor as a slippage indicator. Piezo-electric sensors generate a small voltage spike when deformed. This spike was observed during the slip of a 500 ml soda bottle from the prosthesis' hand. This signal was read by the microprocessor and

plotted with Processing™ software. The typical response can be seen in Figure 3-15. There is an observable spike in the signal when the object starts to slip. This spike ranges from 0.3 to 0.8 V. There is also frequency generated by the slip which averages around 50 Hz. However there is a noise of approximately 50 Hz in the system as well, but this noise has an amplitude of only 0.08 V which can be filtered out in the software.

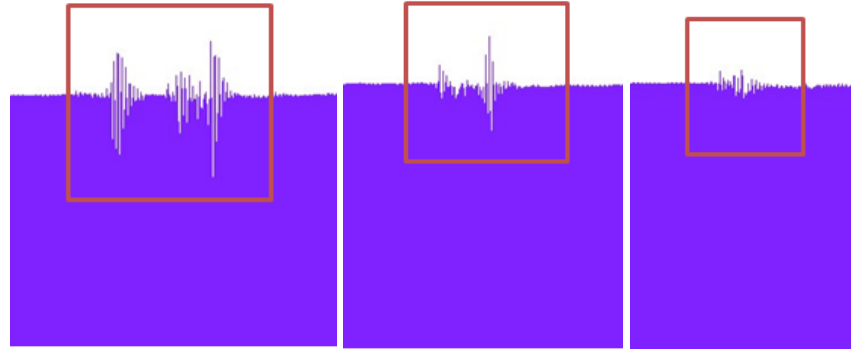


Figure 3-15: Vibration signal at the start of slip

However, the vibration sensor is susceptible to noise in two main forms; natural jerk movements and collisions. These noise creating situations can occur while the amputee is gripping an object and so it is necessary to be able to discern between real slip triggers and false, noise generated triggers. Jerk movements were investigated and plotted in the same way as slippage. The results are shown in Figure 3-16. The natural jerk noise ranges from 0 to 0.3V depending on the intensity of the jerk. This noise is also seen as a spike from the plots, but its shape is very different to that of slippage. Despite its different shape, this noise is difficult to filter out as the shape of the noise is not available in real time.

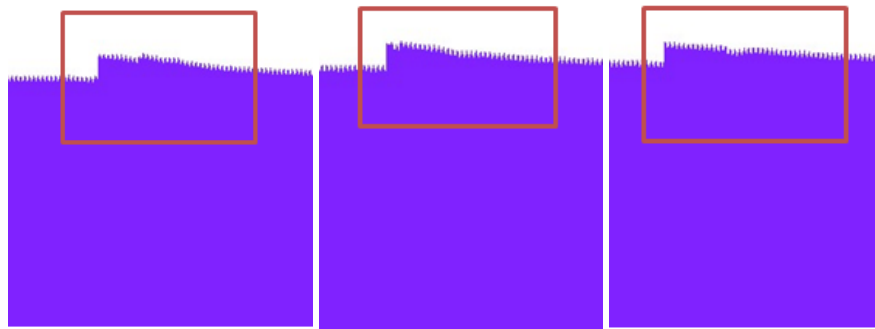


Figure 3-16: Sensor noise resulting from jerk motion

As a natural jerk movement creates noise through its acceleration, and slippage is a frequency signal, the jerk noise can be filtered out by filtering for frequency as well as amplitude. The second form of noise is that of collisions. Large collisions of the prosthetic hand with the external environment could cause more serious problems than dropping the object,

such as mechanical failure of the hand. Three levels of collisions were investigated as a natural and common occurrence that should not result in object drop. Figures 3-17, Figure 3-18 and Figure 3-19 show the result of noise induced through such collisions. These collisions all generate a frequency based noise with a voltage spike increasing to 0.8 V for the heavy collision. However, this frequency, which is in the range of 1 to 2 Hz, is significantly lower than that of the slippage frequency. Therefore filtering for frequency will remove this noise as well.

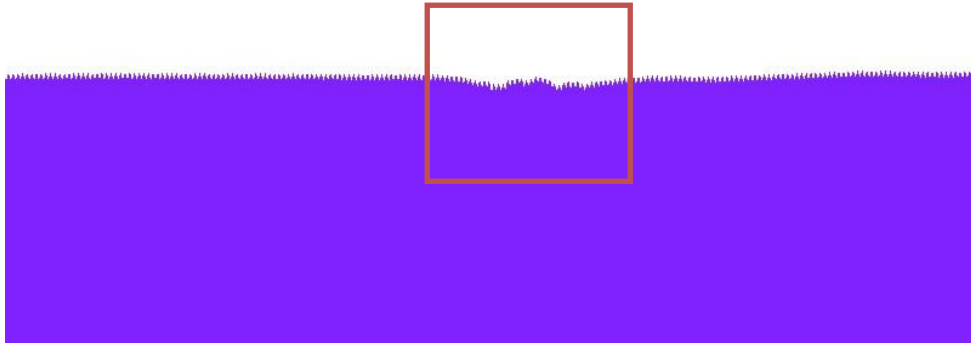


Figure 3-17: Sensor noise from collision 1

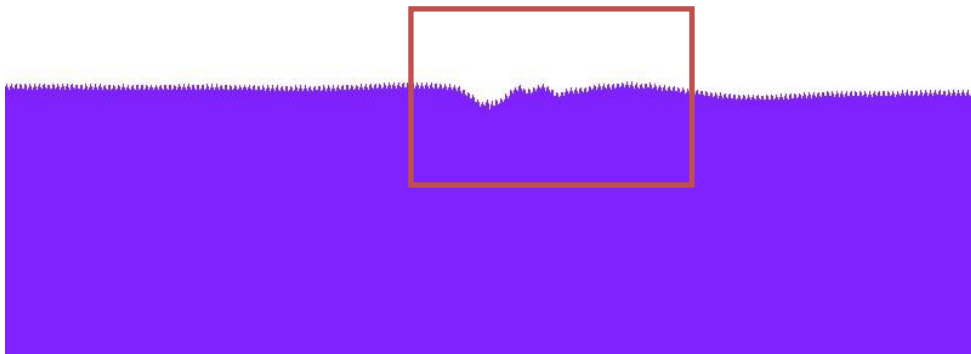


Figure 3-18: Sensor noise from collision 2

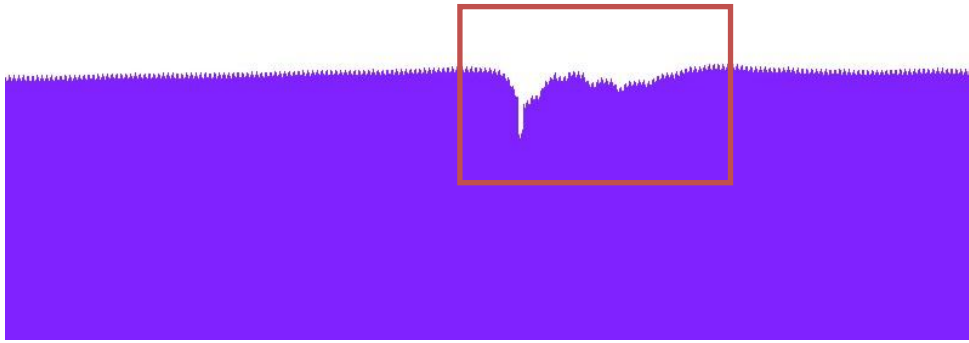


Figure 3-19: Sensor noise from collision 3

As a result of the investigation, it is shown that the vibration sensor is suitable to detect slippage. The signal needs to be filtered for both frequency and amplitude. Slippage information can be filtered in by using a high pass filter set at 40 Hz and a high pass amplitude filter set at 0.3 V. The frequency can be filtered through a high pass filter circuit and the amplitude can be filtered through software.

### 3.1.4 Object texture

An object's roughness is the measure of the vertical deviations as compared to a perfectly flat surface. Both the amplitude and frequency of these deviations is used to quantify roughness. In order to measure texture, the vibration induced in the finger as a result of stroking the object surface was measured. To distinguish between stroking and gripping an object, these vibrations would only be measured if the hand was in an open state. In order to distinguish between object texture and vibrational noise in the environment the texture finger (the little finger) was also equipped with a force sensor. Therefore, object texture vibration is only measured if the hand is open and the texture finger is detecting contact (through the force sensor). The same MiniSense 100 vibration sensor used for object slip was used to investigate texture detection.

Eight different surfaces were tested and their respective frequencies documented to show the difference between different surface textures. These relationships are shown in Figure 3-20 through Figure 3-27. The vibration signal, during the stroke of the surface, is highlighted by a red box.



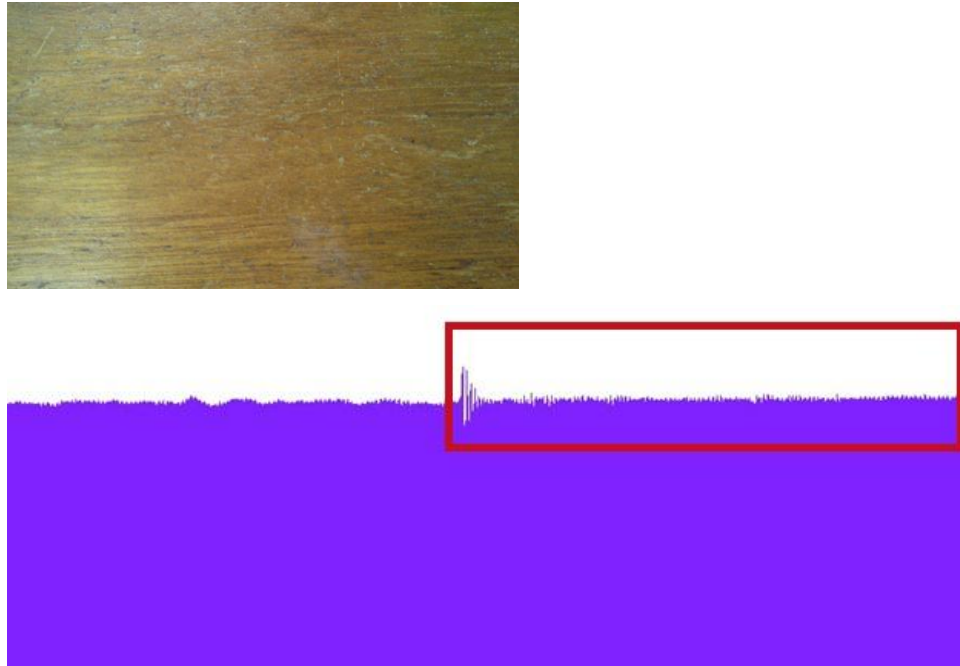


Figure 3-20: Texture vibration signal for smooth varnished wood

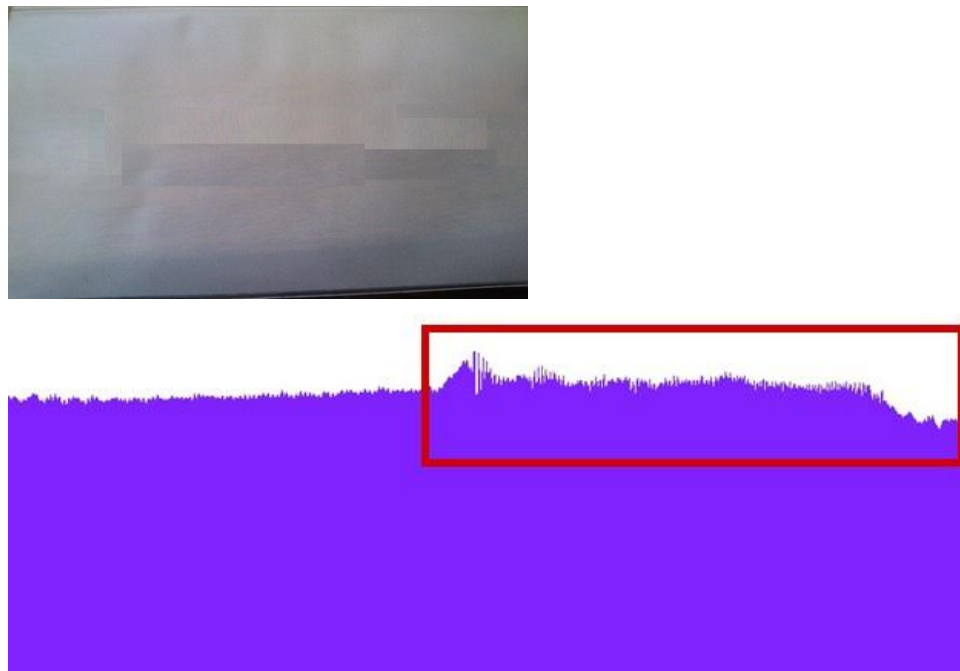


Figure 3-21: Texture vibration signal for semi-smooth plastic

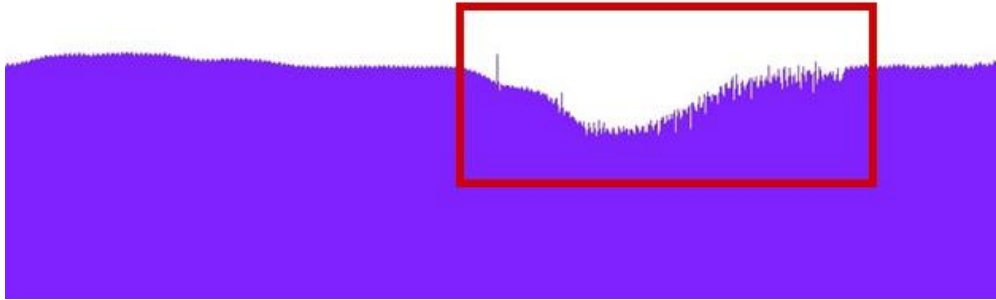


Figure 3-22: Texture vibration signal for smooth ridged plastic

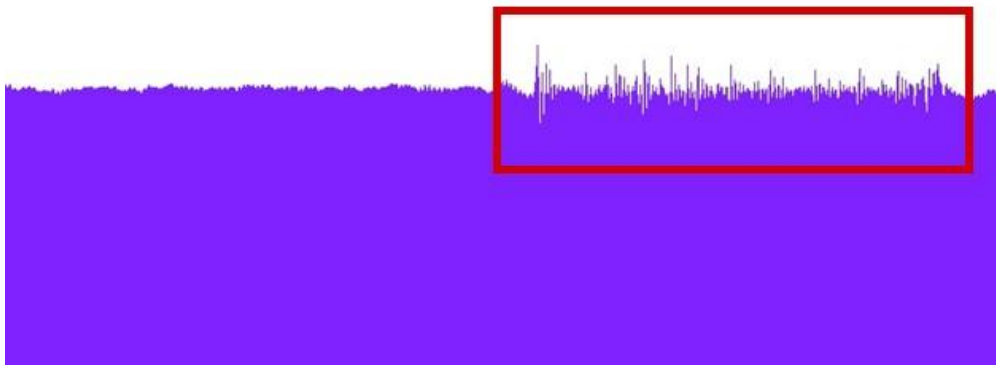


Figure 3-23: Texture vibration signal for smooth metal mesh

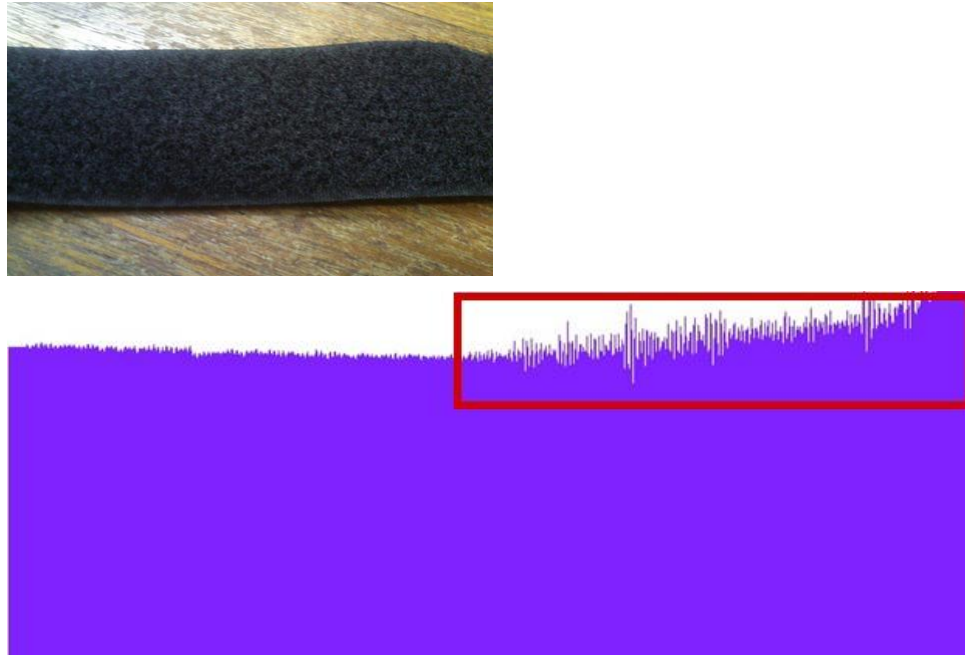


Figure 3-24: Texture vibration signal for Velcro, soft side

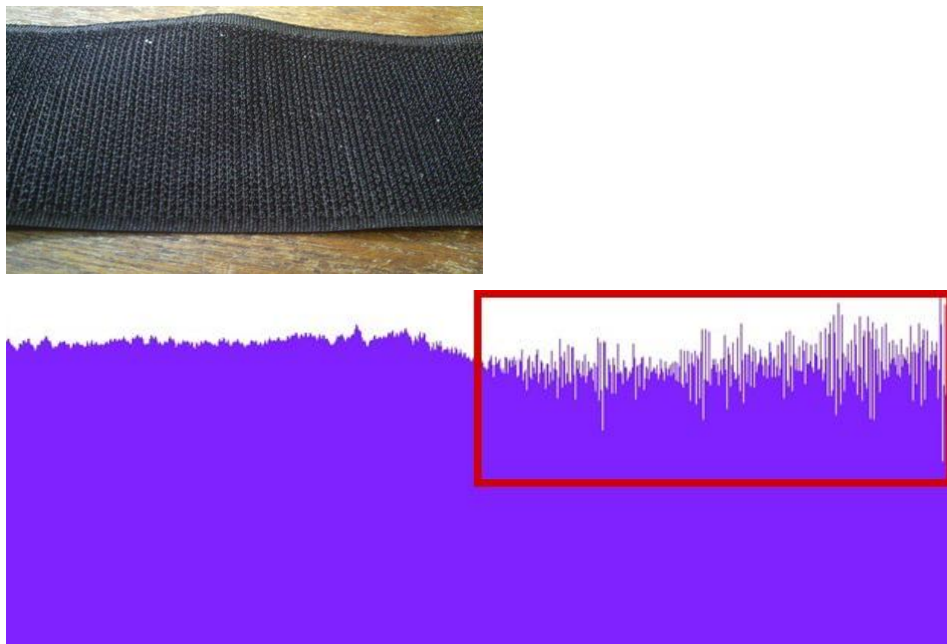


Figure 3-25: Texture vibration signal for Velcro, rough side

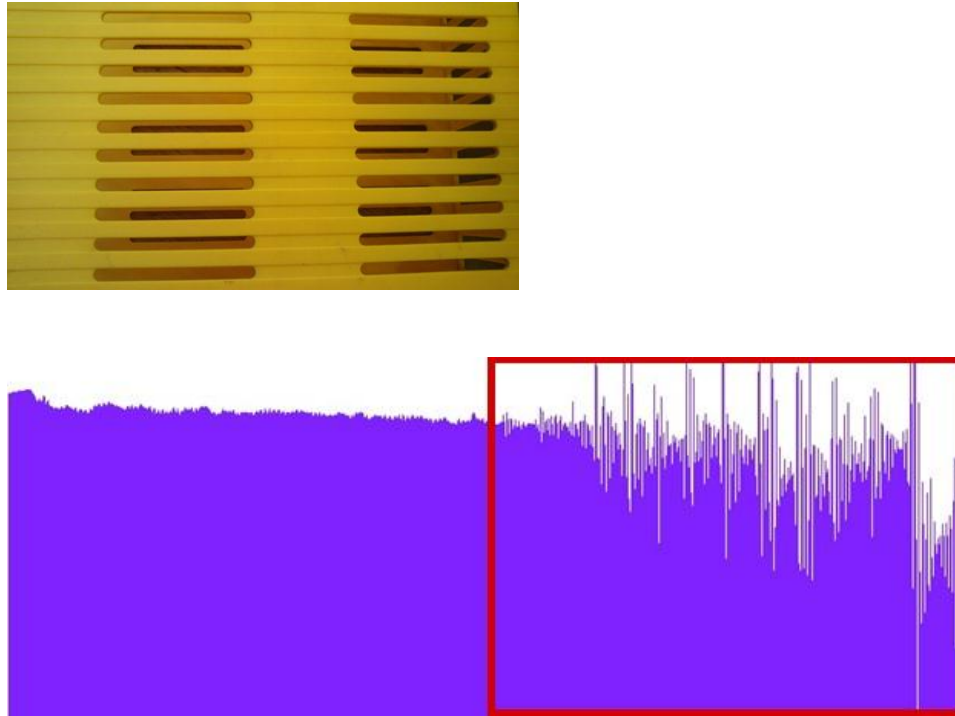


Figure 3-26: Texture vibration signal for bumpy plastic



Figure 3-27: Texture vibration signal for a keyboard

The vibration signal varies in both frequency and amplitude for the different surfaces according to their respective roughness. It must be noted that the frequency of the vibration signal is significantly affected by the relative velocity between the finger and the object. It is not possible to control or measure this velocity. Therefore the frequency cannot be used accurately

to determine roughness. The amplitude of the vibration signal varies proportionally to the amplitude roughness of the surface. The hand's proposed texture sensor is then capable of only distinguishing in part between different surface textures. The investigated system of texture detection is suitable for base texture discrimination between smooth, grainy and bumpy surfaces. In future work, a low resolution system can be drawn up to aid an amputee in distinguishing from such surface types, thus restoring the sense of touch.

### **3.2 Electromyography**

EMG signals are bio-signals generated by muscles in the body when they are contracted. When a human muscle is contracted, a small potential difference is generated between the core and end of the muscle. This voltage can be read with simple surface electrodes that are placed on the skin, directly above the centre and end parts of the muscle respectively (Castellini and van der Smagt, 2009). A reference electrode is also required to equate the skin's natural voltage to ground. The voltage generated this way is proportional to the extent of contraction in the muscle. However, this signal is very small and perfect positioning of the sensors is required to read the signal.

Most amputees retain their muscles in their residual stump, which are ideal for controlling the prosthesis as these muscles were used to control the hand before amputation. The basic dual-channel technique of collecting muscles signals has been kept the same as that of most contemporary upper extremity prosthetics. Two EMG sensors were used to extract the flexion and extension muscle signals from the existing forearm or from the bicep and triceps for transradial and transhumeral amputees respectively. The EMG sensors were purchased from Advancer Technologies and were selected because of their low-cost and ease of integration with Arduino circuit boards. The reference electrode is placed on a neutral/boney location such as the elbow. Figure 3-28 shows one of the EMG electrodes used. The black electrode is the reference electrode, the red electrode is placed over the centre of the muscle and the blue electrode is placed at either end of the muscle.

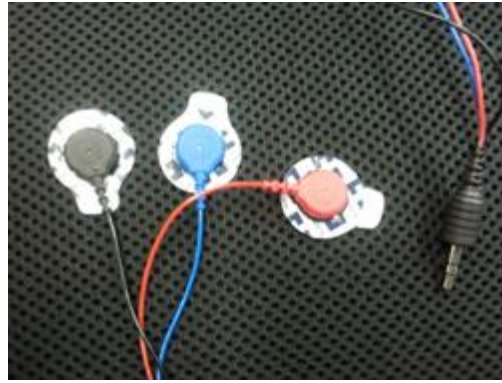


Figure 3-28: Myoelectric sensors

In EMG prosthetics, the prosthetist will conduct an EMG test with the patient to identify the best placement of the EMG sensors. The amputee's prosthetic socket is built with slots in the corresponding areas where the electrodes can be placed comfortably. This method allows for easy wearing of the prosthesis without having to first fit the EMG sensors. For testing purposes the EMG sensors were kept separate from the prosthetic socket. Figure 3-29 shows the electrodes mounted on the surface of a normal human forearm. The signal produced by the raw EMG signal is rectified, smoothed and amplified before it is plugged into an analogue port of the microcontroller. Filtering of the EMG signal is done digitally.



Figure 3-29: Surface mounted electrodes on forearm

### 3.3 Haptic feedback and user interfacing

Feedback is important in prosthetics as it is used to share information collected by the sensors in a prosthetic hand with its user. This feedback is vital for the controlled use of a prosthetic limb as well as allowing the prosthetic limb to be used for explorative and manipulative purposes. In doing so a prosthetic limb comes closer to being a complete replacement for the human limb (van der Riet et al., 2013a).

When someone loses a hand through amputation, they do not only lose their ability to manipulate objects but also their ability to explore their environment. Vibrotactile feedback technology is cheap and non-invasive (Rombokas et al., 2013). Therefore vibrotactile feedback is an important research focus area as it can provide a simple, low-cost solution to the sensory feedback problem in contemporary commercial myoelectric prosthetics. Research has shown that Vibrotactile feedback improves the ability of grip force control in manipulation tasks using EMG control (Rombokas et al., 2013). It has also been found that slip feedback information has equal to greater value than grip force control (Witteveen et al., 2012).

Vibrotactile feedback in literature generally uses two main components to communicate feedback. These two devices are tactors or vibration motors (Witteveen et al., 2012). A tactor displays vibrotactile feedback through amplitude modulation perpendicular to the skin and its frequency can be easily controlled. 250 Hz has been proved to be the most sensitive frequency on human skin (Rombokas et al., 2013). Vibration motors use a rotating internal mass to create vibrations at a tangent to the skin and are significantly less expensive than tactors. Vibration motors have shown comparable results to that of tactors despite their lower accuracy in frequency control applications (Witteveen et al., 2012). Vibration motors have shown promising two-site spatial discrimination results with accuracies around 90% (Cipriani et al., 2012). Vibration motors were selected for haptic feedback because of their lower cost.

Simultaneous multi-sensory feedback for upper extremity prosthetics has not been described before. Studies have explored more than one feedback sense, such as grip force and slippage. However, these studies have not attempted to communicate both of these indicators simultaneously (Witteveen et al., 2012).

### **3.3.1 Methodology**

In order to communicate through a haptic interface with a person, there needs to be a set communication protocol in place (van der Riet et al., 2013a). A protocol based on the location and the duration of vibrations within a short period of time was designed. The location on the forearm of the vibration represents the sense being communicated and the duration of the vibration represents the intensity of that sensation.

#### **3.3.1.1 Sensory extraction**

Sensory data for the grip force, object slip, object temperature and object texture is all available from currently available sensors (Fishel and Loeb, 2012). The sensors used are capable of detecting grip forces between 0 N and 20 N, slippage from no slip (0 mm/sec) to great slip (100 mm/sec), object temperature between 35 °C and 100 °C and texture from smooth to rough. These ranges can all be measured with currently available sensors. In order to remove



unnecessary variables, all sensor data was simulated, creating a controlled environment which was only dependent on the haptic feedback and the test subject's ability to interpret it.

### 3.3.1.2 Feedback design

The vibrotactile feedback system was designed using four 3.4 mm button-type vibration motors. The button-type motors were chosen because of their low-cost and simplicity. The vibration motors are used to communicate the four different sensations; grip force, object slip, temperature and texture. The intensity of each sense is displayed by the length of a pulse of vibration within a 1500 millisecond pulse. The vibration frequency is fixed at 200 Hz. As the sense intensity increases the length of the vibration pulse increases proportionally.

Figure 3-30 shows the circuit design. Four digital I/O pins were used to control the four vibration motors. A surge protection diode was used to protect the power source. The BC337 transistor was selected as a suitable low power transistor.

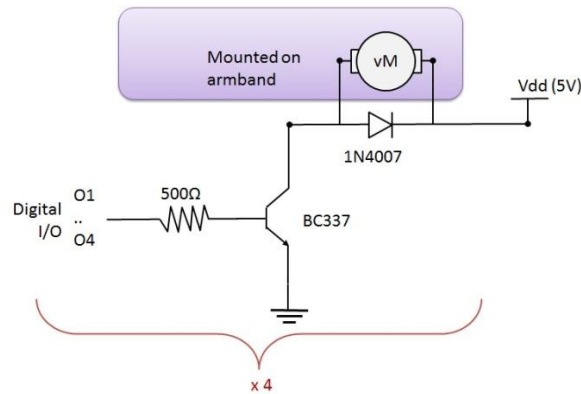


Figure 3-30: Circuit design for the haptic feedback armband

The current limiting resistor was used to protect the MCU and was calculated by selecting the base current limit of 10 mA and the output voltage of the MCU (5 V), as seen in Equation 3-6.

$$R = \frac{V}{I}$$

$$R = \frac{(5)}{(0.01)} = 500 \, \Omega \quad (3 - 6)$$

### 3.3.1.3 Placement

The vibrotactile armband, seen in Figure 3- 31 (van der Riet et al., 2013b), was designed to be fitted inside the prosthetic socket of the amputee or placed elsewhere on the amputees arm. If the vibration motors are placed in the prosthetic socket, they would need to be suspended in the socket so as to prevent any vibration from moving into hand. The armband provides a



compact solution to the haptic feedback problem in prosthetics. It has been shown that spatial discrimination can be successfully used in vibrotactile displays (Cipriani et al., 2012). For this reason the four vibration motors are placed 90 degrees apart around the test subject's forearm. The placement allows for the test subject to use spatial discrimination to discriminate between the four different senses. The corresponding position of each different signal on the arm can be seen in Figure 3-32.

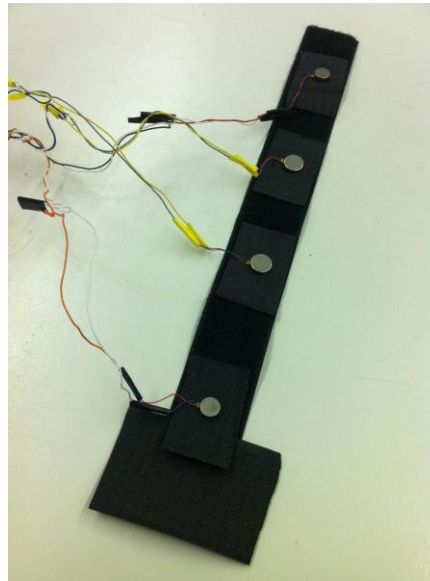


Figure 3-31: The vibrotactile armband

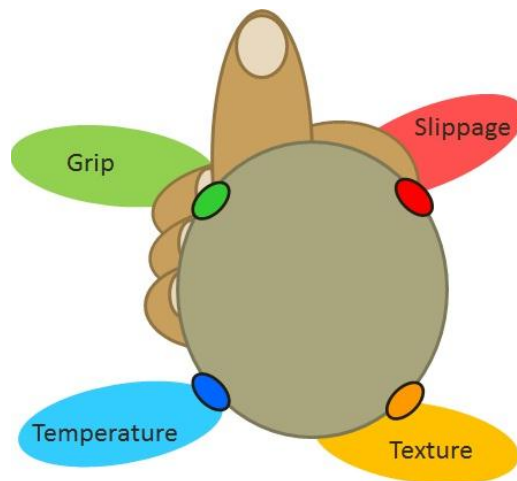


Figure 3-32: Haptic feedback placement on transradial amputee

### 3.3.2 Haptic user interfacing

HUI refers to a method of communication between the prosthetic hand and the amputee. The HUI system uses a haptic medium (vibrotactile motors) to display information to the

amputee in place of a visual display. This allows the amputee to free up his vision for other tasks and allows a more natural (haptic) communication between the prosthesis and the amputee. This communication method and its corresponding navigation menu are detailed in the Control chapter. The HUI system uses a similar approach of communication to that of the sensory feedback. It uses an addition two vibration motors to communicate with the user. The placement of these vibrators in relation to all the other haptic feedback devices is shown in Figure 3-33 with the extension vibration (referring to an upward navigation in the menu) on the top and the flexion vibration (referring to a downward navigation in the menu) on the bottom of the forearm. This design allows the HUI vibration motors to fit inside the amputees socket along with the sensory feedback vibration motors. It is possible to move the vibrotactile displays to any part of the body to allow for customizable, best-fit solutions.

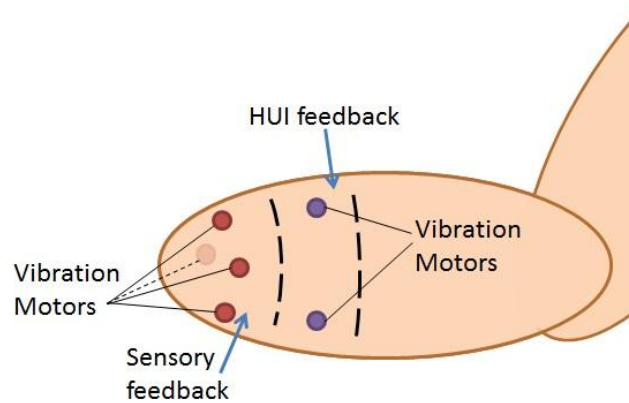


Figure 3-33: Haptic feedback placement on transradial amputee

### 3.4 Actuating and position feedback circuitry

All mechatronic projects contain some moving parts that are controlled through the electronic circuitry. This is normally done with the aid of a microcontroller and drivers. A closed loop control setup is required for accurate movement of the moving parts in the mechatronic system. Closed loop control is achieved through some form of sensory feedback regarding the movement of the mechatronic system. These aspects of the mechatronic design are discussed in detail in this section.

#### 3.4.1 Electronic hardware integration

Motor drivers were required to run the motors in the hand. The stall current on each motor is 1.6 A thus a motor driver needed to be selected that could handle 1.6 A. The TB6612FNG Dual H-bridge motor drive has a 1.2 A current rating per channel with a peak of 3.2 A per channel (“TB6612FNG,” 2007). It was also the most cost effective driver as a single

board drove two motors. Figure 3-34 shows the selected motor driver. It must be noted that these drivers are not suitable to high voltage motors that could draw more than 3A of stall current.

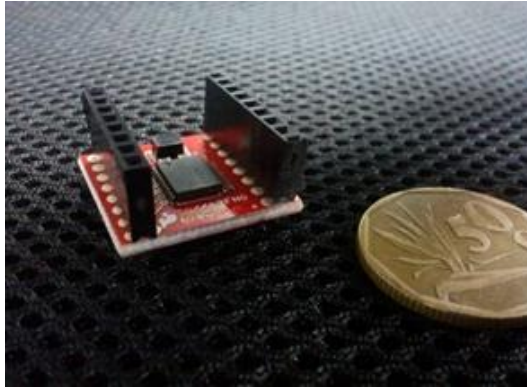


Figure 3-34: TB6612FNG Dual motor driver

A stacked layout for assembling the components in the hand was designed. The first layer housed the actuation. For the second layer a 2 mm perspex mounting plate was bolted to the mounting holes positioned on the palm unit. The microcontroller and circuitry were mounted on this perspex mounting plate. Figure 3-35 shows the microcontroller mounted onto the clear perspex plate.

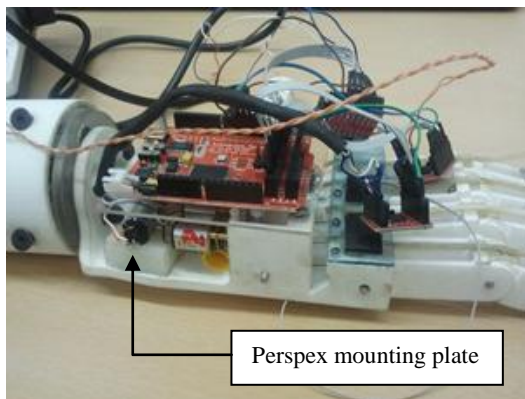


Figure 3-35: Multiple layers involved in assembling the hand

Once the final position of the microcontroller and motor drivers assembly was established it was possible to implement the wiring needed to connect all the components. A custom wire ribbon was created to tighten up the wiring and ensure reliable connections. Figure 3-36 shows the wiring ribbon created to connect the motor drivers to the microcontroller.



Figure 3-36: Custom wire ribbon used to connect

The new wiring ensured that the hand looked neat and that all connections were secure. The hand also utilized resistive flex sensors for position control. Figure 3-37 (Spectra Symbol, 2014) shows a photo of the flex sensors used. The flex sensors reduce their resistance in proportion to the degree that they are bent. They were placed along the length of each finger so that they bent with each finger. The flex sensors allowed the position of each finger to be accurately tracked.



Figure 3-37: 4.5" Flex sensors used for position control of the fingers

A voltage divider circuit was used to convert the flex sensor's resistance into a readable analog voltage signal which was read by the microcontroller. The voltage divider circuit was soldered onto Vera-board and mounted on the perspex plate as shown in Figure 3-38. The flex sensors allowed for a closed loop control of the motors.

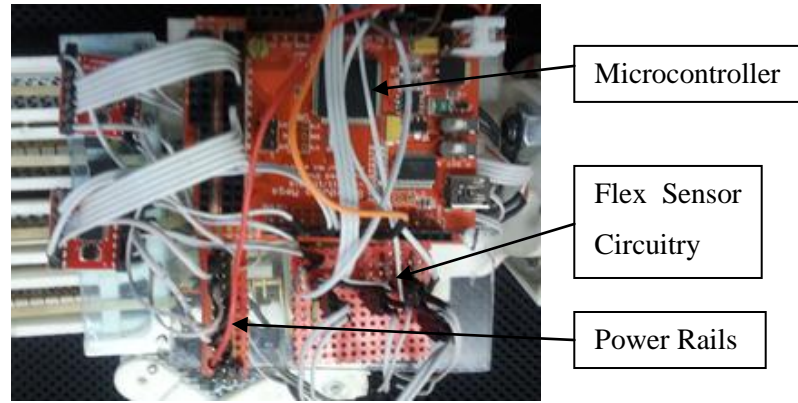


Figure 3-38: Complete electronics layer

It was important that the actuation system layer and the electronics layer did not interfere (mechanically or electrically) with one another. All wiring had to be kept well away from entangling with the moving parts on the actuation system layer. The mechanical layer should not affect the electronics by means of vibration and electromagnetic interference. During the electronic testing phase of the hand it was confirmed that no significant interference was observed. The cables connecting to the servo motor in the wrist were given enough slack to allow for the 90 degree rotation of the wrist in either direction.

### 3.4.2 Complete assembly of the hand

The complete physical assembly of the hand was brought together once the actuation and electronic layers were complete. The hands overall dimensions are in essence anthropomorphic, however it remains minimally larger than that of an average human hand. The complete assembly of the hand is shown in Figure 3-39.

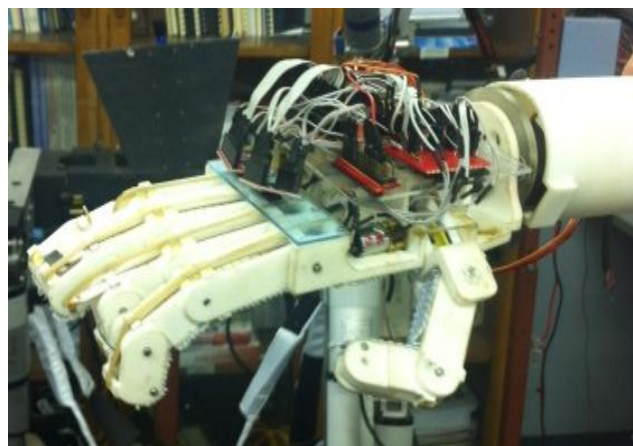


Figure 3-39: Complete assembly of the hand incorporating both actuation and electronic layers

### 3.5 Chapter summary

The electronic design of the prosthetic hand represents a simple, cost effective solution to the sensing, control and actuation of the hand. The hand is equipped with simple, low-cost sensors that are well suited to measuring all the required tactile information from the environment to provide the amputee with a sense of touch. The force sensor is of greatest importance as it offers critical information of the grip strength of the prosthetic hand to the wearer. Grip force information allows the amputee to be able to grip both fragile and heavy objects more effectively. Grip force feedback minimizes the failed grips, especially when coupled with a slippage sensor. The temperature sensing is also an essential sensory feature as this can inform the amputee of contact with dangerously hot objects that could harm the amputee and damage the prosthesis. It also can provide very useful information as in determining whether a hot beverage is still hot or a cold drink is still cold.

Electromyography is a tried and proven method for extracting muscle signals from a patient. The use of the residual muscles in the amputees stump is effective in mimicking the natural way in which the body controls the limbs, as the brain is used to sending signals to the muscles to control the hand. Through the suggested EMG extraction of these signals, the brain simply needs to learn the new combination of muscle movements to control the prosthetic limb. Haptic feedback was proposed in this chapter as a suitable form of communication between the prosthesis and the amputee. With the aim of developing a non-invasive prosthesis, sensory communication becomes complicated as the nervous system is the natural communication channel of the body. The skin provides a communication interface between the prosthesis and the amputee. With this method the amputee needs to learn to interpret the skin's vibrotactile stimulation as the transmission of information.

The actuating system uses low-cost closed loop control through the use of the resistive flex sensors. These sensors effectively track the degree of flexion in each finger and allow for simple integration with the microcontroller through a voltage divider circuit. The Seeeduino Mega was selected as a cost effective microcontroller that offers easy configurability. All of the electronic systems work off 5 V and integrate well. The drivers and motors in the hand were suitable for basic gripping tasks. However, if a stronger grip is desired, the drivers would need to be replaced with ones rated for a higher current. A 5 A rating is recommended for each motor driver running a 12 V motor.

## 4. CONTROL

---

The artificial intelligence (AI) of the prosthetic hand plays two key roles. It runs and manages all the systems on the prosthetic hand (movements and positions, hand sensors, and haptic displays) and it creates a platform for the amputee to control the prosthetic hand. The ability to control a prosthetic arm has always been a major limitation in the field of prosthetics. Replacing a person's brain's natural way of controlling limbs through the nervous system is a great challenge as the method of moving one's limb is a very intuitive function. With most EMG pattern recognition systems, the user's movements are coupled directly with a grip function in the prosthetic arm. Another method to control the prosthetic arm uses a very simple interface which chooses between two grips, as is found in contemporary commercial prosthetics. The role of the hands AI is to simplify control while keeping it intuitive and to effectively and efficiently manage all the other systems on the prosthetic hand.

### 4.1 Haptic user interface

The main challenge in controlling a prosthetic arm is getting it to adapt to different situations. The task of simply opening and closing the hand in a fixed grip is rather simple as the number of inputs available to the user matches the number of outputs. The control of the prosthetic arm becomes significantly more complicated with each new freedom introduced to the prosthetic arm as the number of inputs becomes less and less than the number of outputs. An EMG control system that targets the muscles in the amputated arm generally has access to 2 inputs, flexion and extension. This could be flexion and extension of the wrist or forearm, depending whether the amputation is transradial or transhumeral. In most amputations, targeting these muscle groups gives two inputs of variable strength that can be used to control the prosthetic arm.

#### 4.1.1 Navigation

The proposed system creates a HUI with the user, allowing him/her to navigate through a menu of possible grips and muscle movements and then control the selected option directly. This solution allows the user to operate an unlimited number of grips and muscle movements separately. The infinite scale of the control structure is because a list containing infinite items can theoretically be created. The size of the list does not correlate to the ability to select the first items of the list. Rather as the list size increases, the items on the end of the list become increasingly more difficult to access. An overview of the menu designed for the prosthetic hand can be seen in Figure 4-1. The HUI menu is navigated using the flex and extend inputs given by the controlling muscles. These input signals can be entered separately to navigate "up" and "down" through the menu. The flexion for the wrist has been assigned to the "down" command



and extension to “up”. Selection is done by inputting both signals simultaneously and the user can exit back to the “home” position by giving 2 pulses of both inputs. This “home” position can be seen as the darker blue in Figure 4-1.

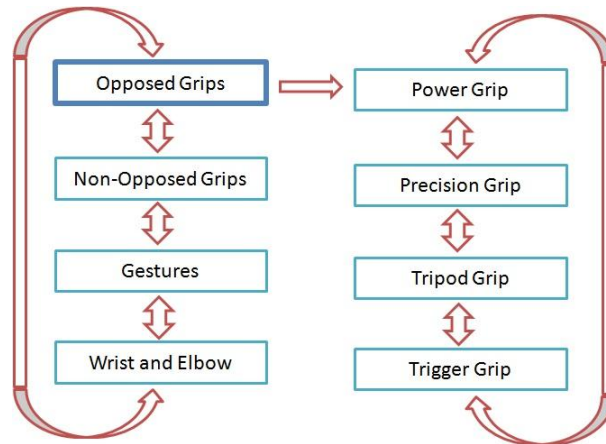


Figure 4-1: Flow diagram example of HUI menu navigation

During training the user will operate the prosthetic hand in front of a computer screen which will be connected to the prosthetic arm. The screen will show the current position in the menu. This training will be done with the accompanying vibration feedback. The menu will always start in the same “home” position, allowing a sequence of navigation commands to be memorized to access a desired command. For example, the input sequence “select”, “down” and “select” would activate the precision grip. Figure 4-2 shows the full menu available in the designed system. After repeated use of the system it is expected that these sequences will become very natural and act as a type of muscle memory. The gesture tab can be expanded to contain a large variety of different gestures in a preset format. The current menu holds seven preset grip types and four independently controllable hand gestures that give it a total of 19 unique hand positions and grip types, excluding the wrist and elbow commands.





Figure 4-2: Overview of HUI menu

Once a grip has been activated, the hand will adjust to the appropriate open grip position. The flex and extend signals will now control the closing and opening of the hand and be sensitive to proportional values to control the grip strength. If a “back to home” command is given the navigation system will first exit to a command menu, as seen in Figure 4-3. This command menu will allow the user to combine useful manipulation commands like rotating the wrist or flexing the wrist or elbow. During these alternative commands the final state of the hand will be maintained. For example, if the amputee wishes to pour a glass of water from a bottle, the amputee would first grip the bottle as usual. Once the bottle is gripped, the amputee can then exit to the command menu and can select the wrist rotation option. The amputee can use the wrist rotation to then pour the bottled water into a glass without dropping the bottle. The hand will automatically maintain the grip on the bottle while the user controls the wrist rotation.

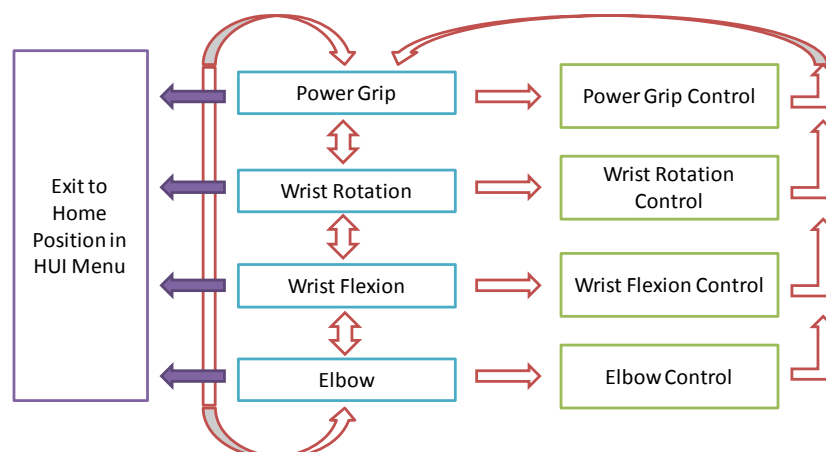


Figure 4-3: Flow diagram of HUI menu navigation

### 4.1.2 Feedback

The user will be informed of every command by means of an appropriate vibration. The two vibration motors used for HUI relate to the two input signals that the user uses to navigate through the HUI menu. If a flexion/extension signal is read, the navigation position will move in the flexion/extension direction and the flexion/extension (“down” / “up”) vibration will be given indicating the successful change in menu position. The HUI feedback will only be used while the user is in the menu. The sensory feedback will be used during grip operation.

A summary of the navigation commands and their corresponding haptic feedback can be seen in Table 4-1.

TABLE 4-1: AVAILABLE INPUTS FOR HUI CONTROL

| <b>Action</b>        | <b>Flexion Signal</b> | <b>Extension Signal</b> | <b>"Up" Vibration</b> | <b>"Down" Vibration</b> |
|----------------------|-----------------------|-------------------------|-----------------------|-------------------------|
| <i>Move Up</i>       | No                    | Yes                     | Short                 | No                      |
| <i>Move Down</i>     | Yes                   | No                      | No                    | Short                   |
| <i>Select Option</i> | Yes                   | Yes                     | Short                 | Short                   |
| <i>Back to Home</i>  | Double Pulse          | Double Pulse            | Long                  | Long                    |
|                      |                       |                         |                       |                         |
| <b>In Grip</b>       | <b>Flexion Signal</b> | <b>Extension Signal</b> | <b>"Up" Vibration</b> | <b>"Down" Vibration</b> |
| <i>Close</i>         | Yes                   | No                      | No                    | No                      |
| <i>Open</i>          | No                    | Yes                     | No                    | No                      |
| <i>Exit to Menu</i>  | Double Pulse          | Double Pulse            | Double Short          | Double Short            |

Only four different input patterns have been taken from the two inputs in order to keep the system simple and to allow for easier tracking through the system using the haptic feedback. In future work the system could be implemented using a pattern recognition system as well, allowing quicker access to desired commands. The logic flow diagram used to extract the pulses used in the HUI navigation from the EMG signals is shown in Figure 4-4.

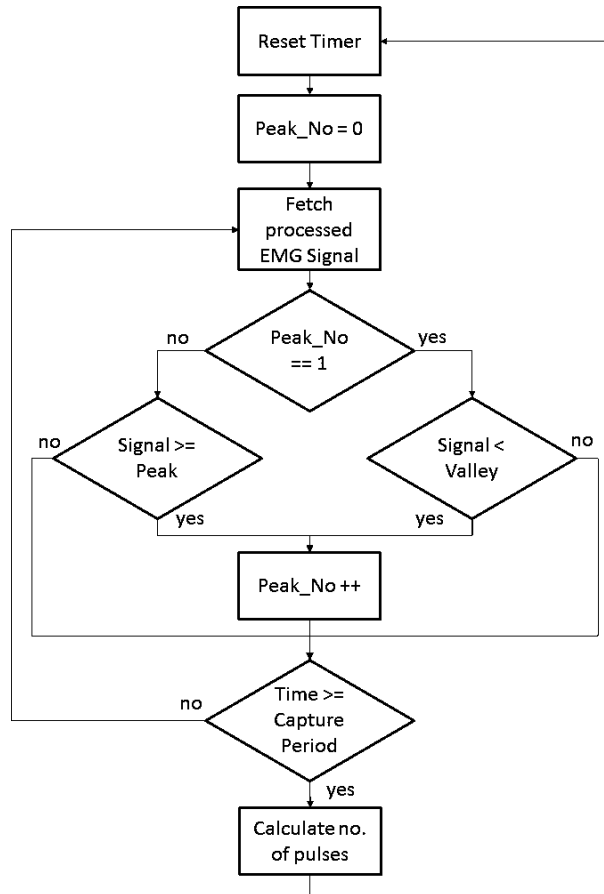


Figure 4-4: Logic flow diagram of pulse counting loop

### 4.1.3 Training

The process of learning the HUI navigation menu requires training. A program has been written to visually display the HUI menu on a computer screen. This program is then run in conjunction with the use of the prosthetic hand for the training period, until the user has memorised the menu. The training technique focuses on motor learning of the muscles being monitored by the EMG sensors. As with all motor learning cases, motor retention is best taught through repetition of tasks during which the tasks become more and more natural to the user. It is the goal of the HUI system approach to control that the memory of the system will migrate completely from working memory to muscle memory.

## 4.2 Electromyography

The algorithm was designed to control the prosthetic hand grip. This was written in C programming language. Figure 4-5 shows the flow diagram for a single grasping operation.

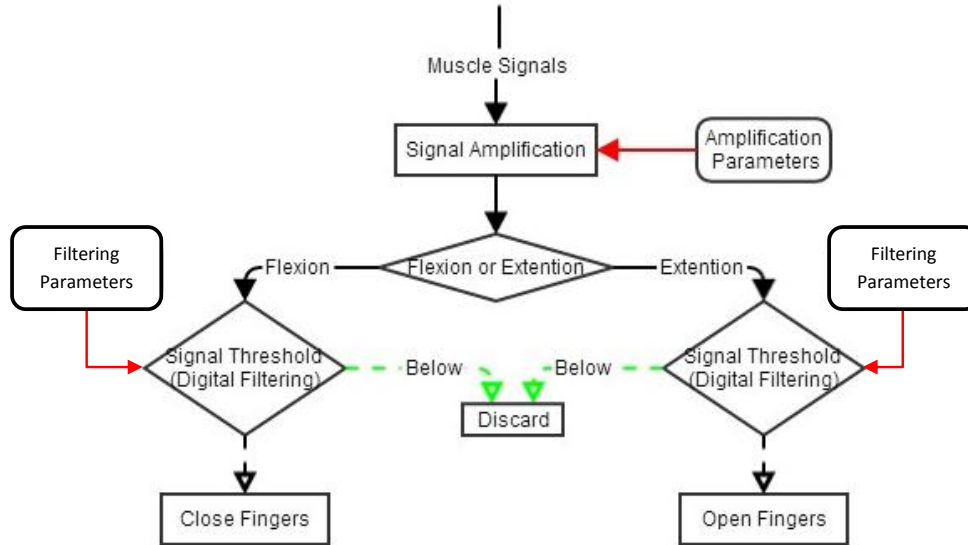


Figure 4-5: Flow diagram for single grasp controlled by muscle flexion or extension

Each amputee has differing signal levels due to the size and strength of the residual muscles, thus causing an inconsistency in the grasping motion. To account for this variation in signal strength and quality the code needs to be calibrated to each amputee's unique signals. Amplification parameters are programmed to account for differing muscle signals and filtering parameters are programmed to cancel out any interfering noise. The amplification and filtering parameters are directly linked since increasing amplification means increasing the vulnerability to noise thus more filtering is needed. Successful implementation of this control system required rigorous testing to achieve repeatable results.

#### 4.2.1 Calibration and filtering

The EMG signal generated by an individual is unique. In order to correctly read an individual's EMG signal the sensors need to be calibrated and filtered. The calibration and filtering parameters need to be adjusted according to each individual. Slight adjustments are also required every time the sensors are reconnected to the muscle as the signals vary with muscle fatigue, sensor placement and arm position (Castellini and van der Smagt, 2009). The EMG signal received by the micro-controller has been rectified and smoothed. This signal however still has a slight tremor as the muscles themselves do not give off a consistent voltage. The strength of the voltage signal varies greatly from person to person. To convert any extracted EMG signal into a meaningful instruction it is necessary to smooth and amplify the received EMG data.

Smoothing is done by calculating a moving average of the signal based on a RMS calculation performed on the most recent data collected in a set time frame. This time frame is

referred to as the “smoothing window” of which the signal is viewed. The larger the window, the more steady and reliable the signal will be to a point, until the window starts to smooth out important data. However the larger the window, the larger the delay in response of the prosthetic hand will be. The smoothing window size relationship is shown in Figure 4-6. The ideal window size will vary from individual to individual depending on the signal received from his/her muscles. The position of the peak of the accuracy plot on the graph depends on the user’s muscle tremors. A user with a larger muscle tremor will require a larger smoothing window to produce the most accurate results.

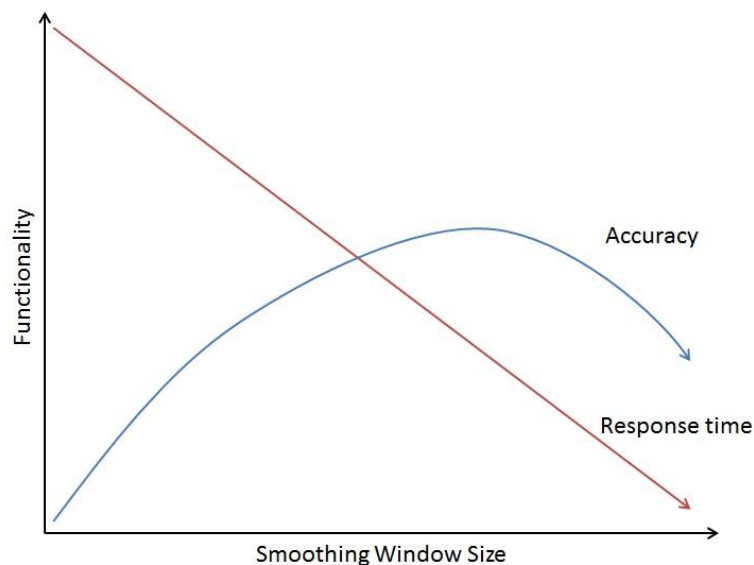


Figure 4-6: Functionality vs smoothing window size for accuracy and response time

Once the correct smoothing has been performed on the EMG signal, it is necessary to map the signal so that it falls within the preset range expected by the controller. The user is required to perform maximum flexion tasks in order to measure the maximum signal the muscle is capable of emitting. The user is encouraged to only perform these tasks to the extent that is comfortable and easy to perform repetitively. These inputs are mapped to the standard range expected by the controller. Each muscle requires individual mapping as they will generate different amplitudes. A correctly calibrated hand allows the user to control the speed and grip force of the prosthetic hand through the changing degree of muscle flexion.

Users also differ in their ability to generate pulse values. Both the frequency and amplitude of muscle pulsing differs and needs to be individually calibrated. The user is asked to perform “pulsing” tasks with his/her muscles, and the frequency and amplitude of these pulses are measured and calibrated into the control system. Filtering is performed by measuring the amplitude of the muscle signal when the muscle is at rest. The maximum amplitude is then taken with a safety factor of 1.5 and used as the high pass filtering threshold. It was found that a

typical value of 5% to 15% of the maximum flexion signal is needed to effectively filter the EMG signal. The calibration of the prosthetic hand takes around 30 minutes to perform manually for a first time user. Once the user's calibration is saved only minor calibration is required every time the sensors are reconnected. It is possible to reduce this time through the development of a specialized calibration and training program that will allow the hand to self-learn the user's individual parameters.

### 4.3 Position control

The motor drivers required two digital inputs along with a single pulse width modulation (PWM) signal to operate the motors. The control algorithm was written in C programming language. Figure 4-7 shows the flow diagram of the program used to control the motors.

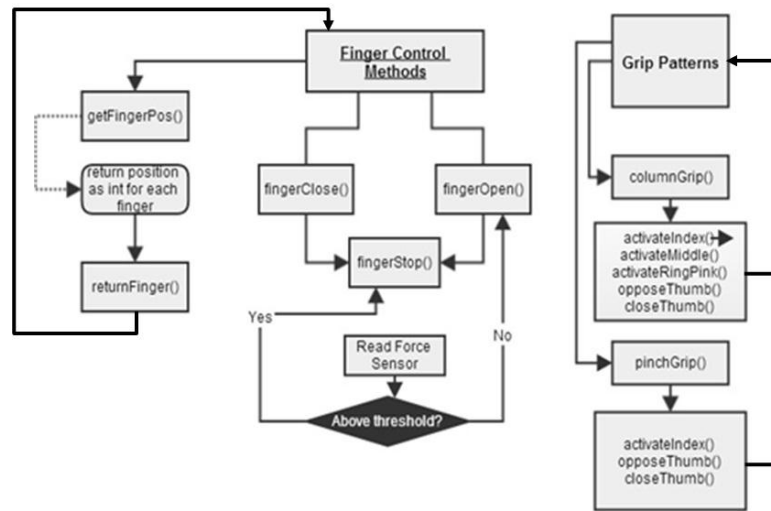


Figure 4-7: Execution methods to be implemented in motor control algorithm

The fundamental motor control code is accessed by the microcontroller when executing the users command. This code is then relayed to the motor driver which executes the motor commands.

Control of the fingers was vital to successful grasping and repeatable results. Since the fingers were actuated by means of a pulley and cable it was imperative that the controller prevent the motors from over-spooling. Over-spooling is caused when the cable slips off the pulley and entangles with the gears, causing a loss of actuation. To prevent this problem, a closed loop control was implemented over the position of the fingers. As each finger has a single degree of freedom (degree of closure), a simple flex sensor was capable of quantifying this variable for each finger. Each finger required individual calibration of its flex sensor position to set fully open and fully closed positional values. The microcontroller continually

checked the value of the flex sensor and stops the finger's motor when the finger crosses the open or closed threshold. By using the software to limit the flexion and extension of the fingers, the controller protects against unravelling of the cable spoil.

### 4.3.1 Grip control process

As the degree of closure is always known by the flex sensors, it is possible for the prosthetic hand to correctly position itself for a new grip. The position control also allows for the addition of proprioceptive sensory feedback of the fingers if desired. The grip control is done through an open loop control system on the controller closed by the user. The user is informed of the current status of the grip through the grip force and slippage haptic feedback as well as visual information from observing the hands position relative to the object. The user can then decide to close or open the hand at varying degrees accordingly. This relationship is shown in Figure 4-8 in the closed loop format.

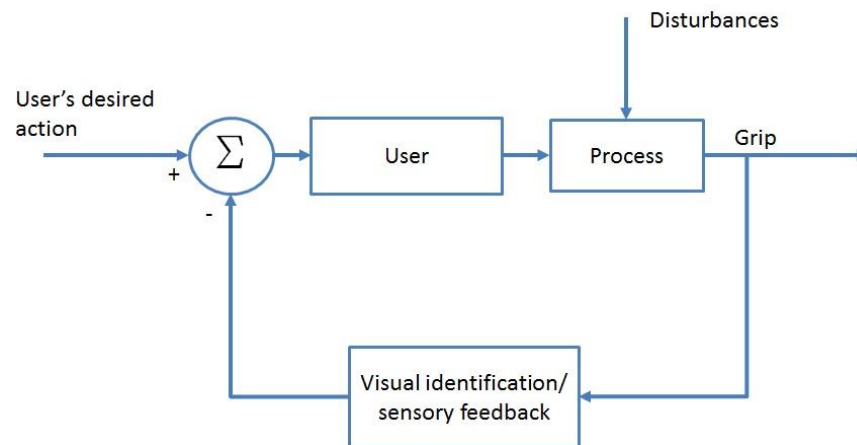


Figure 4-8: User's closed loop control of hand grip

In Figure 4-8 the input of the action is the “user’s desired action” which is weighed in with the degree of completion of this action as measure by the Visual identification/ sensory feedback box. The user replaces the controller in a traditional closed loop control structure as he/she needs to make the decision as to what further action to take. The user communicates his/her desires though the EMG signals read by the prosthetic hand which makes the hand respond accordingly. There are also external disturbances such as noise in the system, inaccuracies in the motors etc. which can affect the outcome.

## 4.4 Haptic sensory feedback

It is necessary to design a communication protocol in order to communicate with the user (van der Riet et al., 2013a). A single vibration motor is allocated to each sensory channel as

mentioned in chapter 3 (Electronic Design). The communication protocol needs to be able to communicate the corresponding sensor value to the user using this single vibrotactile channel.

It has been shown that vibrotactile devices create waveforms in the skin. These waveforms can be sensed up to 80 mm away within the skin (Jones et al., 2010). This doesn't affect single motor systems, but becomes increasingly problematic as the number of vibration motors communicating unique messages increases. Every vibrotactile channel creates its own noise through these vibrational waves. These waves can reach the site locations of other vibrotactile channels.

To solve this problem, the communication system was designed using the maximum vibration frequencies. This system allows each vibrotactile channel to create a noticeable vibration peak of greater intensity than the surrounding noise. Each of the four channels (grip force, slippage rate, object temperature and object texture) are synchronised to start vibrating at the same time. This sequence is repeated every set period of time. The communication protocol is shown in Figure 4-9 (van der Riet et al., 2013b).

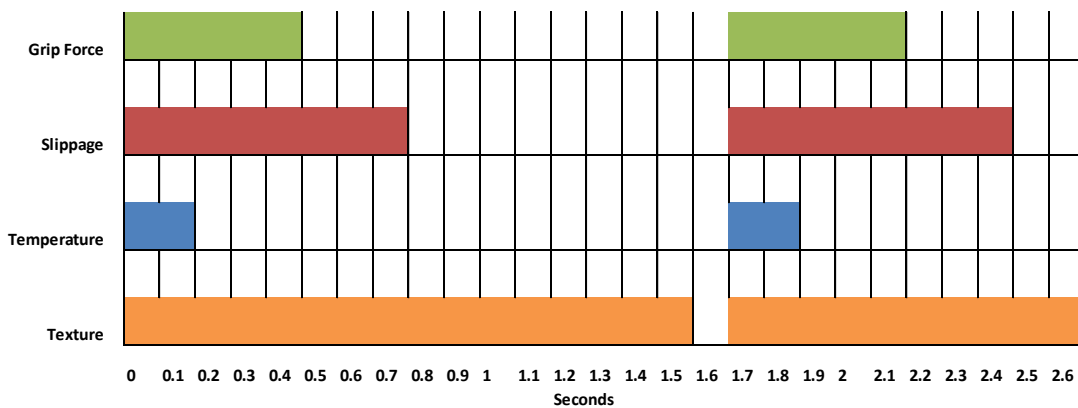


Figure 4-9: Example of the vibrotactile communication protocol

The set period used in the example shown in Figure 4-9, was set to 1.5 seconds. Each sense is active (sensing a signal) and represents a different value (depending on what is being sensed by the sensors). The length of the vibration shown in Figure 4-9 corresponds linearly to the intensity of the appropriate sense. As seen in Figure 4-9, texture has the greatest intensity (100% of the time period) and represents a very rough object surface. The temperature (active for 0.2 seconds which is approximately 10% of the time period) represents an object temperature of 42 °C. Object slip (0.8 seconds) is at 50 mm/sec. The grip force (0.5 seconds) is at 7 N.



## 4.5 Chapter summary

The AI in the hand has three core objectives: functional and efficient control of the prosthetic hand; position control of the hand; and sensory feedback. These objectives are all efficiently met within the code run on the microcontroller. The HUI system provides a familiar, scalable menu system that enable users to select from a pre-set list of grip types or other hand functions while still allowing 2 DOFs of proportional control with each type. This system allows for significant improvement in comparison to alternative finite state machine-type controllers. The HUI menu allows the user to directly select the desired grip without having to scroll through all the undesired grips. With the currently designed menu, the user can select from 19 unique grip and hand positions. The number of unique grip and hand position can be expanded by adding more options in the menu with marginal extra effort required from the user. The HUI system uses simple threshold control and therefore is significantly more robust than pattern recognition systems that suffer from inconsistent user muscle signals and require much longer training periods.

Training of the both the controller to the users muscle signals and of the user to correctly use the prosthetic hand is essential with the hand developed in this research. The calibration process takes about 30 minutes to complete on a first time user with only minor calibration being required after that. The position control methodology works based on a user-closed open loop methodology where feedback information is communicated directly to the user. Flex sensors in each finger are capable of accurately quantifying the fingers' positions. The flex sensors allow for software safety limits to be placed on the extension and flexion of the fingers, preventing the motors from over-unwinding the spools.

The multi-sensory haptic feedback provides a novel approach of communicating multiple senses to the user simultaneously. The feedback is communicated by means of vibrotactile stimulation induced by small, low-cost vibration motors which are worn on the amputee's stump but can be worn anywhere on the amputee's body. A pulse-length communication protocol was developed to communicate with the amputee. Four senses were communicated to the user, namely: grip force, slippage, texture and temperature.

## **5. TESTS AND RESULTS**

---

In order to evaluate the prosthetic hand and subsystems designed through this research various tests were performed. The sensory system was tested to evaluate its effectiveness in interpreting and quantifying environmental conditions of object temperature and grip strength. The haptic feedback system was tested in its ability to communicate to users through the proposed medium. The users' ability to accurately interpret the haptic feedback system was quantified and the results are shown in this chapter. The speed of the HUI control system was analysed. The relationship between the number of commands required to navigate the HUI menu and the time taken to access a specific grip type was determined.

The physical capabilities of the hand were tested through grip force and stability testing, kinematic testing and passive loading testing. These tests were used to quantify the prosthetic hands performance to allow for comparison with other prosthetic hands. The ability of the prosthetic hand to conform to different grip types was also demonstrated. All tests conducted that required test subjects had consent and indemnity forms signed by the test subjects prior to testing.

### **5.1 Sensory system**

The sensors equipped in the hand need to be tested in order to evaluate their final performance within the hand. The hand was equipped with the hand and then underwent two tests. Temperature tests were performed to evaluate the hand's ability to determine the temperature of an object being gripped. A second temperature test was then performed to evaluate the hand's ability to detect dangerous temperatures quickly. The hand's grip force sensors were then used to test the hands gripping force for both power and lateral grip types.

#### **5.1.1 Temperature test**

The temperature sensor in the hand serves both as a functional sensory feature in the hand, allow the amputee to detect hot and cold objects, thus being able to tell the difference between holding a hot or cold beverage with the prosthetic hand. To test this, the hand was equipped with the LM35 temperature sensor placed in the tip of the middle finger. The hand was used to grip a mug containing water of four different temperatures. The hand estimated the temperature of the mug in real time, based on the rate of change in temperature experienced, as discussed in Section 3. Figure 5-1 shows the results of this test collected over a period of 20 seconds. The expected temperature is the average of the expected temperature estimations made every second starting from the time of contact with the mug.

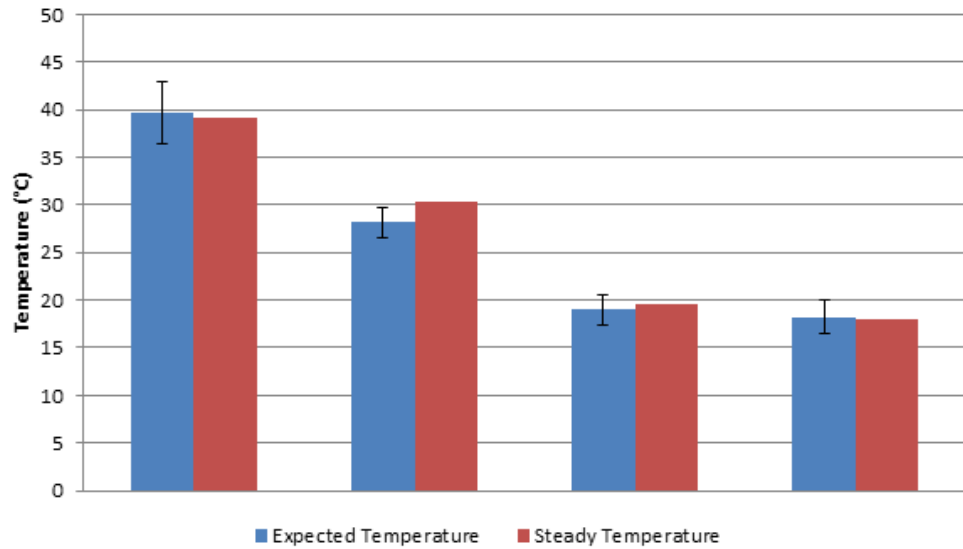


Figure 5-1: Expected temperature versus actual temperature for a period of 20 seconds

In a second test, the performance of the hand in contact with extremely hot ( $150\text{ }^{\circ}\text{C}+$ ) temperatures was investigated. The hand needs to be able to detect these high temperatures before the excessive heat injures the amputee or damages the hand. To test this, a soldering iron set at two known temperatures was placed on the tip of the middle finger of the prosthetic hand. The soldering iron was held in this position for only 5 seconds to prevent damaging the hand. Figure 5-2 shows the results of this test. The final expected temperature shown in Figure 5-2 is the expected temperature calculated 5 seconds after initial contact.

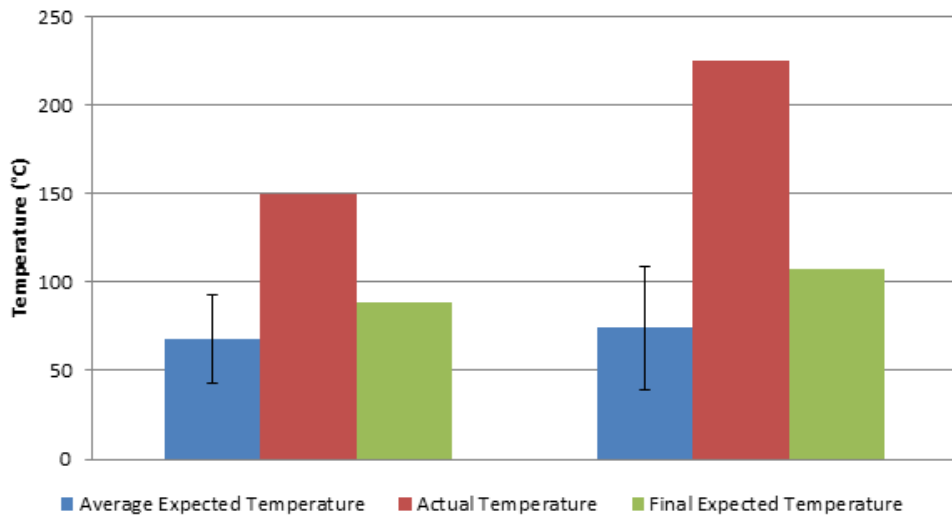


Figure 5-2: Expected temperature versus actual temperature for extreme temperatures

### 5.1.2 Grip force test

The prosthetic hand grip force was tested with a tripod grip of a mug. Force sensors were placed in six locations, at the tip and base of each finger (thumb, index and middle). The hand

was then closed and opened five times in order to determine the grip force distribution. Figure 5-3 shows the results of this test. The circle size is proportional to the force measured at that location. The inner and outer circles represent the standard deviation for each location.

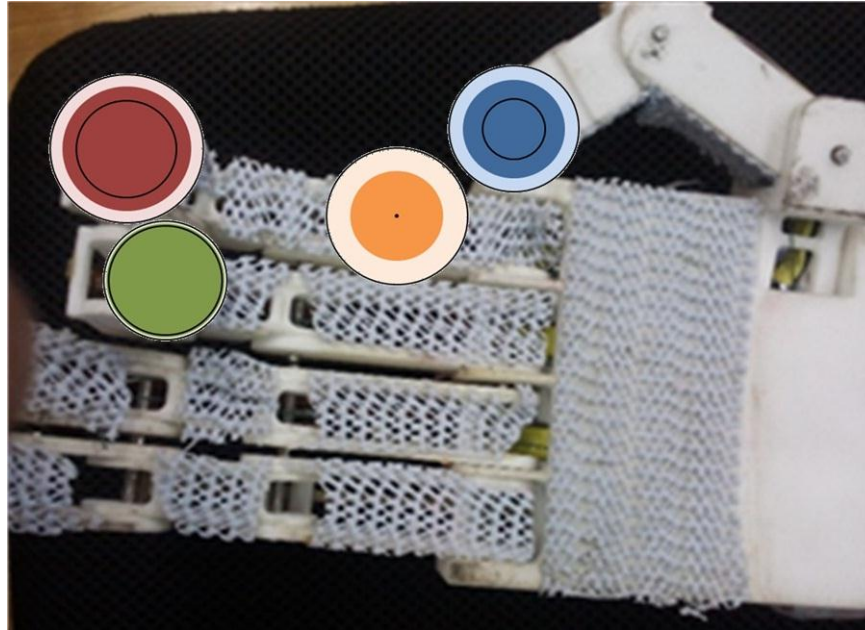


Figure 5-3: Force distribution for tripod grip

The highest force was experienced at the index finger tip (4.22 N) and the lowest force was experienced at both the thumb and middle finger bases (0 N). The thumb tip experienced 2.62 N, the middle finger tip experienced 3.49 N and the index finger base experienced 2.18 N.

### 5.1.3 Discussion

The hand's sensors performed well under the test conditions. The temperature detection for normal temperature (10 °C to 50 °C) objects is satisfactory. The hand is capable of accurately detecting the temperature of the mug within a range of  $\pm 3$  °C and with a standard deviation of  $\pm 1.5$  °C to  $\pm 3.2$  °C for the four tests. This accuracy is well within the required accuracy for prosthetic use. It can be noted that the error increases proportionally with the increase in temperature difference from the hand.

The extreme temperature test showed significant disparities in comparison to the normal object test. This result is partially because of the short time period used in this test. The temperature sensor is programmed to sample over a period of four seconds and so has a lag time of four seconds before the algorithm is working fully with the current data. The average expected temperature, before the four second lag is  $\pm 20$  °C off as a result of the sampling period of the algorithm. The standard deviation is  $\pm 25$  °C to  $\pm 35$  °C. Although the final estimated temperature is  $\pm 100$  °C off from the actual temperature, the results are still useful. The hand still

detects an unusually high temperature and this can be used to signal a warning. In these dangerously hot conditions, the exact temperature of the object is not important but rather the simple knowledge that the object is dangerous. To this objective, the hand is capable of determining that a dangerous temperature is being sensed within 5 seconds of contact with the object during which the hand sustained no damage from contact. Therefore this information can be communicated to the user through the haptic feedback system to warn him/her of the high temperature so that he/she can take appropriate action. Additional warning systems, such as audible or visual can also be implemented to increase the chance of the user noticing the dangerous situation quickly.

## **5.2 Haptic feedback**

This dissertation contributes new work into the examination of the effects of communicating multiple senses (grip force, slippage, temperature and texture) simultaneously using a single vibration motor to display each sense. The study will compare the ability of a user to correctly interpret a single sense feedback with an increasing number of sensory feedbacks. This study will determine the feasibility of such an approach to using haptic feedback.

### **5.2.1 Setup**

The haptic feedback armband designed in the haptic feedback section (3.3) is tested here. Nine test subjects were used. All subjects were healthy and had no upper extremity defects of any kind. Eight of the participants were male and one was female. All were in the age range of 20-25 years. All subjects volunteered to take part in the test and signed consent forms prior to testing.

### **5.2.2 Experimental procedure**

The test subjects were introduced to the vibrotactile armband before testing. The test process and function of the armband was explained to them. The four different senses to be communicated through the armband were also explained.

Following this a training program was run with the subjects. This program highlighted each sense while it was being stimulated. Each sense was shown separately. This was done with an intermediate intensity for each sense (10 N, slight slip of 50 mm/sec, 68 °C and slightly rough). The training program then repeats the senses but with the intensity of the sense also being revealed. The program ran them from 10% through to 100% intensity. This lasted approximately 5 minutes and once it was completed the test subjects were run through four different tests, as shown in Figure 5-4 (van der Riet et al., 2013b). The full test procedure took

between 30 minutes and an hour depending on how quickly the test subjects were able to identify the different sensations.



Figure 5-4: Test subject wearing the armband

#### **5.2.2.1 Test 1 - Spatial discrimination**

The test subject is notified that the test will start with one sense being communicated randomly at a time. After random periods of time the number of senses being displayed will increase until all four senses are communicated at the same time. The order is randomly predetermined and displayed through a vibration of 50% sense intensity. No visual cue is given. The test subject then indicates which of the four senses is felt.

#### **5.2.2.2 Test 2 - Intensity discrimination**

The test subject is told which sense is being displayed but the intensity of the sense is withheld. The intensity, randomly predetermined, is then applied through the corresponding sense. The test subject then indicates on a scale of 0 to 5 on what intensity was perceived. After a number of runs the number of senses being displayed is increased and the test subject is asked to answer for each senses' intensity.

#### **5.2.2.3 Test 3 - Intensity variation discrimination**

This test repeats the process of test 2, but after the intensity has been recorded, the test subject is then told that the intensity may have changed. The test subject then indicates whether the intensity has increased, decreased or remained the same and what the new intensity is.

#### **5.2.2.4 Test 4 - Full spectrum**

Tests 1 to 3 are combined simultaneously. The test subject isn't given any visual cues as to what senses are being displayed. The subject is asked to indicate what senses are perceived and what their respective intensities are. Each time a new change is introduced, the test subject is notified and asked to indicate what changes were perceived.

### 5.2.2.5 Qualitative report

After the test process was completed the test subjects were asked to fill in a survey indicating their satisfaction with the form of feedback. This covered the areas of comfort, comprehension of feedback and difficulty of the tasks.

## 5.2.3 Results

It was found that as the number of sensory channels was increased there was a decrease in performance in all areas. The data was collected from all 9 test subjects and Figure 5-5 (van der Riet et al., 2013b) shows the relationship of spatial discrimination accuracy with the number of sensory channels. These results were gathered from the spatial discrimination test (test A) and the full spectrum test (test D). Figure 5-6 (van der Riet et al., 2013b) indicates the relationship of intensity discrimination with the number of sensory channels using results from the intensity discrimination test (test B), the intensity variation discrimination test (test C) and test D. The results of intensity variation are shown in Figure 5-7 (van der Riet et al., 2013b). Data was taken from tests C and D. All three test focus area averages (spatial, intensity and intensity variation discrimination) were then compared in Figure 5-8 (van der Riet et al., 2013b).

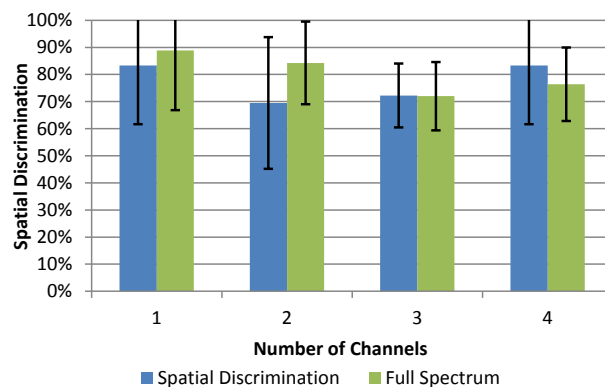


Figure 5-5: Spatial discrimination accuracy percentage ( $\pm$  standard deviation)

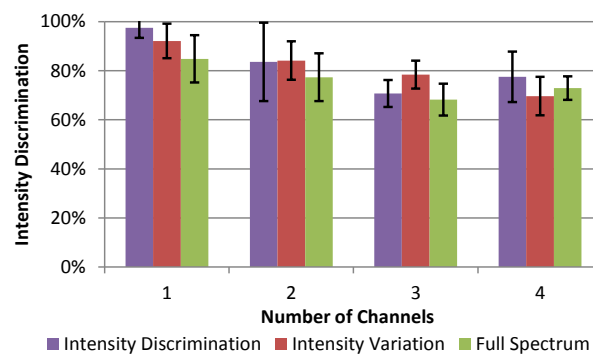


Figure 5-6: Intensity discrimination accuracy percentage ( $\pm$  standard deviation)

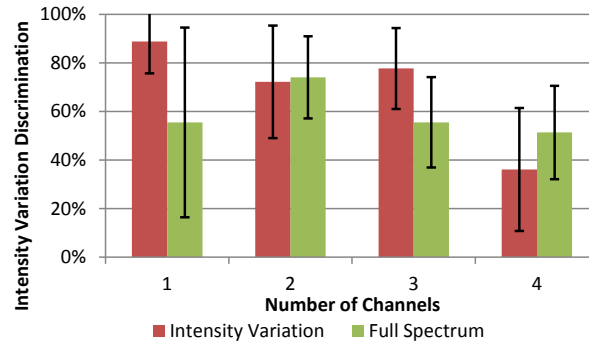


Figure 5-7: Intensity variation accuracy percentage ( $\pm$  standard deviation)

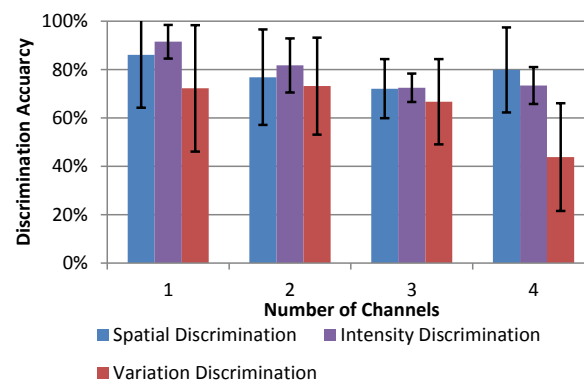


Figure 5-8: Haptic feedback accuracy comparison ( $\pm$  standard deviation)

## 5.2.4 Discussion

The results show that the effectiveness of a vibrotactile feedback system decreases with the increase in the number of sensory channels being displayed simultaneously. Seven out of the nine test subjects indicated that they felt as if they were learning to understand the feedback system as the test progressed. It was stated by some test subjects that if longer training was done, it would improve the ability to correctly interpret the signals being sent. The training could be improved by adding quizzes to help the users to refine their ability to interpret the information communicated through the vibrations.

### 5.2.4.1 Spatial discrimination

It can be seen in Figure 5-5 that there is a general deterioration in the accuracy of localizing the channel being displayed as the number of channels increases. However, this trend doesn't hold when all four channels were being displayed together. There is a noticed improvement of 5% to 10% accuracy between three and four channels. This improvement is due



to the fact that it is possible to tell when all four senses are being displayed by the unbroken vibration around the forearm at the beginning of each period. When only three channels are active, the subject can detect a break, but due to the large amount of vibrational noise in his forearm, it becomes increasingly difficult to localise the active channels.

The standard deviations for spatial discrimination are around 20%. One and two channels were shown to have higher standard deviations. It can be concluded that the ability to learn the system varies between test subjects and that fewer channels are easier to learn. Improved training could result in a quick improvement in the results in these areas. This is confirmed by the increase in accuracy on the full spectrum tests for one and two channels, where unsupervised learning has had immediate effects.

#### **5.2.4.2 Intensity discrimination**

The same trend observed with spatial discrimination can be observed in Figure 5-6 with the intensity discrimination. As the number of channels being displayed increases, the accuracy decreases. However, with intensity discrimination there isn't a noticeable increase in accuracy when all channels are active. Instead, the results for three and four channels are relatively similar. This result could indicate that from three channels upwards; the technique used by the test subjects to determine the intensity stabilises and additional noise doesn't affect this ability.

The accuracy of intensity discrimination has a general decrease over the duration of the test for all numbers of channels. This can be attributed to the fact that the subjects have no reinforcement of what the real intensity values are. Therefore, their reference intensities can drift. The concept of what a 10 N load signal (for example) feels like can change and some test subjects started thinking that 10 N actually has a lower or higher signal intensity that it actually does. This drift would move around 20% from the original intensity, and that is why the accuracies are sitting just under 80%. A decrease in accuracy can also be attributed to an increase in mental fatigue and skin desensitization as the test progressed.

#### **5.2.4.3 Intensity variation discrimination**

The results from the intensity variation vary greatly. The standard deviations for these tests are between 20% and 30%. There is a trend (seen in Figure 5-7) of a decreasing accuracy with the increase in channels. The large standard deviation suggests that proper training can improve the results in this area.

The test also reflected that small changes as well as opposite changes (i.e. one sense increasing in intensity and another decreasing) were much harder to determine accurately. The majority of inaccuracies occurred with these types of changes. These inaccuracies can be

attributed to the vibrational noise in the system inhibiting the test subjects' ability to accurately discern change. The test subjects would need to focus on a sense in order to identify it, thus background changes outside their frame of concentration are missed.

#### **5.2.4.4 Simultaneous multi-sensory feedback**

The full spectrum test can be considered slightly harder than a real life situation. The wearer of a prosthesis will normally be expecting to feel certain sensations when doing certain activities with the prosthetic hand. If a water bottle was being gripped, then the senses of grip and slippage would be expected, if a surface was being touched then texture and possibly temperature would be expected. Daily usage tests could see an improvement to the results as the senses being experienced would be more tangible to the test subjects. One test subject reported that the multi-sensory feedback helped him visualize not only that he was gripping an object, but the texture and temperature of the object being held in his virtual prosthetic hand.

The different forms of discrimination of signals show similar results as seen in Figure 5-8. Intensity discrimination has the highest level of accuracy in all but the four channel system. As stated earlier, spatial discrimination has an advantage when all the channels are being used as this is easier to feel than to identify which channels are active and passive. However, the intensity discrimination accuracies are misleading as it would be very rare to get 0% accuracy, even poor guesses will tend to be within a 50% to 70% range of the true value. Thus, bearing these misleads in mind, it can be observed that spatial discrimination is the most accurate discrimination technique. Both spatial and intensity variation discrimination show a large standard deviation. This large standard deviation suggests that an improved training program could improve the results of the test.

The accuracy of intensity discrimination of approximately 70% suggests that the system would be highly suitable for low resolution channels. Four stages are very accurately interpreted (outside the 30% error margin); in-active, low-intensity, mid-intensity and full intensity. Senses that don't require a high resolution, such as temperature and slippage can be easily interpreted. These results show that multi-sensory haptic feedback is possible and that a single vibration motor per channel is adequate at achieving these goals. This result is very promising in the light of the great need for improved feedback in prosthetic limbs and vibrotactile feedback offers an inexpensive and simple solution to the feedback problem.

### **5.3 HUI control**

The Haptic User Interface is the control method developed in this research that allows the amputee to navigate through a selection of predefined prosthetic hand functions and grip types.

The HUI system uses a 2-channel EMG input to give the user access to an effectively limitless number of predefined hand functions and grip types without sacrificing the ability to access or control the basic grips. In order to evaluate the effectiveness of the HUI control method a timed selection test was done to measure the time it takes to select any of the 7 predefined grips.

The test subject was an unimpaired adult male. The test was performed with a visual feedback of the HUI menu as well as with the aid of the HUI vibrotactile feedback. The subject performed 5 repetitions of each task. The results with their standard deviations are shown in Figure 5-9.

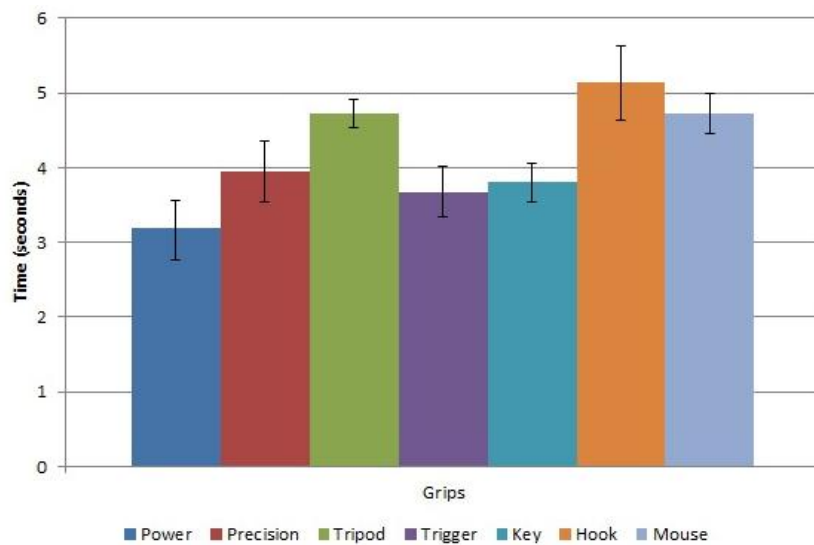


Figure 5-9: Time taken to select a grip with the HUI system

The menu layout gives priority to certain grips over others by giving them a shorter selection path. The minimum number of commands needed to select a grip is 2, used to select the “Power” grip and the maximum number of commands is 4, used to select the “Tripod”, “Hook” and “Mouse” grips. This relationship is shown in Figure 5-10, with the times taken to select each grip being dependent on the number of commands required to select it. A linear trend has been assumed as the time taken to perform each command would not vary with an increased number of commands.

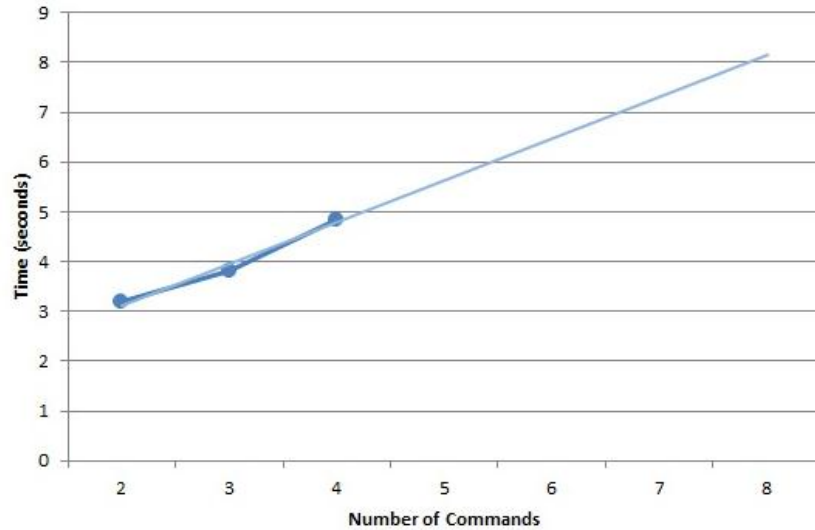


Figure 5-10: Number of commands versus time for the HUI system

The relationship between the number of commands and time is shown in Equation 5-1. Where *Time* is the time taken to select a specific grip, given in seconds, and  $n_c$  is the number of commands required to select the specific grip.

$$Time = 0.8 \times n_c + 2.3 \quad (5 - 1)$$

## 5.4 Physical capabilities

The prosthetic hand's physical performance is tested and discussed in this section. The ability of a prosthetic hand to grip objects is the fundamental purpose of any prosthetic hand and therefore the most critical aspect of the prosthetic hand to test. The prosthetic hand was designed to mimic the natural movements of the human hand. The shape and speed of the prosthetic hand is compared to that of a human hand to evaluate how closely this is achieved. The prosthetic hands ability to hold static loads is also evaluated as this ability determines the maximum loads that the hand can carry. The complete hand with the wrist and all motors and circuitry but without the battery weighs 540 g.

### 5.4.1 Grip force test

One of the most common measures of prosthetic hand effectiveness is done through the measurement of the grip force capable by the prosthetic hand. The power and lateral (key) grips are typically used to measure the grip force. The power grip uses all fingers and the thumb to squeeze an object and is used when gripping a bottle. The lateral grip only uses the thumb and is used to grip and handle keys, cards or other small flat objects. The hand was tested 5 times for

each grip. The results of the tests are shown in Figure 5-11 with their respective standard deviations.

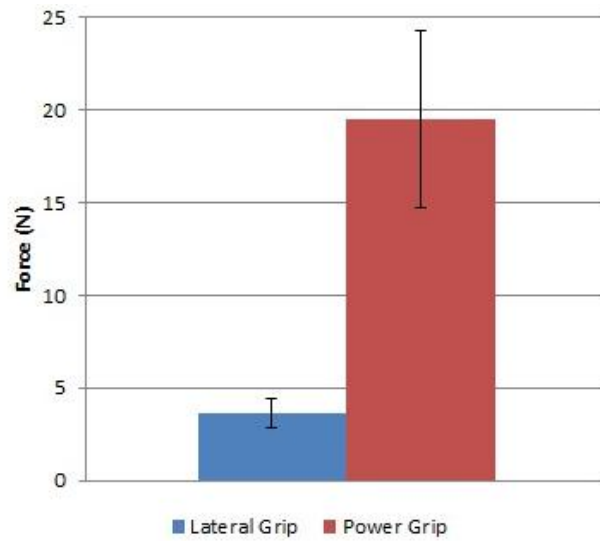


Figure 5-11: Grip force test results

The lateral grip had an average grip force of 3.7 N while the power grip had an average grip force of 19.5 N. The results show a large standard deviation for the power grip. The large standard deviation is due to the fact that the tips of the fingers sometimes slip on the object, as shown in Figure 5-12. The fingertip slipping on the object reduces the effective gripping force as the majority of grip force is transferred through the fingertip as this is where the tendons are connected.



Figure 5-12: Fingertip slip during grip

### 5.4.2 Grip stability test

The grip stability is the ability of the prosthetic hand to grip and hold objects of varying weights. To test the grip stability of the prosthetic hand, a water bottle was used with varying degrees of water levels. This allowed the prosthesis' grip to be tested against a controlled object weight. A 250ml bottle was marked with 9 equally spaced graduation marks as shown in Figure 5-13. A corresponding weight of 28 g for each level increment was measured and calibrated using water.



Figure 5-13: 250ml graduated water bottle

The hand easily grasped the empty bottle. The core aim of this test was to support the application of a nylon non-slip covering on the inner surface of the palm and fingers. The weight of the bottle successfully held with and without the nylon covering was compared. Figure 5-14 shows the hand with the nylon non-slip covering.



Figure 5-14: Nylon non-slip covering to increase grip strength

The grip feel and solidity was given a rating out of 10, with a rating of 10 being a completely secure grip. Each graduation mark represents a different level of grip stability (how easily the object is dropped from the hand during movement of the hand). A rating of 0 represents the complete inability of the hand to lift the bottle. The test was carried out using water as the filling liquid. Figure 5-15 represents the results of this test.

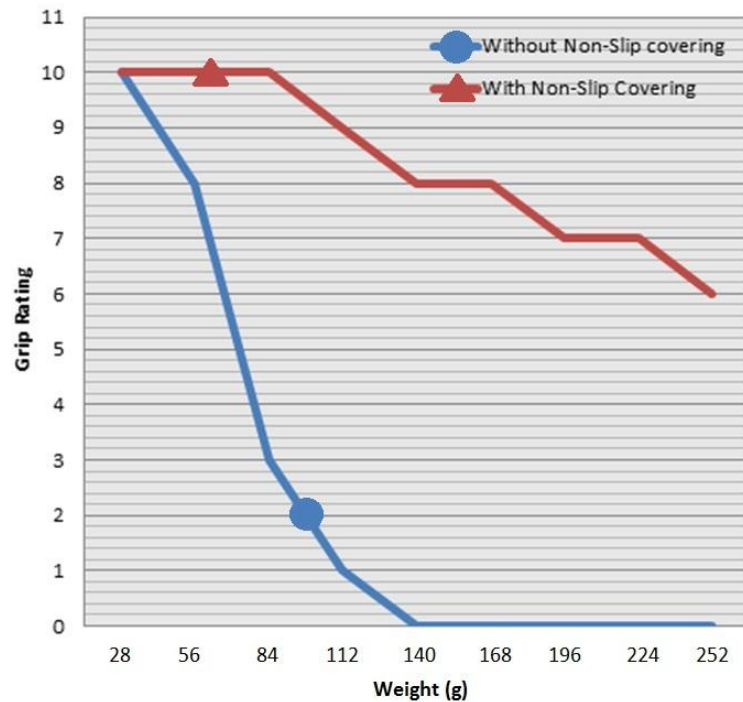


Figure 5-15: Graph showing how secure a grip felt as weight of water bottle increases

It can be seen that the gradient of the circle trend line is steep. The shape of the circle line shows that the grip is unstable when low loads are applied and does not offer a secure grip. The addition of the nylon non-slip cover decreases the gradient of the graph, indicating that the stability and strength of the grip performs better than the hand without the non-slip covering when applying a larger load.

### 5.4.3 Kinematic video analysis

A video analysis of the hand was aimed to validate the prosthetic hand's ability to mimic a human hand in its motion. The open-source video analysis tool Kinovea [14] was used to conduct this analysis. The software is capable of tracking objects in real-time. The joint paths of both the prosthetic hand and human hand were compared using this software. The results showed the kinematic behaviour of the prosthetic hand. It also allowed the maximum joint speeds to be compared.

The analysis procedure involved the setup of a white background to enhance contrast between the object being tracked and the surrounding environment. A reference frame had to be



setup on the white background to give the software a known length and scale. The program is capable of accurately calculating the absolute velocities of the joints with the aid of this reference frame. Figure 5-16 shows a snapshot of the kinematic video analysis at the point where the joints of the human hand are at their maximum. The human hand was recorded closing all fingers in a smooth and natural manner to measure the closing speed of an average human grasp.

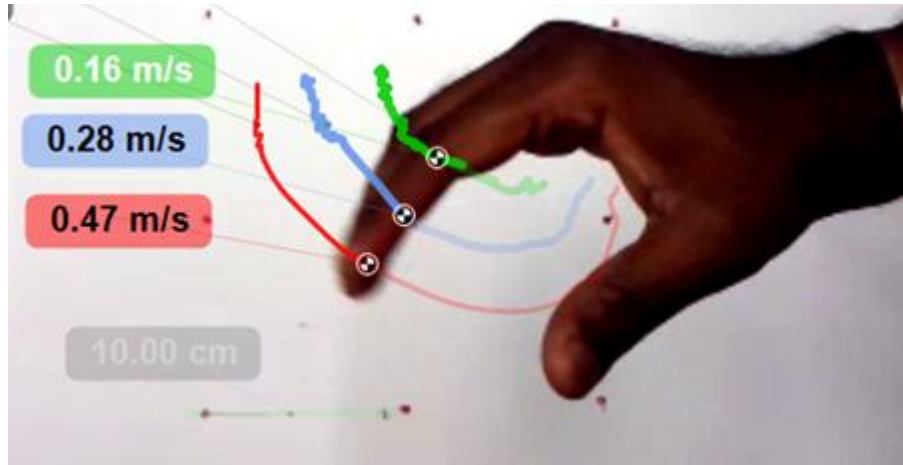


Figure 5-16: Joint paths tracked and velocities measured using Kinovea kinematic analysis software

The prosthetic hand was recorded under the same reference conditions to make sure that the measurements correlated for both the human and prosthetic hand. Figure 5-17 shows a snapshot of the prosthetic arm at its maximum distal joint velocity.

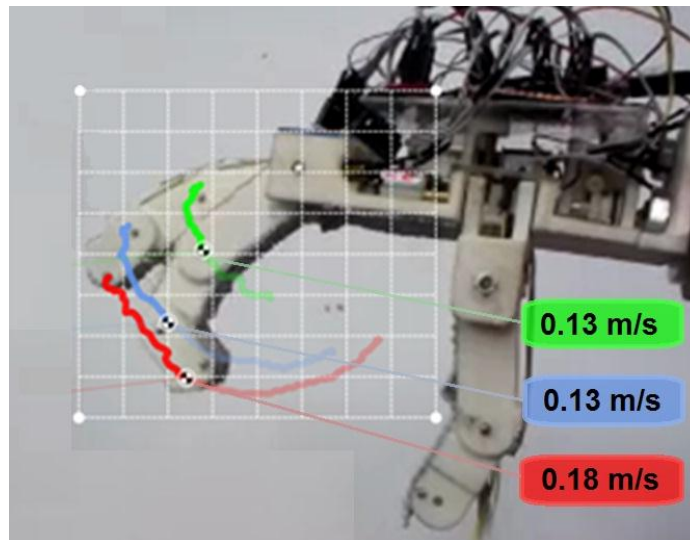


Figure 5-17: Joint paths and velocities tracked of the prosthetic hand

The results showed similar joint paths to that of the human hand. Figure 5-18 shows the graphs of joint velocities against time. The joint velocity graph compares the differences in joint velocity and overall closing time.



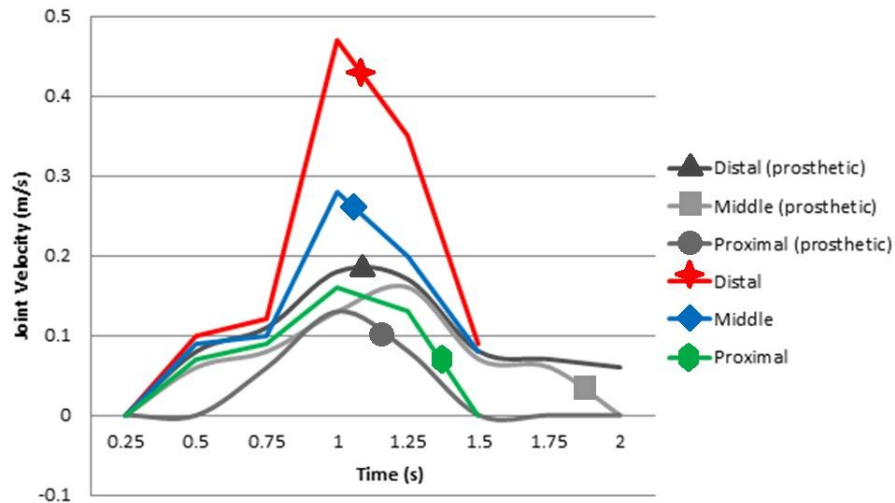


Figure 5-18: Graph of joint velocities for both human and prosthetic hands

It can be seen that the human hand closes faster in the natural closing grip task than that of the prosthetic hand at maximum power. The friction between joints and cables slows the speed of the prosthetic hand. The human hand was measured to close in 1.5 seconds were as the prosthetic hand took 2 seconds.

Positional and displacement data was also extracted from the kinematic video analysis. It is important to compare the motion of the prosthetic hand to a human hand. The prosthetic hand must mimic its biological counterpart as closely as possible to enable controlled grasping and aesthetic appeal.

A radar chart was used in order to compare the kinematic behaviour of the human and prosthetic hand. The radar chart was used because it is a graphical method of showing three or more quantitative variables on the same axes starting from the same point therefore enabling the two motions to be shown. The same reference points and recordings were used to extract displacements in Cartesian coordinates. Figure 5-19 shows the plot of X and Y coordinates in the radar chart.

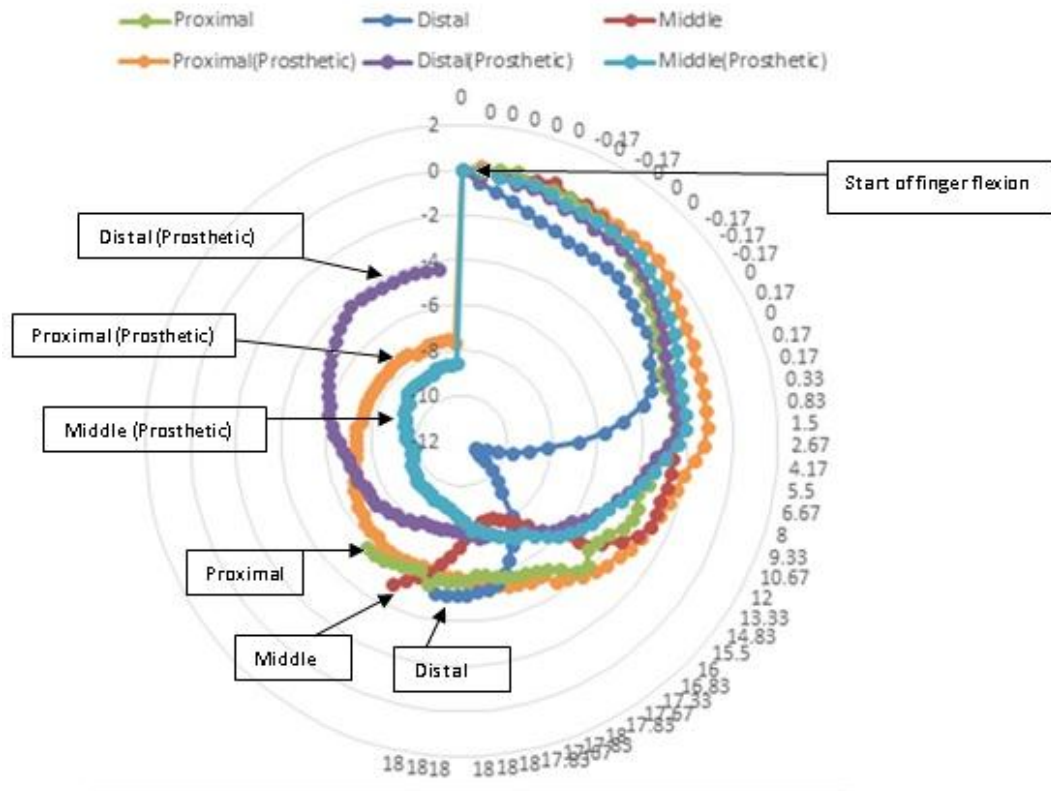


Figure 5-19: Comparison between kinematic behaviour using joint displacements

It can be seen that the displacements of the respective middle, proximal and distal joints follow the same path (show the same displacement) for approximately the first quarter of its motion. The movements of the joints in the prosthetic hand can be seen to start off with very similar kinematic behaviour to that of a human hand. It is then seen that as the finger reaches halfway between its fully open and fully closed position the joint displacement differs from that of the human hand. The rigidity of the prosthetic finger contributes to the variation between it and the human finger during the halfway point of closure. The human proximal joint is a flexible joint with more than one degree of freedom hence allowing the finger to curl through a larger degree than that of the prosthetic finger.

The prosthetic fingers differ in kinematic behaviour compared to the human finger at the latter stages of flexion. This difference is caused because the prosthetic finger only has a single tendon attached to the distal phalanx which causes it to close earlier than the human finger, which has tendons connected to all three phalanges, allowing it to close more uniformly than the prosthetic finger. It can be seen from the radial chart that the distal segment rotates about the distal joint earlier than that of its biological counterpart, this caused inconsistencies in the pinch grip tasks. The fundamental dimensions of the prosthesis' distal segment and the nature of its actuation cause the inconsistency in the pinch grip. The overall behaviour of the prosthetic

fingers is as close to human finger motion. The hand moves in a natural way in which the user can feel comfortable with utilizing.

#### 5.4.4 Passive loading test

The passive loading test is done by gripping a bag in the hook grip position, shown in Figure 5-20. The bag is then increased in weight incrementally until failure occurs. The hand is not powered during this test and so the motors are off, thus the weight is held through the self-locking mechanism of the worm gears. The ability of the hand to hold objects without drawing power is critical in reducing the hands power consumption and extending its battery life.

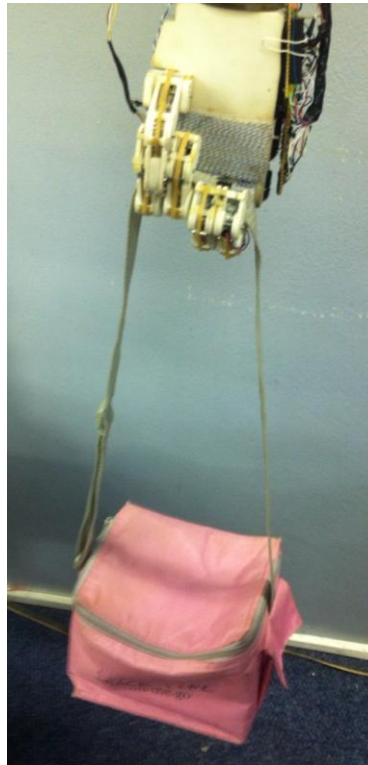


Figure 5-20: Hand gripping bag for passive load testing

Weights were placed in the bag to increase the weight of the bag by 250 g increments. The hand failed at 8.25 kg with the last successful passive load being performed at 8 kg. Stretching in the tendon cables occurred before failure and caused the fingers to extend slightly. This extension did not cause the hand to drop the object and thus the cables performed satisfactorily. Failure occurred in the coupling of the worm wheel and cable pulley shown in Figure 5-21.



Figure 5-21: Weakest point under passive loading test –  
worm wheel and cable pulley coupling

The worm wheels and cable pulleys were coupled with epoxy glue. This adhesive proved to be the weakest point in the design under passive loading. To improve the coupling strength the worm wheel and cable pulley can be 3D printed as a single part. Alternative design approaches would be to use screws to secure the pieces or to design the pieces with a D-shaped male/female mating hole.

## 5.5 Practical testing

As a prosthetic hand's function is to assist an amputee with daily living and to improve his/her quality of life, the prosthetic hand needs to be tested in real life. This section investigates the prosthetic hand's ability to pick up and handle everyday objects. The hand is also tested on a transradial amputee who uses the hand to do basic tasks such as manipulating objects and drinking out of a cup.

### 5.5.1 Gripping objects

The hand's gripping capabilities had to be demonstrated to fully test the effectiveness of the end effector as a functional prosthetic. A simple procedure of gripping objects of different shapes and dimensions was undertaken. The hand was tested with rigid objects as soft objects are easier to grip. The hand's ability to adaptively grasp objects is tested and proven by a range of grip tests. Figure 5-22 illustrates example of square objects being grasped.

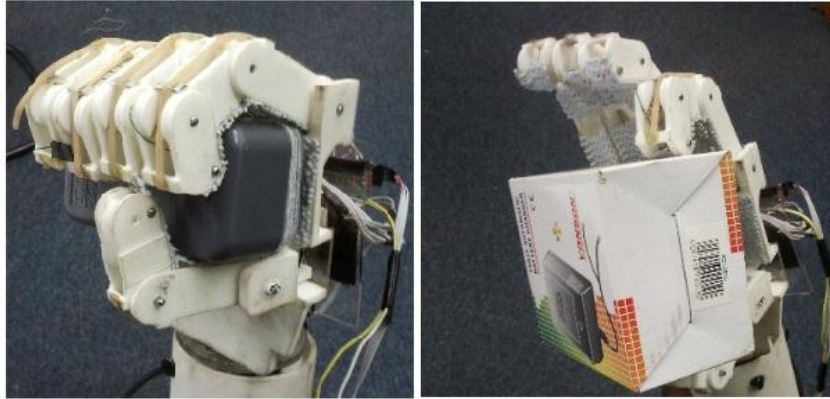


Figure 5-22: Hand gripping square objects

Grasping square objects posed no challenges as the fingers adaptively grasped the corners with ease. Figure 5-23 shows the hand grasping different types of plastic bottles.



Figure 5-23: Hand gripping unusually shaped bottle and a 2 litre bottle

The hand also handles round or spherical objects. Figure 5-24 shows the hand grasping a cricket ball.



Figure 5-24: Hand gripping a spherical object



### 5.5.2 Live testing with a transradial amputee

The prosthetic hand was tested on an adult male double transradial amputee. The amputee had no experience with using EMG controlled prosthetics and owns a pair of body powered prosthetic hands. The amputee went through a period of training which lasted 30 minutes (including calibration) prior to use of the prosthetic hand. This training process is shown in Figure 5-25. In Figure 5-25 the amputee is viewing visual feedback of the two EMG channels on the screen of the laptop. This process helped the amputee to focus on using the correct muscles and control the degree of muscle contraction in order to control the prosthetic hand. Due to the subject's amputation, the two EMG sensors were placed over his bicep and triceps respectively. The amputee had not used these muscles properly since his amputation 20 years prior and it took a lot of concentration to use them to control the prosthetic hand.



Figure 5-25: Amputee training with EMG control of the prosthetic hand

The amputee picked up the use of the prosthetic hand quickly and performed grasping tasks comfortably with the prosthetic hand. The amputee is shown in Figure 5-26 using the prosthetic hand to drink from a cup. The amputee also was capable of pouring water from a bottle into a cup. The amputee used the prosthetic hand for 4 hours continually during this session and reported that the prosthetic hand was comfortable to use and performed satisfactorily.



Figure 5-26: Sequence of the amputee grasping and drinking out of a cup with the prosthetic hand

It was noted that the amputee's muscles experienced fatigue over the course of the 4 hour exercise. As a result of the muscle fatigue, the EMG signals weakened and the amputee felt that controlling the prosthetic hand became strenuous. Muscle fatigue would lessen with continual use of the EMG prosthetic hand.

## 5.6 Chapter summary

The prosthetic hand performed satisfactorily according to the amputee, and is capable of gripping a variety of differently shaped objects. The amputee experienced fatigue while using the prosthetic hand continually for 4 hours. However, as the amputee had no prior experience with EMG prosthetics and had not properly used the muscles used to control the prosthesis in 20 years, fatigue was expected. As an amputee continually uses the same muscles to control the EMG prosthetic hand, his/her muscle strength, endurance and skill in using the hand will improve (as with any muscle exercise). Through this learning method, the prosthetic hand is very natural in comparison to any other physical activity.

The prosthetic hand also mimics the movement of the human hand to a satisfactory degree. The prosthetic hand takes 2 seconds to fully close, which is slower than a human hand. The hand is capable of lifting 8 kg with the hook grip in a passive loading situation. The hand can provide up to 19.5 N of grip force with a power grip and 3.7 N of grip force with a lateral grip. The gripping strength of the prosthetic hand is satisfactory and is capable in daily use. However, the prosthetic hands grip strength is lower than that of other contemporary prosthetic hands (van der Riet et al., 2013a). The results from the grip stability test showed significant improvement with the use of the non-slip covering. The hand is capable of lifting suitable weights for eating and drinking purposes and meets the initial specifications. Increasing the motor power would improve grip strength and hand speed. However, a more powerful motor would be larger and heavier than the motors currently selected. Therefore a balance between size, weight and grip strength needs to be decided upon. Using more powerful motors will also increase the overall cost of the prosthetic hand. The motor's gear ratio controls the balance of

torque to speed. Grip strength was indicated as being more important than hand closing speed by the amputee at the beginning of the research. The decision was made to favour grip strength over speed.

The hand's sensors were shown to satisfactorily detect temperature and grip force. The ability of the hand to detect extreme temperatures quickly is inaccurate. The hand's prediction grew more accurate as the time passed, especially after the four second window lag time. The hand can satisfactorily determine when it is in contact with dangerously hot objects.

The haptic feedback test investigated the potential for multi-sensory haptic feedback. A vibrotactile armband was designed to communicate four different channels using a single vibration motor for each channel. This armband was worn on the forearm of the test subjects. The test subjects were tested on three different discrimination abilities: spatial, intensity and intensity variation. It was found that spatial discrimination was the most accurate ability. The tests showed promising results and the proposed armband has potential to be used as a solution to multi-sensory haptic feedback for low resolution senses. The results from this test will be used as a reference from which further improvements to multi-sensory haptic feedback can be made. The haptic communication protocol and training programs both can be improved greatly in future studies. With the hands current 2 channel sensory setup of grip force and temperature, the test subjects' accuracy in interpreting the information is  $\pm 75\%$ . The communication protocol can be improved to further increase the accuracy of interpretation.

The HUI system provides a novel method of accessing an effectively limitless number of grip types and hand gestures within a relatively short time and with high accuracy. The tests showed that there is a linear relationship between the number of commands required and the time needed to select a grip. The hand is capable of performing 7 different grip types and an additional 12 hand positions and gestures. The user can select from any of the 7 grip types within 5 seconds. The selection speed is satisfactory and gives the hand a good dexterity to speed ratio.



## 6. CONCLUSION

---

The prosthesis developed through the course of this research is a low-cost, modular prosthetic hand/arm capable of being used by both transradial and transhumeral amputees. The prosthetic hand was manufactured through 3D printing techniques. The fingers are actuated with 6V DC motors through a worm gear and spool coupling to wind/unwind the single cable in each finger to act as a tendon to close the finger. The wrist is controlled through a servo motor allowing 180 degrees of rotation. The proposed prosthetic arm uses two air muscles to replicate the actions of the bicep and triceps.

The kinematics of the hand and fingers show a good range of motion, allowing it to mimic the basic natural motion of a human hand. The current design offers a simple, lightweight and low-cost solution for prosthetic hands. Adding the full DOFs found in a human hand to the prosthetic hand would greatly increase its complexity, cost and weight, and so falls outside the objectives of this research. The size of the hand is slightly larger than a human hand and its size should be reduced in future versions. The connecting adapters were all made from stainless steel which increased the weight of the prosthesis. With the new technology of 3D printing they can be reproduced and be made from a much lighter material such as titanium.

The prosthetic hand contains a microprocessor and circuitry allowing it to control the six DC motors and the servomotor. The hand uses flex sensors to measure the degree of closure in each finger and is also equipped with a modular sensory system. The sensory system consists of pressure, temperature and vibration sensors which are used to detect grip force, temperature, object slippage and texture. These sensors can accurately detect grip force (to 0.1 N) and temperature (to the nearest degree Celsius). Methods for detecting object slippage and texture using the vibration sensors are proposed. The hand is controlled with a 2 channel EMG control system. The hand is equipped with six vibrotactile displays; two vibration motors are used to communicate navigation information from the HUI control method and four vibration motors are used to provide simultaneous multi-sensory feedback to the amputee.

The novel HUI control method allows the user to navigate through a limitless list of pre-set grip types and hand gestures. The HUI method provides a highly accurate and relatively fast selection of grip types through its use of threshold-triggered navigation. A novel simultaneous multi-sensory feedback system was developed using four vibrotactile displays and a novel communication protocol. The communication protocol allows four different sensory channels to be communicated simultaneously with an accuracy of 70% showing that simultaneous multi-sensory feedback is possible.

The prosthetic hand was successfully tested with a transradial amputee. The overall system was built within a small budget of US\$ 1'000. The low-cost design and manufacturing of the prosthetic hand achieves the low-cost goal of the research.

## **6.1 Research achievements**

A summary of the prosthetic hand developed through this research, the UKZN Touch Hand, is given in Table 6-1 in comparison to other contemporary prosthetic hands. The rows in which the UKZN Touch Hand improves upon the other contemporary prosthetic hands are highlighted in green.

TABLE 6-1: SUMMARY OF UKZN HAND VERSUS CONTEMPORARY UPPER EXTREMITY PROSTHESES

|  | UKZN Touch Hand                      | i-limb ultra (Touch Bionics, 2013) | BeBionic3 (RSLSteeper, 2013) | Michelangelo (OttoBock <sup>b</sup> , 2013) | SmartHand (Cipriani et al., 2011) | Vanderbilt University Hand (Dalley et al., 2010) | Southampton Hand (Cotton et al., 2006) | MARCUS (Kyberd et al., 1995) |
|--|--------------------------------------|------------------------------------|------------------------------|---|-----------------------------------|--|--|------------------------------|
| <b>Grip Strength (N):</b>                            |                                      |                                    |                              |   |                                   |  |  |                              |
| <b>Power Grip<sup>**</sup></b>                       | 19.5                                 | 136                                | 140                          | 70  | 36                                | 50   | - <sup>*</sup>                         | - <sup>*</sup>               |
| <b>Lateral Grip<sup>***</sup></b>                    | 3.7                                  | 34                                 | 27                           | 60  | 8                                 | - <sup>*</sup>                                   | - <sup>*</sup>                         | - <sup>*</sup>               |
| <b>Passive Load (kg) - Hook Grip (Suitcase Hold)</b> | 8                                    | 90                                 | 45                           | - <sup>*</sup>                              | 10                                | - <sup>*</sup>                                   | - <sup>*</sup>                         | - <sup>*</sup>               |
| <b>Degrees of Freedom</b>                            | 7                                    | - <sup>*</sup>                     | - <sup>*</sup>               | - <sup>*</sup>                              | 16                                | - <sup>*</sup>                                   | 6                                      | 2                            |
| <b>Closing Speed - Power Grip (sec)</b>              | 2                                    | 1.2                                | 1.0                          | - <sup>*</sup>                              | 1.5                               | 0.3  | - <sup>*</sup>                         | - <sup>*</sup>               |
| <b>Grip and Hand Positions</b>                       | 19+                                  | 11                                 | 14                           | 7   | - <sup>*</sup>                    | 8  | 6                                      | 3                            |
| <b>Control</b>                                       | 2 Channel Myoelectric                | 2 Channel Myoelectric              | 2 Channel Myoelectric        | 2 Channel Myoelectric                       | Myoelectric                       | Myoelectric                                      | Myoelectric                            | Myoelectric                  |
| <b>Actuators</b>                                     | DC Motors                            | DC Motors                          | DC Motors                    | DC Motors                                   | DC Motors                         | DC Motors  | DC Motors                              | DC Motors                    |
| <b>Touch Sensors</b>                                 | pressure, slip, temperature, texture | No                                 | No                           | No  | pressure                          | No   | pressure, slip, temperature            | pressure, slip               |
| <b>Feedback Displays</b>                             | 6 vibrotactile displays              | No                                 | No                           | No  | 5 vibrotactile displays           | No   | No                                     | No                           |
| <b>Weight (g)</b>                                    | 540                                  | 479                                | 598                          | 600   | 530                               | - <sup>*</sup>                                   | - <sup>*</sup>                         | - <sup>*</sup>               |
| <b>Cost (US\$)<sup>****</sup></b>                    | 1'000 (materials)                    | 40'000                             | 35'000                       | 75'000                                      | - <sup>*</sup>                    | - <sup>*</sup>                                   | - <sup>*</sup>                         | - <sup>*</sup>               |

data unavailable    <sup>b</sup>this grip uses all the fingers and the palm with the thumb is in the opposed position and its used to grip objects such as a bottle

<sup>\*\*\*</sup>this grip is between the thumb and the side of the finger with the thumb in the non-opposed position and its used to grip objects such as a key

<sup>\*\*\*\*</sup>cost is approximate and varies greatly according to the amputation

The UKZN Touch hand met all the research objectives of this research. The hand introduces improvements to prosthetic hands in the categories of control, sensory feedback and cost. The hand introduces a novel EMG control method that allows the user to choose from a limitless number of possible grip types and hand gestures. The UKZN Touch hand utilizes 19 grip types and hand positions. The hand is capable of measuring grip force and temperature, as per the research objectives but is also capable of measuring texture and object slippage. The hand's haptic feedback system provides a novel method of communicating all sensory information simultaneously to the user. The prosthetic hand cost US\$ 1'000 in materials (excluding the prosthetic arm extension) which is well below the cost of other contemporary prosthetic hands.

To re-iterate the contributions, specifications and objectives stated in the Introduction chapter, the following was achieved:

- grip with a force of 15 N (19.5 N was achieved) using a power/cylindrical grip type and to grip with a force of 3 N (3.7 N was achieved) using a lateral/key grip (only using the thumb)
- hold 4 kg (8 kg was achieved) in a static (motors off) hook grip
- fully close the hand in 3 seconds (2 seconds was achieved)
- a multi-dexterous design, with individual actuation of each finger
- sense the grip force of the hand
- measure the temperature of objects being touched
- a novel sensory feedback system to communicate all sensory information simultaneously to the user
- be controllable using only two EMG channels
- introduce a novel method of control, allowing for more than 14 grip-type and hand gesture options (19 grip-type and hand gesture options were achieved)
- a modular design allowing for use with a transradial or transhumeral amputee
- a low-cost design with total the material cost under US\$ 3'000 (total material cost under US\$ 1'000 was achieved)

## 6.2 Future work

For future recommendations, it is acknowledged that a more efficient system for actuation can be developed. The grip force in the prosthetic hand needs to be increased in future versions of the hand. The grip force can be increased by implementing a more expensive and higher

power motor into the hand. The increased motor power would come with increased cost, and so a trade-off will need to be done. A modular solution could be implemented allowing the motors to be swapped out as the user desires and can afford. The wrist was designed with only a single DOF (rotation) to reduce the cost and weight of the prosthetic hand. However the flexion and extension movements are also important in daily life and inclusion of this second DOF would improve the overall function of the prosthetic hand. However, an additional DOF would bring added complexity, weight and cost to the hand. A modular approach could be taken here, allowing for the second DOF to be an attachable part to the prosthetic hand, allowing it to be used as necessary.

The monocoque design offered structural rigidity but there was little room for tools to reach inside, making the assembly very time consuming. The design should be modified to allow for the easy installation of the mechanical and electrical components. Further consideration could be given to allowing the hand to have modular mechanical and electrical components. This would allow for a high degree of customizability and would allow the amputee to choose only the components he/she wants to be in his/her prosthetic hand.

### 6.2.1 Control

The process of identifying the ideal location for the placement of the EMG sensors can be slow and difficult. Effective software needs to be developed to aid in the process of identifying the ideal location on the amputees stump needs to be developed. This program would visually show the signal readings while the EMG sensors are placed in different locations. The calibration process currently takes up to 30 minutes to do manually. This software could also assist in the calibration process, allowing the hand to calibrate itself by running a calibration exercise with the user. This technique would also significantly reduce the calibration time for return users.

Training software would also be beneficial to the amputee to allow him/her to practice controlling the prosthetic hand with the aid of a computer program. This program will show the amputee the effectiveness of every action he/she performs. The training software will also give a visual display of the HUI interface aiding the amputee to memorize the menu layout. Visual description of the sensory feedback system would also be beneficial to the amputee in learning to interpret the haptic sensory feedback given for different sensory triggers.

The pulse-length haptic sensory feedback communication protocol was found to be difficult to quantify because of the lack of a reference point. Alternative communication

protocols should be investigated to determine the ideal protocol. It is suggested that a pulse-count protocol be investigated as counting pulses is easily quantifiable.

### **6.2.2 Haptic feedback**

Through the course of the haptic feedback tests, a number of areas were identified for improvement. Only one type of communication was used in this dissertation. Future work needs to be done to evaluate which communication protocol is the most effective at communicating multi-sensory feedback. Tests should be done to investigate the maximum number of channels an individual is capable of interpreting.

Although this study sought to provide a haptic feedback solution that could be placed within the socket of the prosthetic arm, alternative and optimal locations and distances between channels should be investigated to maximize the efficiency of the feedback system. The training provided to test subjects before the tests was a simple demonstration. Supervised training procedures should be investigated to assess whether improved training programs and an increased duration of training time improves the accuracy interpretations.

Vibrotactile multi-sensory feedback tests need to be performed with real prosthetic hands and sensors, communicating real values back to the test subjects. These tests will provide a much more accurate picture on the feasibility of this approach to vibrotactile multi-sensory feedback. The test subjects can then be assessed on their ability to correctly identify object properties instead of merely identifying sensor values. The test should be conducted on subjects that have amputated upper extremity limbs. The study should also be conducted with an increase in sample size and repetitive testing over a period of days to weeks to improve the reliability of results.

## **6.3 Chapter summary**

This research has shown the low-cost design and development of a modular multi-sensory prosthetic hand with novel EMG control. The prosthetic hand has been shown to meet all of the objectives set out in the introduction chapter, being capable of satisfactory gripping objects and sensing and communicating the grip force and temperature of those objects. The sensory feedback is achieved through a novel simultaneous multi-sensory haptic feedback display that uses a single vibrotactile displays to communicate each sense. This research has produced a novel control system that is capable of allowing the user to select from a limitless list of preset grips and hand gestures. For future research it is proposed that alternative communication

protocols are investigated to design the optimum communication protocol for the designed multi-sensory haptic display device.

## 7. REFERENCES

- American Society for Surgery of the Hand, [Online]. Available: [www.assh.org](http://www.assh.org), date viewed: 28 February 2013.
- Anatomy Universe: [Online]. Available: [www.anatomyuniverse.com](http://www.anatomyuniverse.com), date viewed: 19 June 2013.
- Antfolk, C., Alomzo, M., Controzzi, M., Lundborg, G., Rosén, B., Sebelius, F. and Cipriani, C., "Artificial redirection of sensation from prosthetic fingers to the phantom hand map on transradial amputees: vibrotactile versus mechanotactile sensory feedback," *IEEE Transactions on Neural Systems and Rehabilitation Engineering*, Vol. 21, No. 1, January 2013.
- Arnould-taylor, W., *A Text Book of Anatomy and Physiology*, 3rd ed., vol. 3. Nelson Thornes, 1998.
- Artificial Joint Replacement of the Finger, [Online]. Available: [www.eorthopod.com](http://www.eorthopod.com), date viewed: 21 May 2013.
- Bark, K., Wheeler, J., Lee, G., Savall, J. and Cutkosky, M., "A wearable skin stretch device for haptic feedback," *Eurohaptics Conference and Symposium on Haptic Interfaces for Virtual Environment and Teleoperator Systems*, Salt Lake City, UT, USA, March 2009.
- Carrozza, M., Vecchi, F., Sebastiani, F., Cappiello, G., Roccella, S., Zecca, M., Lazzarini, R. and Dario, P., "Experimental analysis of an innovative prosthetic hand with proprioceptive sensors," *IEEE International Conference on Robotics & Automation Taipei, Taiwan*, September 2003.
- Castellini, C. and van der Smagt, P., "Surface EMG in advanced hand prosthetics," *Biological Cybernetics*, pp. 35-47, 2009.
- Celanese, [Online]. Available: [www.plastics.ides.com](http://www.plastics.ides.com), date viewed: 20 June 2013.
- Cipriani, C., Controzzi, M. and Carrozza, M., "Objectives, criteria and methods for the design of the SmartHand transradial prosthesis," *Robotica*, Vol. 28, Iss: 6, pp. 919-927, October 2010.
- Cipriani, C., Controzzi, M. and Carrozza, M., "Progress towards the development of the SmartHand transradial prosthesis," *IEEE International Conference on Rehabilitation Robotics Kyoto International Conference Center, Japan*, June 2009.
- Cipriani, C., Controzzi, M. and Carrozza, M., "The SmartHand transradial prosthesis," *Journal of Neuroengineering and Rehabilitation*, 2011.
- Cipriani, C., D'Alonzo, M. and Carrozza, M., "A miniature vibrotactile sensory substitution device for multifingered hand prosthetics," *IEEE Transactions on Biomedical Engineering*, Vol. 59, No. 2, February 2012.
- Cotton, D., Cranny, A., Chappell, P., White, N. and Beeby, S., "Control strategies for a multiple degree of freedom prosthetic hand," *UKACC Control, Mini Symposia*, pp. 211-218, August 2006.
- Dalley, S., Varol, H. and Goldfarb, M., "A method for the control of multigrasp myoelectric prosthetic hands," *IEEE Transactions on Neural Systems and Rehabilitation Engineering*, Vol. 20, No. 1, January 2012.
- Dalley, S., Wiste, T., Varol, H. and Goldfarb, M., "A multigrasp hand prosthesis for transradial amputees," *International Conference of the IEEE EMBS Buenos Aires, Argentina*, 2010.
- Damian, D., Lundersdorfer, M., Kim, Y., Arieta, A., Pfeifer, R. and Okamura, A., "Wearable haptic device for cutaneous force and slip speed display," *IEEE International Conference on Robotics & Automation RiverCentre, Saint Paul, Minnesota*, May 2012.
- Dietrich, C., Walter-Walsh, K., Preibler, S., Hofmann, G., Witte, O., Miltner, W. and Weiss, T., "Sensory feedback prosthesis reduces phantom limb pain: proof of a principle," *Neuroscience Letters*, Vol. 507, pp. 97-100, 2012.
- Docstoc, [Online]. Available: [www.docstoc.com](http://www.docstoc.com), date viewed: 21 May 2013.
- Finger Joint Anatomy, [Online]. Available: [www.fingerreplacement.com](http://www.fingerreplacement.com), date viewed: 21 May 2013.
- Fishel, J. and Loeb, G., "Sensing tactile microvibrations with the BioTac - comparison with human sensitivity," *4th IEEE International Conference on Biomedical Robotics and Biomechatronics, Roma, Italy*, pp. 1122-1127, June 2012.
- Geng, B., Yoshida, K., Petrini, L. and Jensen, W., "Evaluation of sensation evoked by electrocutaneous stimulation on forearm in nondisabled subjects," *Journal of Rehabilitation Research & Development*, Vol. 49, No. 2, pp. 297-308, 2012.
- Gurari, N., Kuchenbecker, K. and Okamura, A., "Perception of springs with visual and proprioceptive motion cues: implications for prosthetics," *IEEE Transactions on Human-Machine Systems*, Vol. 43, No. 1, January 2013.
- Hargrove, L., Scheme, E., Englehart, K. and Hudgins, B., "Multiple binary classifications via linear discriminant analysis for improved controllability of a powered prosthesis," *IEEE Transactions on Neural Systems and Rehabilitation Engineering*, Vol. 18, No. 1, February 2010.
- Hayward, V. and Cruz-Hernandez, J., "Tactile display device using distributed lateral skin stretch," *Symposium on Haptic interfaces for Virtual Environment and Teleoperator Systems, IMECE Conference*, November 2000.
- Henshaw, J., "Tour of the senses," *The John Hopkins University Press*, 2012.
- Interlink Electronics, [Online]. Available: [www.interlinkelectronics.com](http://www.interlinkelectronics.com), date viewed: 13 February 2014.
- Jiang, N., Englehart, K. and Parker, P., "Extracting simultaneous and proportional neural control information for multiple-DOF prostheses from the surface electromyographic signal," *IEEE Transactions on Biomedical Engineering*, Vol. 56, No. 4, April 2009.
- Jones, L., Held, D. and Hunter, I., "Surface waves and spatial localization in vibrotactile displays," *IEEE Haptics Symposium, Waltham, Massachusetts*, pp. 91-94, March 2010.
- Khushaba, R., Kodagoda, S., Takruri, M. and Dissanayake, G., "Toward improved control of prosthetic fingers using surface electromyogram (EMG) signals," *Expert Systems with Applications*, Vol. 39, pp. 10731-10738, 2012.
- Kim, K. and Colgate, J., "Haptic feedback enhances grip force control of sEMG-controlled prosthetic hands in targeted reinnervation amputees," *IEEE Transactions on Neural Systems and Rehabilitation Engineering*, Vol. 20, No. 6, November 2012.
- Kinovea, [Online]. Available: [www.kinovea.org](http://www.kinovea.org), date viewed: 12 February 2014.
- Kruijff, E., Schmalstieg, D. and Beckhaus, S., "Using neuromuscular electrical stimulation for pseudo-haptic feedback," *Proceedings of the ACM Symposium on Virtual Reality Software and Technology*, pp. 316-319, New York, NY, USA, 2006.
- Kyberd, P., Holland, O., Chappell, P., Smith, S., Tregidgo, R., Bagwell, P. and Snaith, M., "MARCUS: a two degree of freedom hand prosthesis with hierarchical grip control," *IEEE Transactions on Rehabilitation Engineering*, Vol. 3, No. 1, March 1995.
- "LM35 precision centigrade temperature sensors," *National Semiconductor*, November 2000.
- MacLean, K., "Designing with haptic feedback," *IEEE International Conference on Robotics & Automation San Francisco, CA*, April 2000.
- Matrone, G., Cipriani, C., Carrozza, M. and Magenes, G., "Real-time myoelectric control of a multi-fingered hand prosthesis using principle components analysis," *Journal of NeuroEngineering and Rehabilitation*, 2012.
- Measurement Specialties, [Online]. Available: [www.meas-spec.com](http://www.meas-spec.com), date viewed: 13 February 2014.
- Mediscape, [Online]. Available: [www.emedicine.medscape.com](http://www.emedicine.medscape.com), date viewed: 21 May 2013.



- Okamura, A., "Methods for haptic feedback in teleoperated robot-assisted surgery," *Industrial Robot: An International Journal*, Vol. 31 Iss: 6, pp. 499 – 508, 2004.
- OttoBock<sup>a</sup>, [Online]. Available: [www.ottobock.com](http://www.ottobock.com), date viewed: 18 February 2013.
- OttoBock<sup>b</sup>, [Online]. Available: [www.living-with-michelangelo.com](http://www.living-with-michelangelo.com), date viewed: 25 February 2013.
- Otto Bock Healthcare, [Online]. Available: [www.ottobock-export.com](http://www.ottobock-export.com), date viewed: 19 June 2013.
- Pololu, [Online]. Available: [www.pololu.com](http://www.pololu.com), date viewed: 16 September 2013.
- Richards, L. and Loudon, J., "Bone and joint structure," [Online]. Available: [www.kumc.edu](http://www.kumc.edu), date viewed : 21 May 2013.
- Rombokas, E., Stepp, C., Chang, C., Malhotra, M. and Matsuoka, Y., "Vibrotactile sensory substitution for electromyographic control of object manipulation," *IEEE Transactions on Biomedical Engineering*, vol. 60, pp. 2226-2232, March 2013.
- RSLSteeper, [Online]. Available: [www.bebionic.com](http://www.bebionic.com), date viewed: 25 February 2013.
- Rutkowski, J. and Levin, B., "Acrylonitrile–butadiene–styrene copolymers (ABS): Pyrolysis and combustion products and their toxicity—a review of the literature," *Fire and Materials*, Vol. 4, pp. 93-105, September 1986.
- Science Kids, [Online]. Available: [www.sciencekids.co.nz](http://www.sciencekids.co.nz), date viewed: 19 June 2013.
- Seed Studio, [Online]. Available: [www.seedstudio.com](http://www.seedstudio.com), date viewed: 18 February 2014.
- Skeletal System: Bone, Bone Tissue and Joints, [Online]. Available: [www.rapidlearningcenter.com](http://www.rapidlearningcenter.com), date viewed: 21 May 2013.
- Spectra Symbol, [Online]. Available: [www.spectrasymbol.com](http://www.spectrasymbol.com), date viewed: 18 February 2014.
- "TB6612FNG," Toshiba, 30 June 2007.
- Tejiero, C., Stepp, C., Malhotra, M., Rombokas, E. and Matsuoka, Y., "Comparison of remote pressure and vibrotactile feedback for prosthetic hand control," *IEEE RAS/EMBS International Conference on Biomedical Robotics and Biomechatronics Roma, Italy*, June 2012.
- Touch Bionics, [Online]. Available: [www.touchbionics.com](http://www.touchbionics.com), date viewed: 25 February 2013.
- Van As, R. and Owen, I., "Coming up short handed (the Robohand blog)," [Online]. Available: [www.comingupshorthanded.com](http://www.comingupshorthanded.com), date viewed: 13 February 2013.
- van der Niet, O., Reinders-Messelink, H., Bongers, R., Bouwsema, H. and van der Sluis, C., "The i-limb hand and the DMC plus hand compared: a case report," *Prosthetics and Orthotics International*, Vol. 34, pp. 216–220, June 2010.
- van der Niet, O., Reinders-Messelink, H., Bouwsema, H., Bongers, R. and van der Sluis, C., "The i-limb pulse hand compared to the i-limb and DMC plus hand," *MyoElectric Controls/Powered Prosthetics Symposium Fredericton, New Brunswick, Canada*, August 2011.
- van der Riet, D., Stopforth, R., Bright, G. and Diegel, O., "An overview and comparison of upper limb prosthetics," *IEEE AFRICON Conference, Mauritius*, September 2013.
- van der Riet, D., Stopforth, R., Bright, G. and Diegel, O., "Simultaneous vibrotactile feedback for multi-sensory upper limb prosthetics," *6<sup>th</sup> IEEE Robotics and Mechatronics Conference of South Africa*, Durban, October 2013.
- Wheeler, J., Bark, K., Savall, J. and Cutkosky, M., "Investigation of rotational skin stretch for proprioceptive feedback with application to myoelectric systems," *IEEE Transactions on Neural Systems and Rehabilitation Engineering*, Vol. 18, No. 1, February 2010.
- Witteveen, H., Rietman, J. and Veltink, P., "Grasping force and slip feedback through Vibrotactile stimulation to be used in myoelectric forearm prostheses," *34th Annual International Conference of the IEEE EMBS, San Diego, USA*, August 2012.
- Zhe Xu , Kumar, V., Matsuoka, Y. & Todorov, E., "Design of an anthropomorphic robotic finger system with biomimetic finger joints," *4th IEEE RAS & EMBS International Conference on Biomedical Robotics and Biomechatronics*, pp. 568-574, June 2012.

## 8. APPENDIX A

### 8.1 Mechanical drawings of hand

